CT5060 MSc Thesis

DESIGN CRITERIA FOR HIGH STRENGTH STEEL JOINTS

Leary Pakiding
1289047

Structural Engineering - Delft University of Technology
Huisman-Itrec B.V

Preface

Part of this research was conducted at Huisman-Itrec B.V, a company specialized in heavy lifting equipment based in Schiedam the Netherlands. This research is part of the modules which has to be fulfilled in order to obtain an MSc degree in Structural Engineering in Delft University of Technology-The Netherlands.

Acknowledgements are given to people who their supports make this research can be accomplished. Firstly it goes to the thesis committee: Prof. Dr. ir. L.J. Sluys, Dr. ir. P.C.J. Hoogenboom, Ir. E. Romeijn (Huisman-Itrec B.V) and Dr. ir. A. Romeijn who give valuable supervision. Secondly, for M. Stofregen and A. Bereznitski (Huisman-Itrec B.V) that their contributions to this project really appreciated. Thirdly, for the SPMU-TPSDP USTJ who provides financial support for my study. Fourth, it goes to the ISC-Delft community and finally, to my family: Cecilia, Archangela and Aurelia who always be there with their love and encouragement.

Delft,   May 2007
Leary Pakiding

Contents

Notations

E = modulus of elasticity
K = coefficient in power law formula
R_e = yield strength
R_m = ultimate strength
S = steel grade
T = thickness
f_{av} = average stress
f_y = yield stress
a = weld throat
l = weld length
l_y = weld length in the direction of the width of base material
f_u = ultimate tensile stress
n = exponent in Ramberg Osgood relation
np = exponent in power law formulation
F/Fu = ratio between corresponding yield load and ultimate load
Δ_{pl}/ Δ_{el} = ratio between displacement plastic and displacement elastic from load displacement curve
α_m = ratio of failure strain to ultimate strain
α_s = coefficient in parabolic relation of engineering stress strain based on the position of ultimate stress and failure stress
β_m = ratio of failure stress to ultimate stress
ε_{eng} = engineering strain
$\varepsilon_{eq,p}$ = equivalent plastic strain
ε_f = failure strain
ε_0 = characteristic failure strain
ε_{true} = true strain
ε_u = ultimate tensile strain
γ_{Mw} = partial safety factor for welded connections
σ_{eng} = engineering stress
σ_{eq} = equivalent Von Mises stress
σ_h = hydrostatic stress
σ_{true} = true stress
$\sigma_{\perp}$ = normal stress perpendicular to weld
$\tau_{\perp}$ = shear stress perpendicular to weld
$\tau_{//}$ = shear stress parallel to the weld
σ_{weld} = normal stress in the weld
ν = Poisson ratio

List of Figures

List of Tables

Summary

Finite Element (FE) analysis has been done to determine the β value which appears in the design formula of fillet weld connection based on stress directional method. In this case the determination of the β value for steel S1100 is the main concern. This FE analysis is related to the experimental work [6] regarding Very High Strength Steel. For this analysis, there are three different types of connections which are modelled and are labelled as connection type A1, connection type 2 and connection type 3. Only connection type A1 corresponds to experimental work [6]. The other connections are modelled mainly to see the influence of stress combinations occurring in the weld in order to calibrate the β value. For each type of connections, there are two types of geometry with differences in material thickness.

Before starting with the FE analysis, material input is developed in terms of true stress strain relation. These material input are created for each material (for base and weld material). Provided with these input, FE analysis starts with modelling of tensile test specimen for base and weld material in order to validate the material properties which are used as the input. This modelling also serves as a trial to see how the nonlinear analysis works in ANSYS. After validation of the results of this analysis it continues with modelling the three types of connection using steel S1100 and steel S355.

Convergence tests are done for each type of connection to determine the type of element and mesh size which will be used for further analysis. For this particular case, only connections using steel S1100 are modelled. These tests use different types of meshes which start from coarse mesh to fine mesh. Special integration points are applied in the elements in order to prevent locking problems

Further analysis to determine the corresponding failure load is done for each type of connection. The determination of the failure load for connections using steel S1100 is based on the Lemaitre criterion which relates the point of failure to the triaxiality and plastic strain present. Several nodes are investigated to determine where failure starts in the connections. On the other hand, for connections using steel S355 the determination of the failure load is based directly from the FE analysis results which can be seen clearly from corresponding load displacement curve of each connection.

Furthermore, the calculation of β value is performed. This value is calculated based on three standards [3], [8], [10] which have the same formulation with different criteria. The first step in the determination of this value is by determining the yield load criteria which state when yielding starts in the connections. This criterion is based on the ratio of plastic displacement (non-linear response to elastic displacement (linear response) in the load displacement curve of each connection. This criterion is used because of the fact that the determination of yield load (non-linear response) is difficult to determine from the experiment. Using this criterion, the ratio of corresponding yield load to failure load F/Fu can be determined which in return gives the corresponding β value for each connection. It can be seen later in this report that the resulting β values according to those standards give a large scatter. The β value is taken simply from the average of each connection analysed. Additionally, a statistic analysis is performed in order to determine the probabilistic failure of the connection using the chosen β value. This is done in order to accommodate the problem related to the large scatter in the results of β values from FEA. Monte Carlo simulation is used in this case. Only connections using steel S1100 are analysed using Monte Carlo analysis. The results of this analysis show that the factor β = 2.24 is a safe value for designing fillet weld connection using high strength steel S1100. It is shown by the lower failure probability of Monte Carlo simulation compared to that of codes of practice.

Finally, a proposed formula is derived for designing fillet weld connections of steel S1100. This formula is based on the resulting failure load of each connection from the Lemaitre criterion. The corresponding stress components which occur in the weld are calculated then using linear regression analysis a design curve is produced. Based on this analysis, the corresponding design formula of fillet weld connection for steel S1100 is produced after some elaborations. This formula is only valid for fillet weld connections where $\sigma_\perp$ and $\tau_\perp$ are coupled.

Chapter 1 Introduction

1.1 Introduction

Recent developments in steel production give the opportunity to use high strength steel with yield strength up to 1100 N/mm² in structures. This improvement brings many advantages not only for production companies but also for clients as well as for designers. One of the benefits is that lighter structures can be made which in turn can give savings in material used, reducing the transportation costs and reducing the construction time. In addition, large steel structures for instance heavy lifting cranes are only possible when use is made of this type of material.

The level of safety and serviceability are the main considerations in using high strength steel and need to be controlled in design and fabrication. In design of statically loaded connections the deformation capacity is one of the main considerations. In fabrication, special attention is given to imperfections in the base material and in the weld which can reduce the strength of structures.

Traditionally in welded connections, the static strength of the weld material is larger than the material of the adjacent steel plates. This situation is called overmatched. As a consequence, at high loading yielding will occur in the plates and not in the welds. At continued loading yielding will extent to a large area of the plates providing large ductility before finally the connection breaks. However, when the plate material has yield strength of 1100 N/mm² the connection might be under-matched because welding material can only reach yield strength up to approximately 900 N/mm². As a consequence, most yielding is confined to the welds and the connection might fail with little ductility. Reduced ductility of connections can result in reduced safety of a structure because its connections would fail one after another instead of sharing to carry the load.

A project has been conducted by TNO, TU-Delft and several companies entitle “Integrity of High Strength Steel” [4, 5, 6, and 7]. It included fabrication and testing of 48-different high strength steel welded connections. The results justify design of high strength steel connections using the well known formula for mild steel connections from NEN 2062 [10]

$$\sigma_c = \beta\sqrt{\sigma_\perp^2 + 3\left(\sigma_\perp^2 + \tau_{//}^2\right)} \tag{1.1}$$

where β is an empirical factor that differs for the type of steel grade. This design formula is based on the yield condition of Von Mises [2]. In this form it is often referred to as the formula of Hubert-Hencky. In Huisman-Itrec B.V the following β values are used for high strength steel fillet weld connections. They are not provided by the Code of Practice but based on experimental results [6].

S355 β = 0.85
S460 β = 1.00
S700 β = 1.00
S900 β = 1.15
S1100 β = 1.38

1.2 Problem Statement

Though regularly applied by industry, high strength steel welded connections are not studied as thoroughly as mild steel connections. It is not clear whether the mechanical behaviour of such connections can be predicted correctly by the current state of finite element analysis software. If it can be shown that finite element model is sufficiently accurate then other connections can be analysed without resorting to expensive experiments. Moreover, the current design formula can be extended to other material strengths, connection types and loading conditions.

1.3 Objectives

The main objective of this research is to find the β values in equation (1.1) for high strength steel S1100. In addition the β value for steel S355 is also calculated in order to have a comparison with that mentioned already in the code [10].

1.4 Approaches

The approaches which are used in this project to solve the problem are listed as follow.

1. Study ANSYS
2. Model several connections for which experimental results are available.
3. Determine the sensitivity and appropriate values of modelling parameters.
4. Determine the limitations in what can be predicted reliably.
5. Model several connections for which no experimental data is available.
6. Compute the behaviour of these connections.
7. Compare the results with the design formula and propose improvements.

Chapter 2 Material Properties

2.1 Introduction

Two material properties (like yield strength (R_e), ultimate tensile strength (R_m) and maximum elongation (ε_u)) are given for steel S1100 and steel S355 which will be used in the FE analysis. These material properties are used in developing the material input for the FE analysis.

2.2 Material Properties of steel S1100

In order to apply real material properties of steel S1100 that are used in the experiment, all material properties for the FE model are adopted from a TNO report [4]. These material specifications are given in Table 2.1. This table also include some parameters such as K and np which will be used later in creating the stress strain relationship which will be used as an input in the FEA. These parameters are derived from an iterative procedure using FE modelling of tensile test specimens that explained in [4].

Table 2.1 Material properties steel S1100

Specimen	Plate/ Weld	T [mm]	S (MPa) O/U	R_e [Mpa]	R_m [Mpa]	ε_u [Mpa]	K [Mpa]	np [-]
4A1	Plate	10	1100	1179	1432	11%	1500	0.003
	Weld	Undermatched		728	777	15%	950	0.05
5A1	Plate	40	1100	1106	1325	11%	1375	0.0001
	Weld	Undermatched		931	1061	14%	1250	0.037

In addition, based on [7] these material specifications are applied to the type of connections which is shown in Figure 2.1. For this project, only connection type A which will be analysed in detail regarding the fillet weld connection.


Connection type A


Connection type B


Connection type C

Figure 2.1: Type of connections

2.2.1 Stress strain relation steel S1100

To perform nonlinear analysis which includes material nonlinearity, the true stress strain curve is needed. The curve is created based on the material specifications shown in Table 2.1 where the modulus of elasticity is taken 210000 N/mm^2. Moreover, the same procedure and assumption based on [4] is used to create the curves. Firstly, 3 points are plotted based on the data in Table 2.1. These points are Re positioned at strain εe, Rm which is put at an assumed strain of one third εu and the failure stress (approximately 0.6Rm) which positioned at εu. The resulting plot of these points is shown in Figure 2.2.

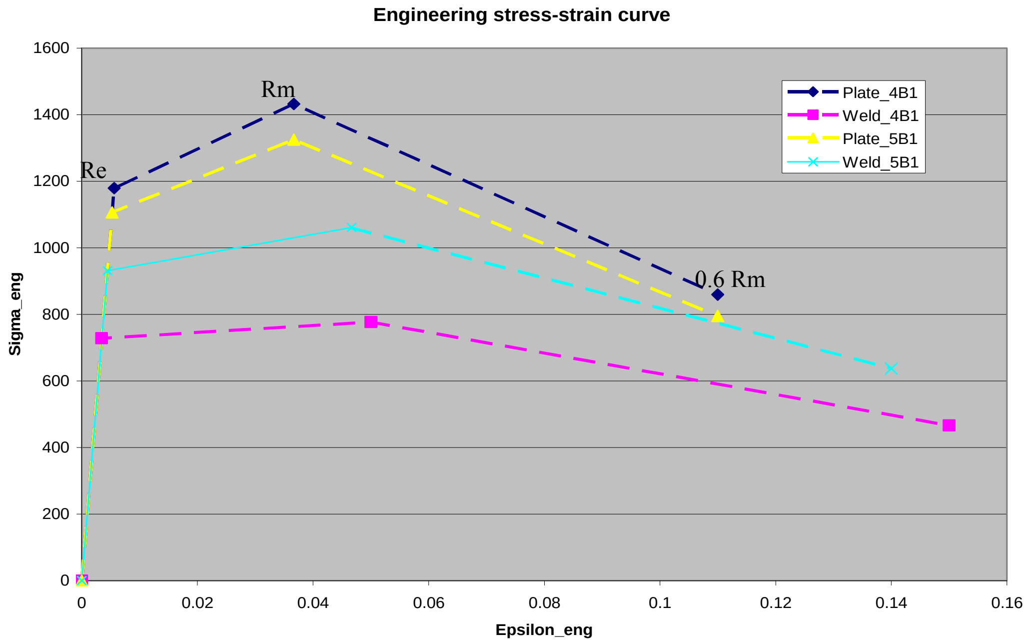

Figure 2.2: The approximated engineering stress strain curves

Consequently, based on Figure 2.2 the engineering stress-strain curve is made. The steps to create this curve are based on [4] and are given as follow.

1. The first upward part of the approximated engineering stress strain curve for each material is approximated by Ramberg-Osgood relation.

$$\varepsilon_{eng} = \frac{\sigma_{eng}}{E} + 0.002\left(\frac{\sigma_{eng}}{Re}\right)^{n} \tag{2.1}$$

2. The second downward part is approximated by a parabolic relation.

$$\sigma_{eng} = R_m - \alpha_s\left(\varepsilon_{eng} - \frac{\varepsilon_u}{3}\right)^2 \tag{2.2}$$

where

$$\alpha_s = \frac{R_m(1-\beta_m)}{\varepsilon_u^2(1-\alpha_m)^2}$$

β_m=0.6 ; α_m=1/3

Finally, the true stress strain relation is created. The theoretic formula below is used to approximate the first upward plastic part of the true stress strain curve. ε_{eng} and σ_{eng} are taken from the result of equation (2.1).

$$\varepsilon_{true} = \ln(1+\varepsilon_{eng}) \tag{2.3}$$
$$\sigma_{true} = \sigma_{eng}(1+\varepsilon_{eng}) \tag{2.4}$$

Based on [4] the so called Power Law formula is used to approximate the hardening part of the true stress strain curve.

$$\sigma_{true} = K \cdot \varepsilon_{true}^{np} \qquad (2.5)$$

The resulting true stress strain curves for the base and weld material are shown in Figure 2.3.

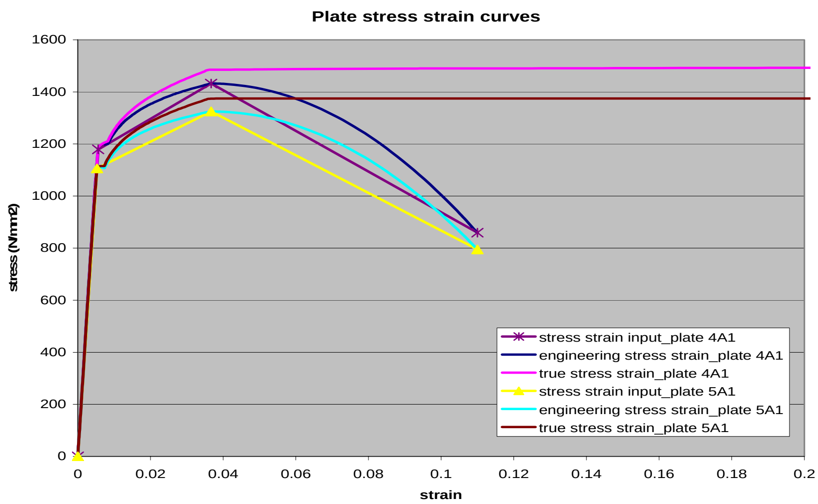

(a)

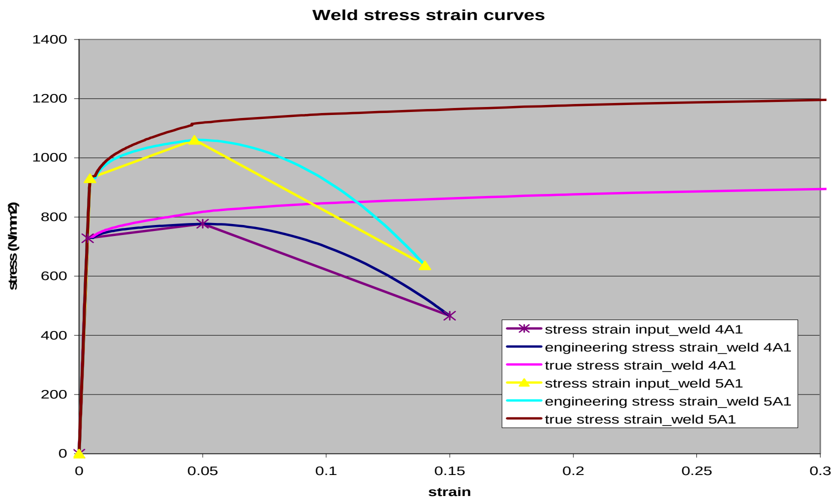

(b)

Figure 2.3: Resulting true stress strain curves
(a) base material, (b) plate material

A flow chart to create the true stress strain curves is given in Figure 2.4.

<u>Plot input data:</u>
Re positioned at ε_e
Rm positioned at $1/3\varepsilon_u$
0.6Rm positioned at ε_u

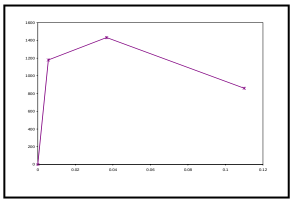

<u>Engineering stress strain curve is made.</u>

- Fitted the first upward part using Ramberg Osgood relation:

$$\varepsilon_{eng} = \frac{\sigma_{eng}}{E} + 0.002\left(\frac{\sigma_{eng}}{Re}\right)^n$$

- Fitted the downpart using parabolic relation:

$$\sigma_{eng} = R_m - \alpha_s\left(\varepsilon_{eng} - \frac{\varepsilon_u}{3}\right)^2$$

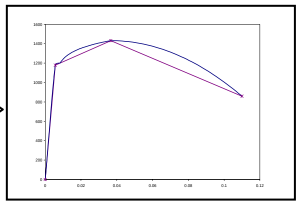

<u>True stress strain curve is made.</u>

- The first upward plastic part is approximated using theoretic relation:
  $\varepsilon_{true} = \ln(1+ \varepsilon_{eng})$
  $\sigma_{true} = \sigma_{eng}\,(1+ \varepsilon_{eng})$

- The hardening part is approximated using parabolic relation:
  $\sigma_{true} = K \,.\, \varepsilon_{true}^{np}$

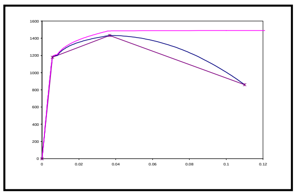

Figure 2.4: Flow chart for creating the true stress strain curve

In figure 2.4, for true stress strain curve the number of points which are used to build this curve is 100.

2.2.2 Tensile test simulation

In order to validate the true stress strain curves obtained from the previous approximation for steel S1100 materials, the tensile test is performed numerically using the FE package ANSYS. This analysis also serves as a trial in order to test the nonlinear analysis in this FE package. The geometries of the tensile test specimens for the base material and for the weld material are shown in Figure 2.5. These geometries are chosen to resemble the geometries which are used commonly in the tensile test experiment. For the weld tensile test specimen, the circular section is common in practice because sometimes it happens that the size of the weld is quite small and therefore it is difficult to obtain a rectangular section.

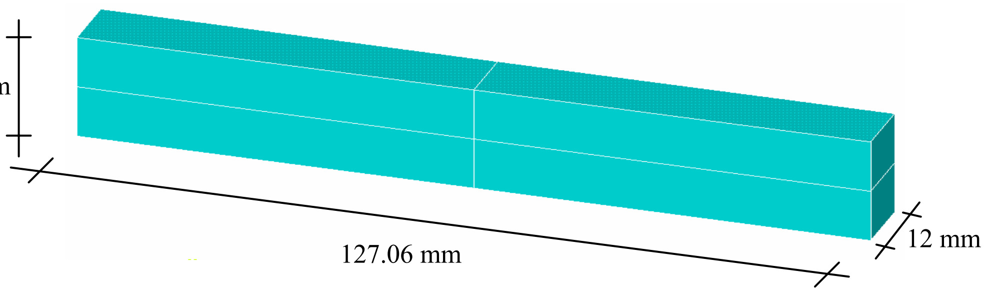

(a)

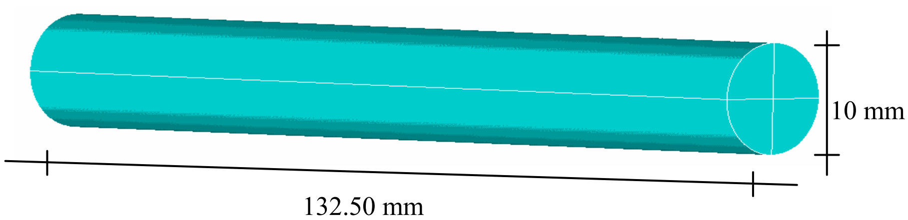

(b)

Figure 2.5: Geometry of the tensile test specimen
(a) base material, (b) weld material

Due to symmetry in geometry and loading, only one fourth of the base material specimen is modelled and for the weld material specimen it is only one eight.

The type of element which is used in this analysis is SOLID185 (8 nodes brick element) and the explanation of this material model regarding the numerical integration point is given in Appendix B. For this particular case selective reduced integration is chosen for this type of element. The material properties input are Modulus of elasticity E= 210000 MPa and Poisson's ratio 0.3. These material properties are used for all tensile test specimens. To include material nonlinearity, the true stress strain curve is used as the input. The isotropic hardening rule and Von Mises plasticity are chosen for these materials. The kinematic hardening rule does not work for these materials.

Mapped mesh (Appendix C) is used to mesh the geometry and there is no preference for the number of elements. In the analysis options large displacement and large strain are activated. The full Newton Rapshon iterative procedure is used with automatic time stepping. The boundary conditions only applied in the area of symmetry. Finally, for the loading, displacement control is used where this load is increased gradually for each sub-step.

In order to have necking in the appropriate part of the tensile test specimens which is located at half of the height of the specimens, an imperfection is introduced in the geometry. This is done by reducing 2% of the height of the specimen part where the necking is expected to occur.

The results of the analysis are shown in Figure 2.6 and Figure 2.7

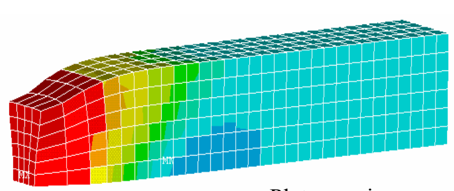

Plate specimen

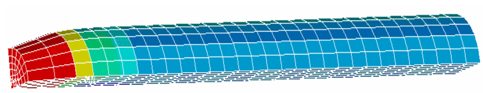

Weld specimen

Figure 2.6: The necking phenomena

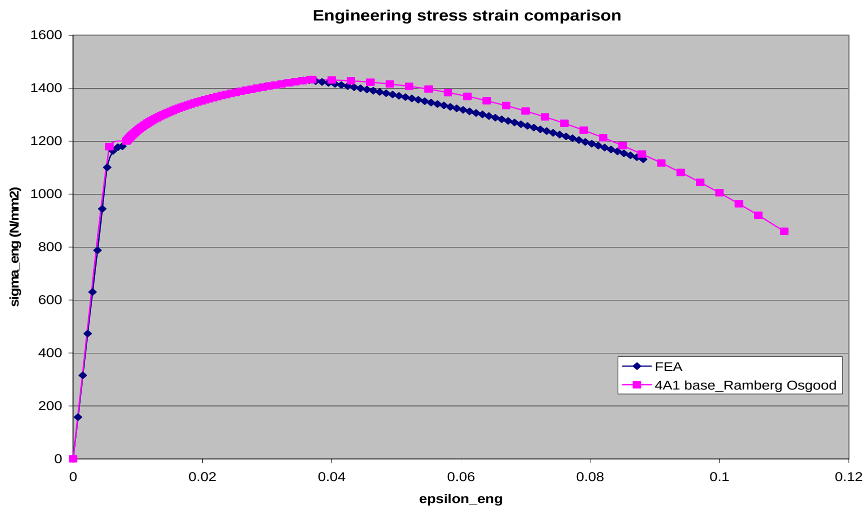
Engineering stress strain comparison
sigma_eng (N/mm2)
epsilon_eng
FEA
4A1 base_Ramberg Osgood
0
200
400
600
800
1000
1200
1400
1600
0
0.02
0.04
0.06
0.08
0.1
0.12

(a)

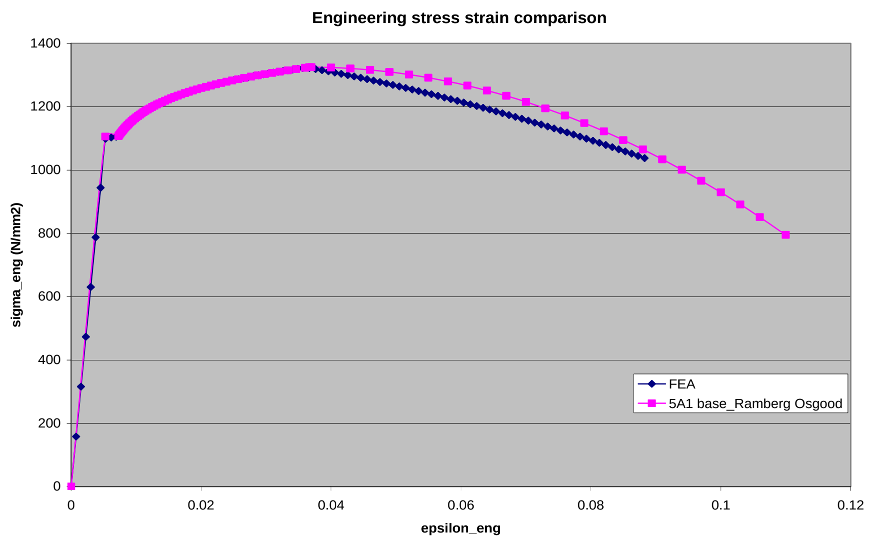
Engineering stress strain comparison
sigma_eng (N/mm2)
epsilon_eng
FEA
5A1 base_Ramberg Osgood
0
200
400
600
800
1000
1200
1400
0
0.02
0.04
0.06
0.08
0.1
0.12

(b)

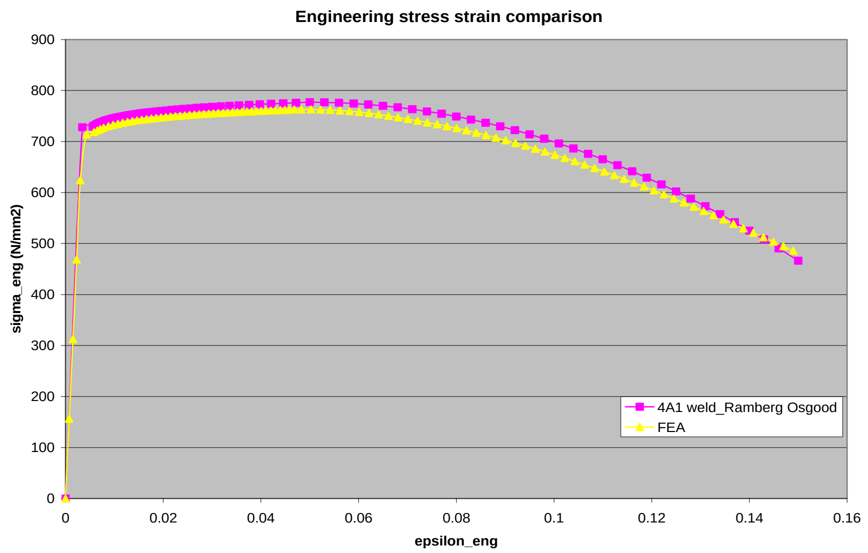
Engineering stress strain comparison
sigma_eng (N/mm2)
epsilon_eng
4A1 weld_Ramberg Osgood
FEA
0
100
200
300
400
500
600
700
800
900
0
0.02
0.04
0.06
0.08
0.1
0.12
0.14
0.16

(c)

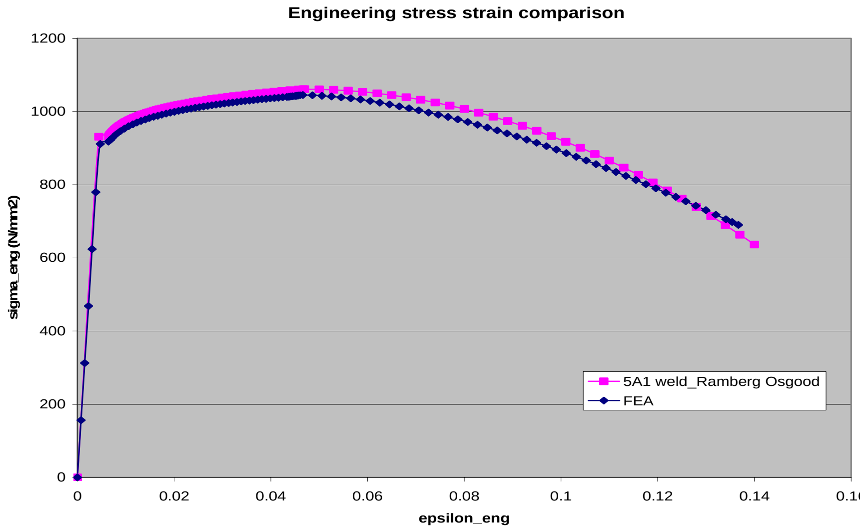

(d)

Figure 2.7: Engineering stress strain curves comparison
(a) 4A1 base material, (b) 5A1 base material, (c) 4A1 weld material, (d) 5A1 weld material

Based on the necking phenomena in Figure 2.6 it can be concluded that the simulation of the tensile specimens are very accurate. This is also validated by the engineering stress strain curves comparison in Figure 2.7 where the stress strain curves of FE analysis results can track the path of the engineering stress strain curves based on Ramberg Osgood formula although for the weld materials there are very small differences.

Furthermore, in order to know the sensitivity of the down part of the engineering stress strain curve related to the element size of the necking part, a convergence test is done using finer mesh and higher order brick element (SOLID 186) which its numerical integration point is also given in Appendix B. The result of this test is shown in Figure 2.8.

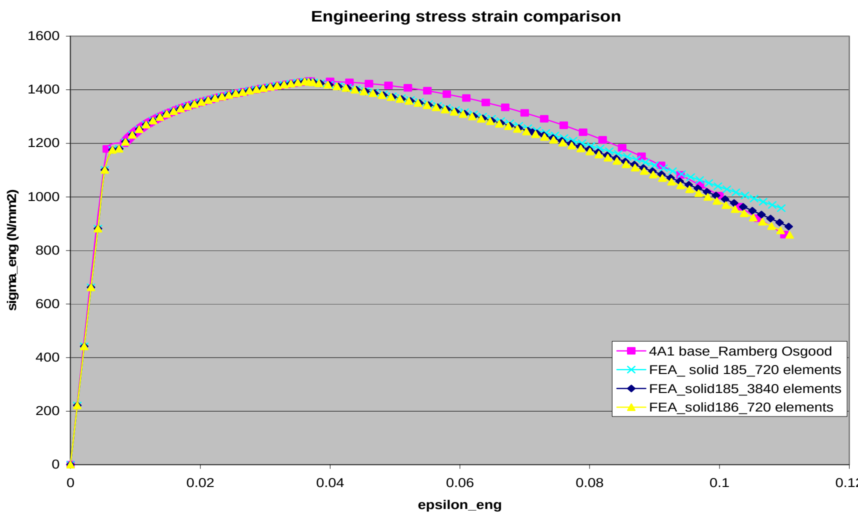

(a)

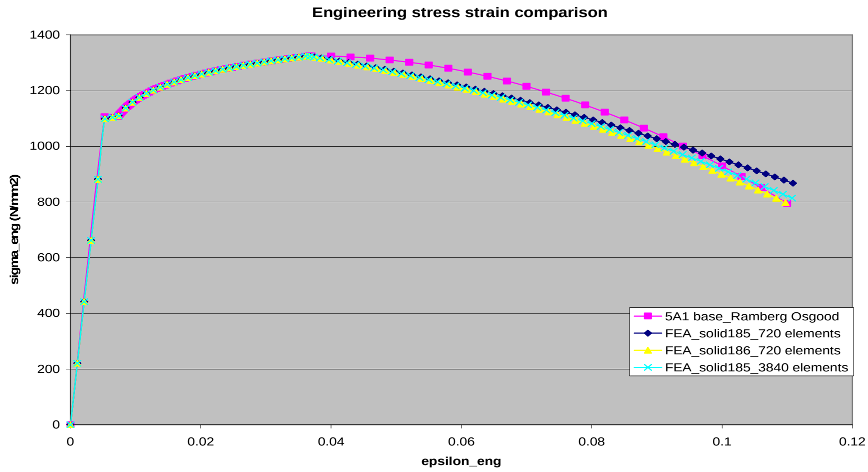

(b)

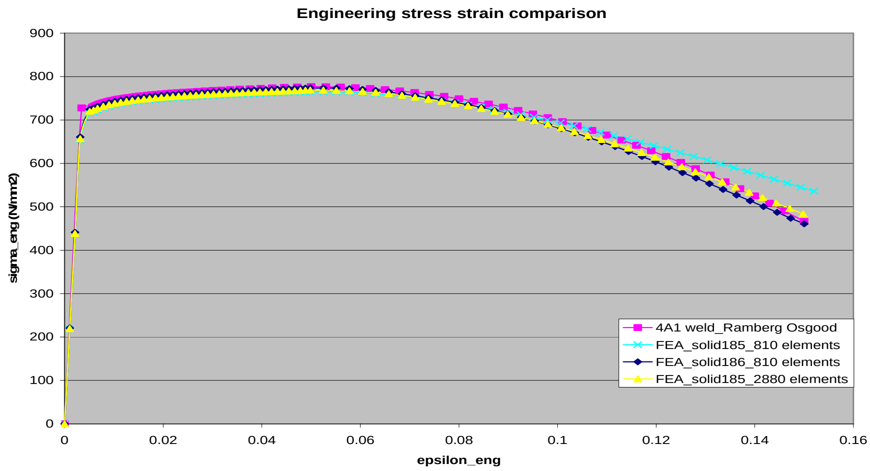

(c)

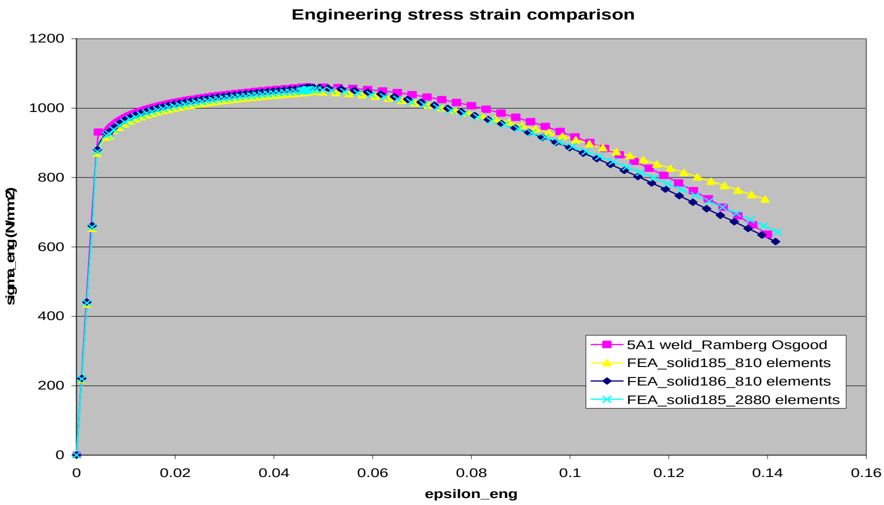

(d)

Figure 2.8: Engineering stress strain curves which show the sensitivity of the down part (a) 4A1 base material, (b) 5A1 base material, (c) 4A1 weld material, (d) 5A1 weld material

Figure 2.8 shows that the downward part of the engineering stress strain curve is influenced by the size of the element and also by the type of element used. The smaller the size of the element at necking part is the steeper the slope of the downward part of the stress strain curve and the same condition also happens for using higher order element. However the difference is not remarkable.

Moreover, the sensitivity at the necking part of the specimen is also investigated based on variation of element size and the use of different type of elements. The results of this investigation are shown in Figure 2.9. According to this figure, the influence of using different element size at the necking part gives remarkable differences especially by fining the mesh at the area of the necking which results in steeper slope for that area. It implies that in this part there is an influence of mesh sensitivity to the necking phenomenon.

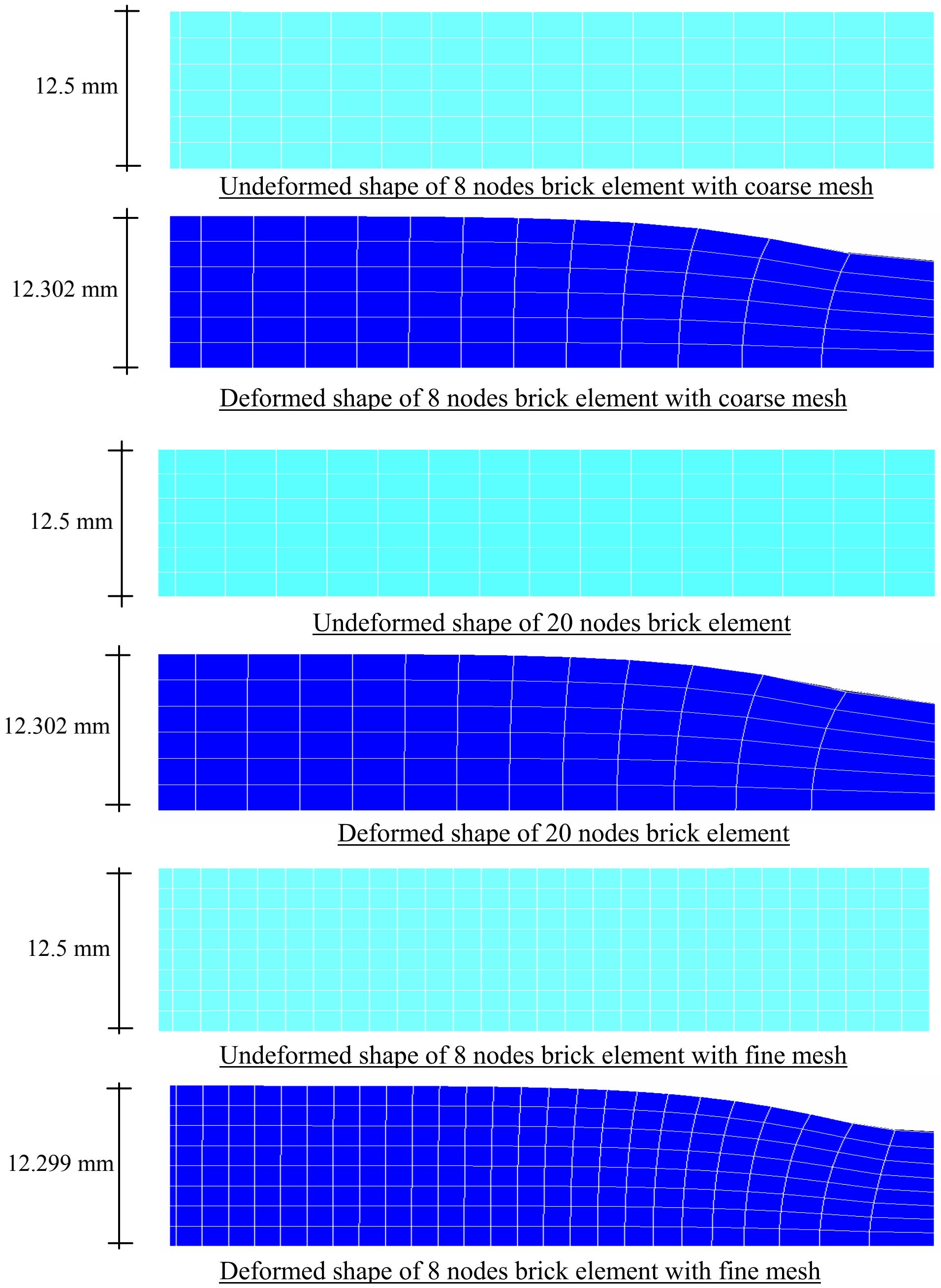

Figure 2.9: Sensitivity of the element around the necking part of the specimen

2.3 Material Properties of steel S355

Table 2.2 Material properties steel S355

Plate/ Weld	T [mm]	S (MPa) O/U	Re [MPa]	Rm [MPa]	εu [MPa]	K [MPa]	np [-]
Plate	10 and 40	355	391	531	32.2%	879	0.19
Weld	Overmatched		480	600	30%	805.96	0.0852

The material properties for steel S355 which will be used in the FE modelling is given in Table 2.2. The properties of the base material are based on report [11]. For the weld, consumable MEGAFIL 710 M which can be found in [12] is used as the typical consumable for overmatching condition. An approximation based on [9] is done to determine the K and np value because there is no available engineering stress strain relation for the weld that results from experiment tensile test which can be used as a comparison if the FE iterative procedure wants to be performed to determine this value.

2.3.1 Stress strain relation steel S355

For this type of steel, the data which is given in Table 2.2 is used to create the true stress strain relation. The procedure which is given in Figure 2.4 is used to create the stress strain relation for weld material. The corresponding result of this approach is given in Figure 2.10b. As mentioned before, for the plate material the resulting true stress strain curve is based on [11] and it is shown in figure 2.10a .

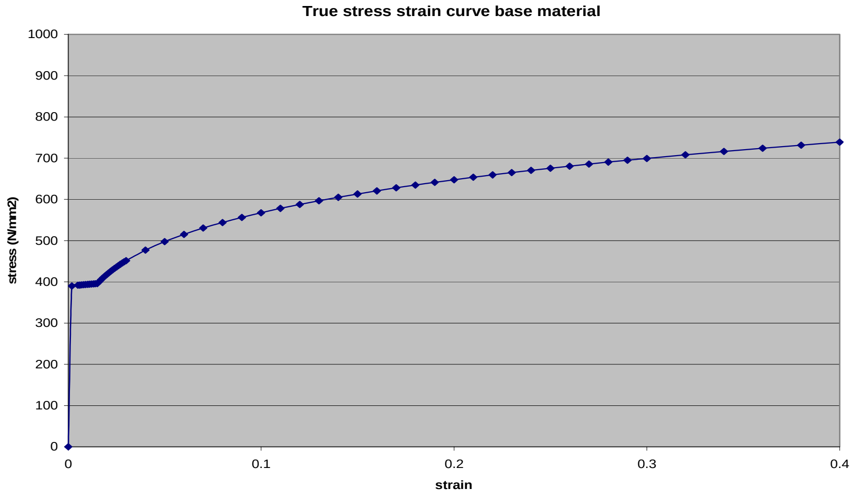

(a)

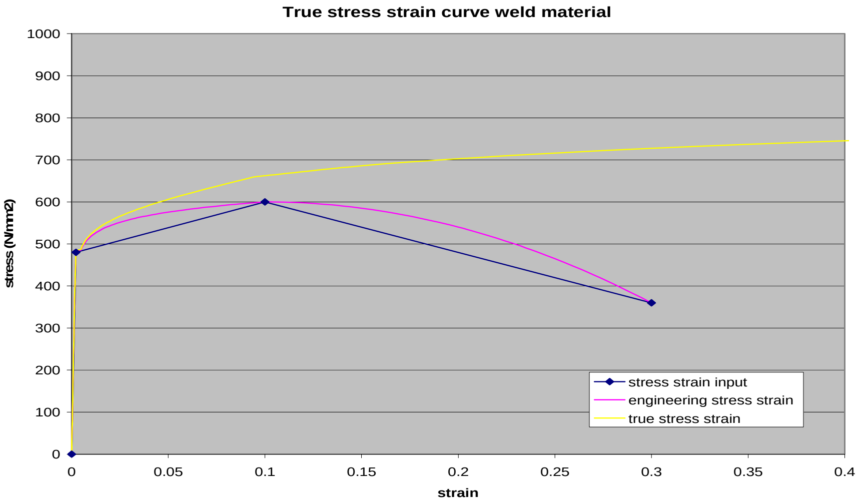

(b)

Figure 2.10: True stress strain relations and engineering stress strain relations
(a) base material, (b) weld material

Chapter 3 FE Modelling of Connections

3.1 Introduction

This chapter explains the Finite Element Modelling of fillet weld connections which is done using FE package ANSYS. Two types of steel; steel S1100 and steel S355, are used for the connection to simulate over-matching and under-matching condition in fillet weld connections respectively. Three types of connections are modelled which are labelled connection type A1, connection type 2 and connection type 3. To determine the failure load of connection which use steel S1100 a so called Lemaitre criterion is adopted while for connections use steel S355 the failure load directly determined based on load displacement curve plot.

3.2 FEM of connections

3.2.1 FEM connections using steel S1100

3.2.1.1 Connections type A1

The geometry of the connections which are modelled is shown in the Figure 3.1. These geometries are based on the geometry of the experiment reported by [6]. It can be seen that only one fourth of the geometry configurations are modelled because of symmetry in geometry and loading.

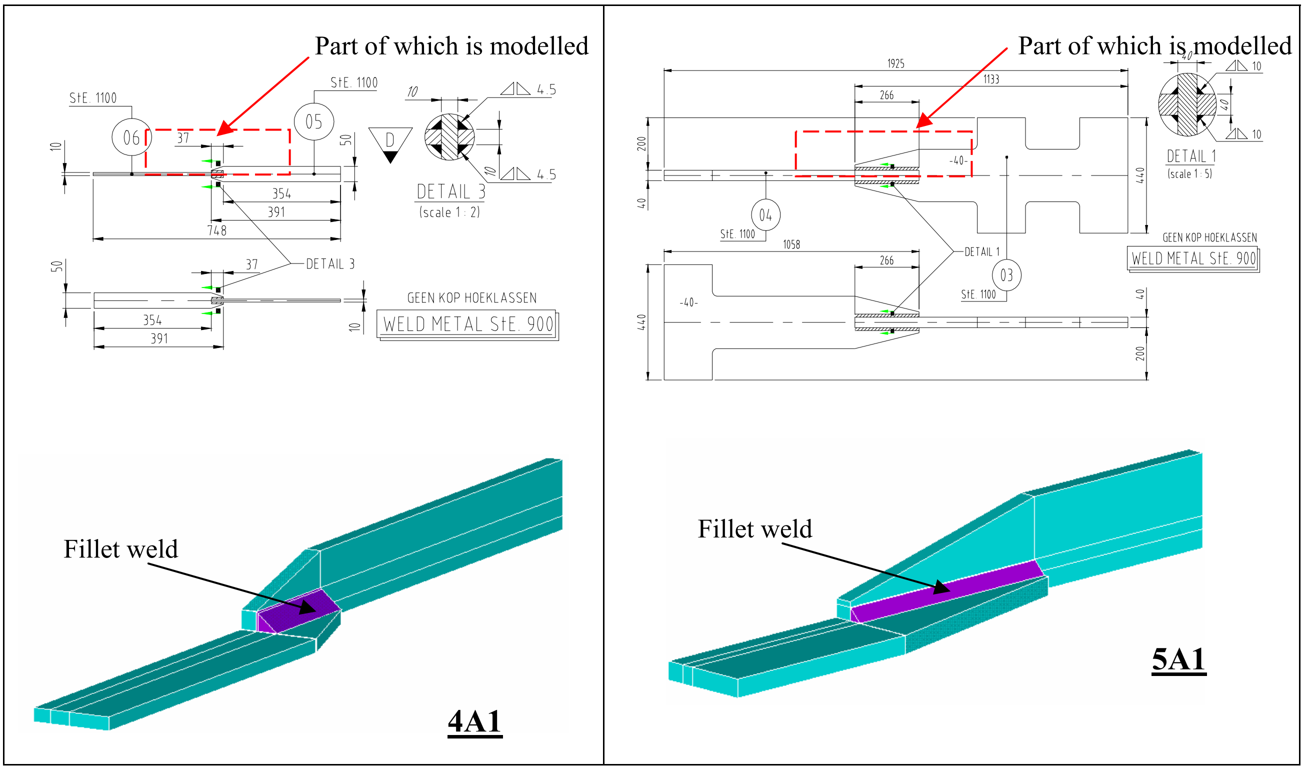

Figure 3.1: Geometry of connections type A1

The types of element that are used for the model are SOLID185 and SOLID186. These elements are used for the 3-D modelling of solid structures. They are defined by eight nodes and twenty nodes respectively and have three degrees of freedom at each node: translations in the nodal x, y, and z directions. These elements have plasticity, hyper-elasticity, stress stiffening, creep, large deflection, and large strain capabilities. A distinction is used regarding SOLID185 and SOLID186 to show the influence of higher order element behaviour.

For the material properties, there are two different material properties which are the material for the base plate and material for the fillet weld. Both of this materials having Modulus of elasticity E=210.000 N/mm^2 and Poisson ratio ν=0.3. In order to include material nonlinearity in the model, the true stress strain relation is input using isotropic hardening rule with Mises plasticity. The true stress strain curves which are input in ANSYS are shown in Figure 3.2 (see also Figure 2.3).

Mapped mesh is used to mesh the model. The number of elements is made starting from coarse mesh to fine mesh in order to perform convergence testing.

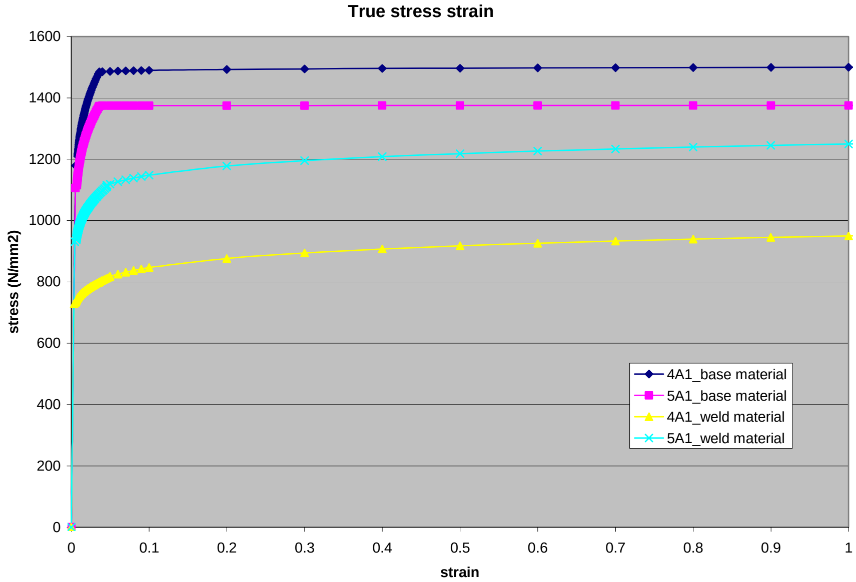

Figure 3.2: True stress strain curves

Static analysis is performed with large displacements and large strains. The full Newton Raphson iterative procedure is activated with automatic time stepping. The displacement control is used for the loading procedure which is increased gradually every sub-step in order to apply the load slowly to prevent convergence problems.

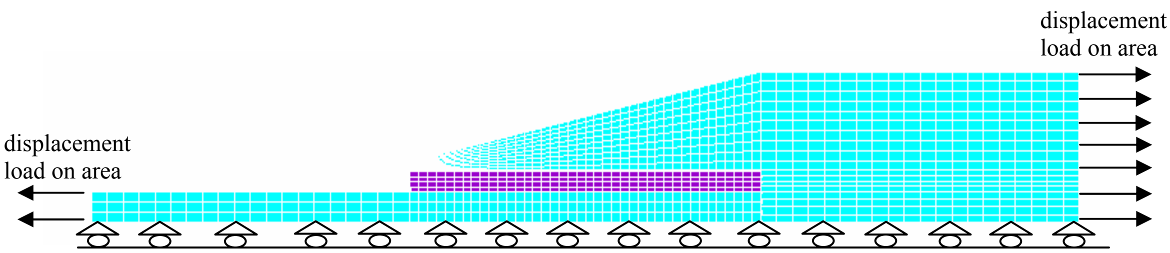

Front view

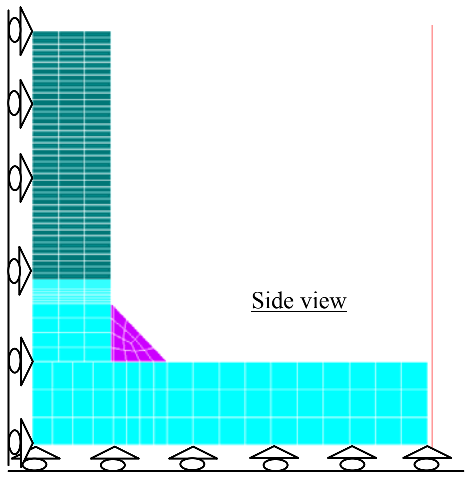

Figure 3.3: Boundary conditions

The boundary conditions are applied only in the symmetric part of the model. These boundary conditions are shown in the Figure 3.3. In this figure, all the boundary conditions are applied in the area which will be transformed later on by ANSYS to the finite element model (nodes) before the analysis started. The advantage of the application of the boundary conditions on the area is that the change of the solid model mesh will not change the boundary conditions. The following section gives detailed explanation regarding the modelling of both connections (type 4A1 and type 5A1) and also the determination of the failure load.

1. Connection type 4A1

Convergence tests are done firstly to determine the size of the element which will be used later in the analysis for this type of connection. This test is based on the element size and calculation time on a modern PC. The types of mesh by means of mesh refinement which are used in this convergence tests are shown in Figure 3.4. The results of the analysis are shown in Table 3.1 and Figure 3.5.

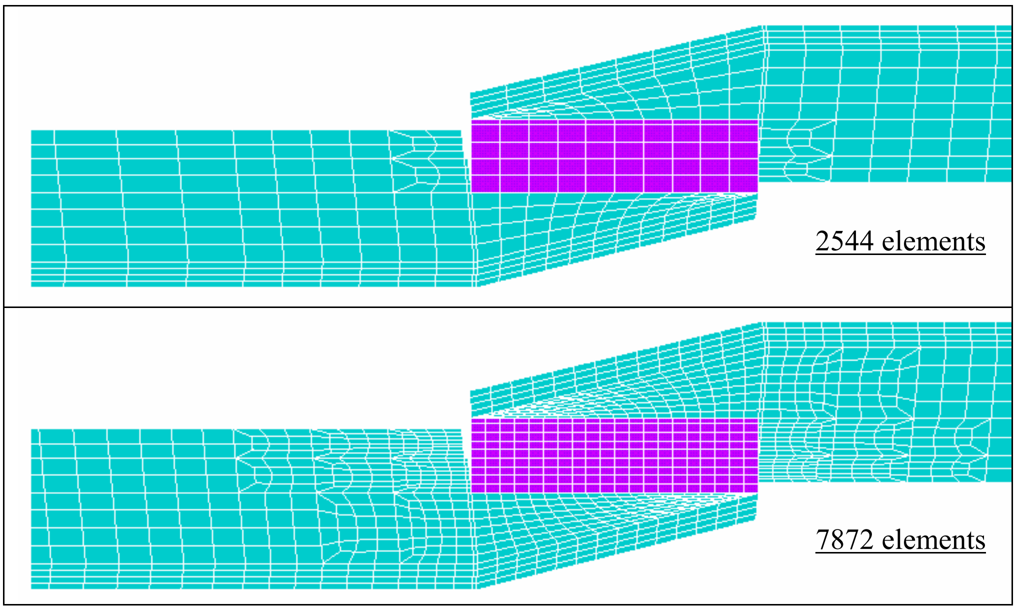

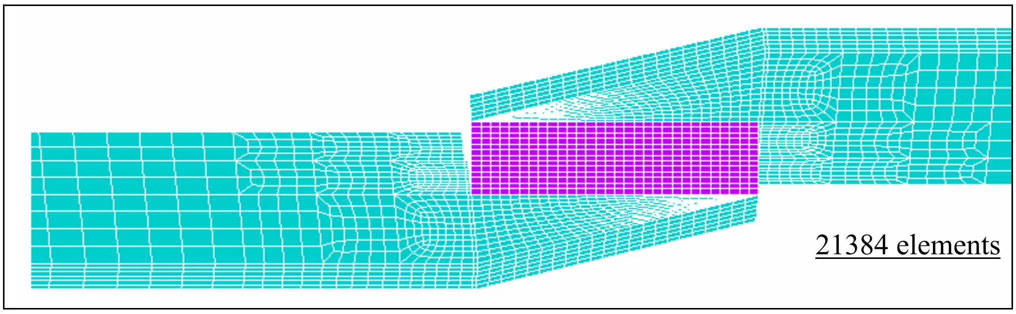

Figure 3.4: Types of mesh

Table 3.1 Convergence test results

No.	Type of elements	Calculation time
1.	8 nodes brick element (2544 elements)	7 minutes
2.	20 nodes brick element (2544 elements)	33 minutes
3.	8 nodes brick element (7872 elements)	26 minutes
4.	20 nodes brick element (7872 elements)	8 hours and 38 min.
5.	8 nodes brick element (21384 elements	1 hour and 2 min.

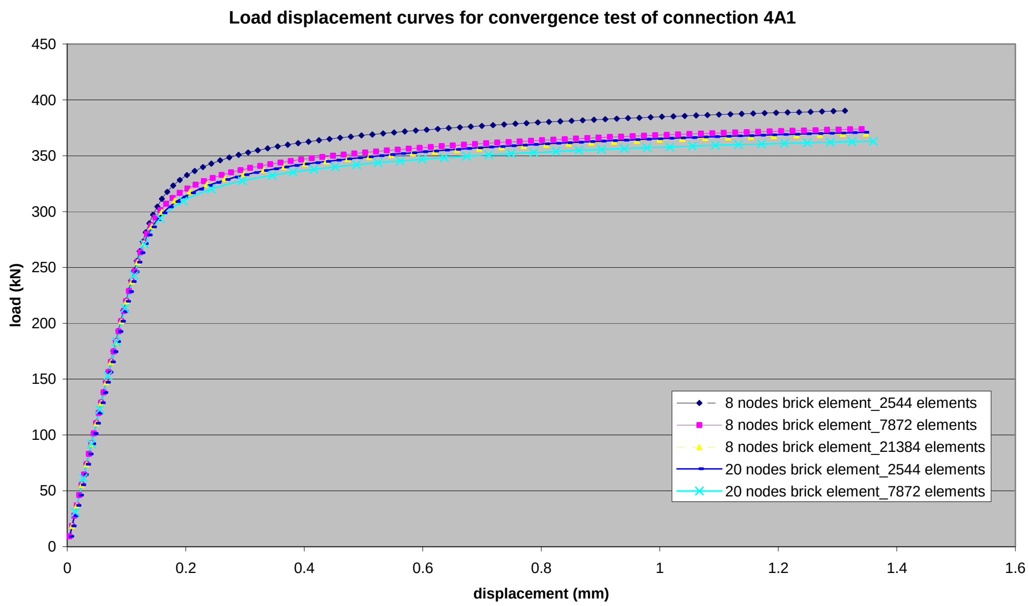

Figure 3.5: Convergence test results

From Figure 3.5 it can be seen that by using 20 nodes element with a coarse mesh refinement, the convergence is faster to achieve compare to that of using 8 nodes element with 21384 elements. Also the numbers of element needed are less if using 20 nodes element with less computational time. Based on this result, for further analysis only 20 nodes element will be used with 2544 elements.

In addition, another test is conducted to see the influence of the distance where the load applied. In previous analysis, the distance where the load applied is 200 mm from the end of the weld and is compared to that of 100 mm load application from the weld. Figure 3.6 shows the different distance of load application.

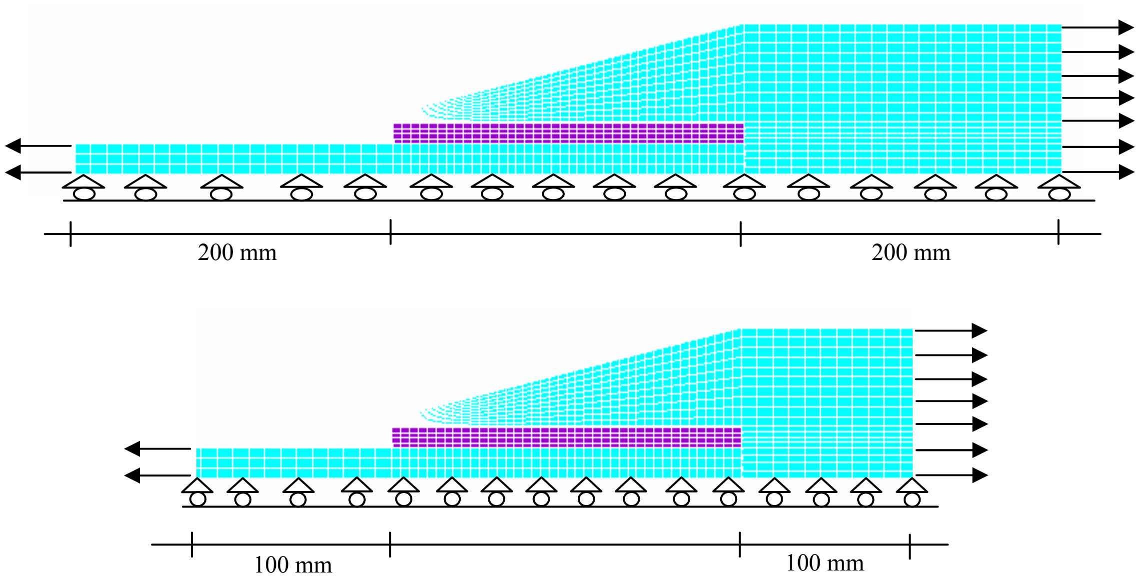

Figure 3.6: Load application distance

The result of this comparison is shown in Figure 3.7.

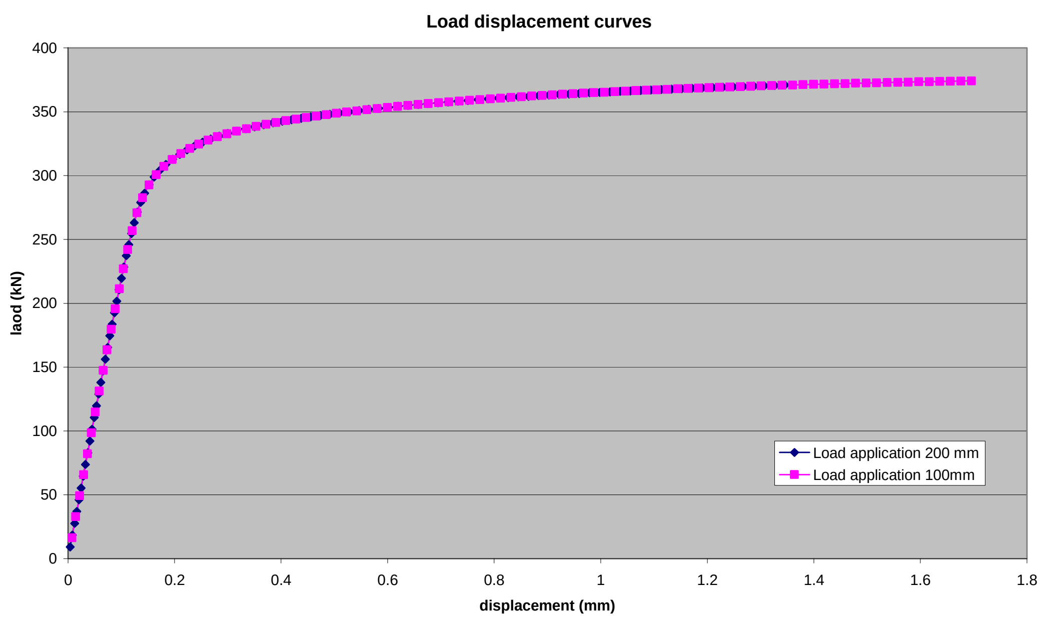

Figure 3.7: Comparison result based on load application

The result of Figure 3.7 shows that there is no visible influence of the load application distance. It can be seen that the load displacement curve for both situations are almost the same.

To validate the performed analysis a comparison with the experimental results based on [6] is made. The result of the related connection from [6] is replotted and it is compared to the FE analysis result. The measured length of the displacement in the FE analysis model is exactly the same to the LVDT positions (Figure 3.8) in the experiment for particular connections [6]. It is achieved by measuring the displacement on the node which represents one end of the LVDT in the experiment (node that positions at the parent material). The result of this comparison is given in Figure 3.9.

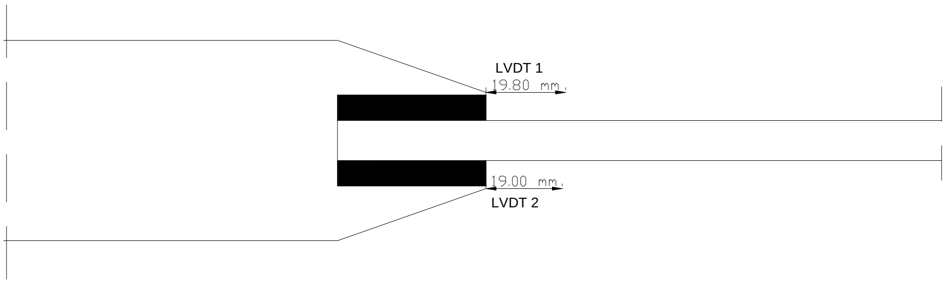

Figure 3.8: LVDT positions

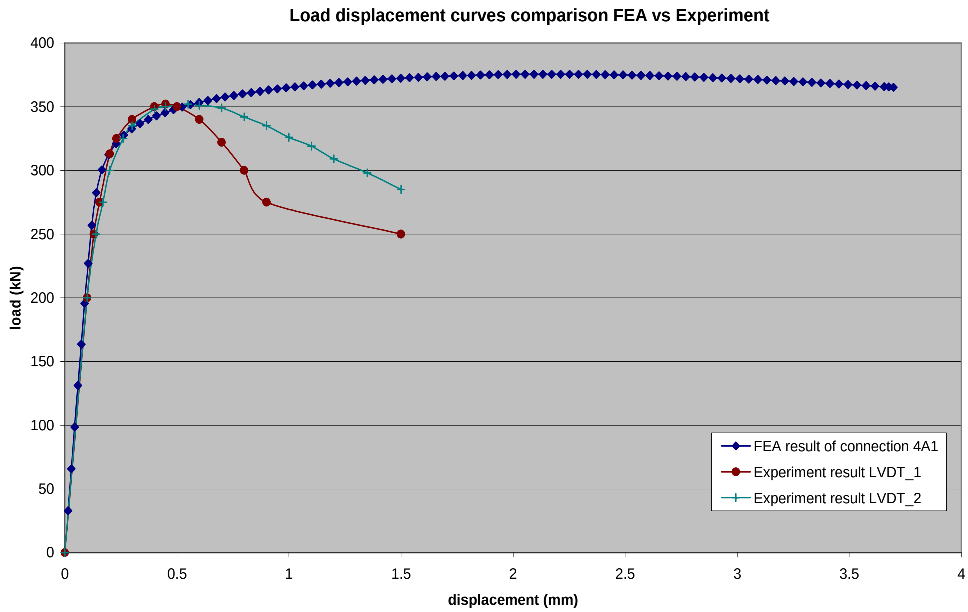

Figure 3.9: Comparison of FEA result and experiment result

The result presented in Figure 3.9 shows that the FEA result only matches to that of experiment result in the elastic and partly elastic plastic region. After that region the result show some differences. The first notably difference can be seen in the load capacity of the connection. Based on the experiment, the maximum load capacity which can be taken by the connection is 352 kN. On contrary it is 375 kN which can be taken by the connection based on FEA. Such a difference of approximately 6% is assumed to be negligible. Secondly, the FEA result shows that the connection has much more ductility compared to that of the experiment result. The main reasons why there are differences in the area after elastic region are the fact that in the real model there are so many influencing parameters and imperfections which occur in the weld that are not accurate taken into account in the FE model for instance, shrinkage of the weld, post heat treatment, the influence of HAZ, geometry of the weld and etc.

Furthermore, Lemaitre criterion is calculated in order to determine the failure load corresponding to the occurrence of the first failure in each connection. A curve which is called master curve that gives limitation of failure is made. Several nodes in the connection especially those which give significant indication where failure starts is investigated.

For connection type A1, these failure loads will be compared to see the difference between the experimental results and the FE analysis results.
Lemaitre criterion is used according to the following formula [5].

$$\varepsilon_{\mathrm{f}} = \frac{\varepsilon_0}{\frac{9}{2}\frac{1-2\nu}{1+\nu}\left(\frac{\sigma_h}{\sigma_{eq}}\right)^2 + 1} \tag{4.1}$$

Where:

$\sigma_h = \frac{1}{3}(\sigma_1 + \sigma_2 + \sigma_3)$ → Isotropic stress

$\sigma_{eq} = \sqrt{\sigma_1^2 + \sigma_2^2 + \sigma_3^2 - \sigma_1\sigma_2 - \sigma_2\sigma_3 - \sigma_3\sigma_1}$ → Von Mises yield criteria

$\varepsilon_0 = 1.0$

With σ_h / σ_{eq} is the so-called tri-axiality.

For ε_0 value, in this project it is taken 1.0 however the value of ε_0 can varied for different type of steel as reported in [11]. The master curve of Lemaitre criterion for ν=0.3 is shown in Figure 3.10. The equivalent plastic strain $\varepsilon_{eq,p}$ in the Figure 3.10 is the accumulated plastic strain. The complete formula for this term in ANSYS is given in Appendix E. In addition, Figure 3.10 also shows that this curve depends strongly upon triaxiality ratio.

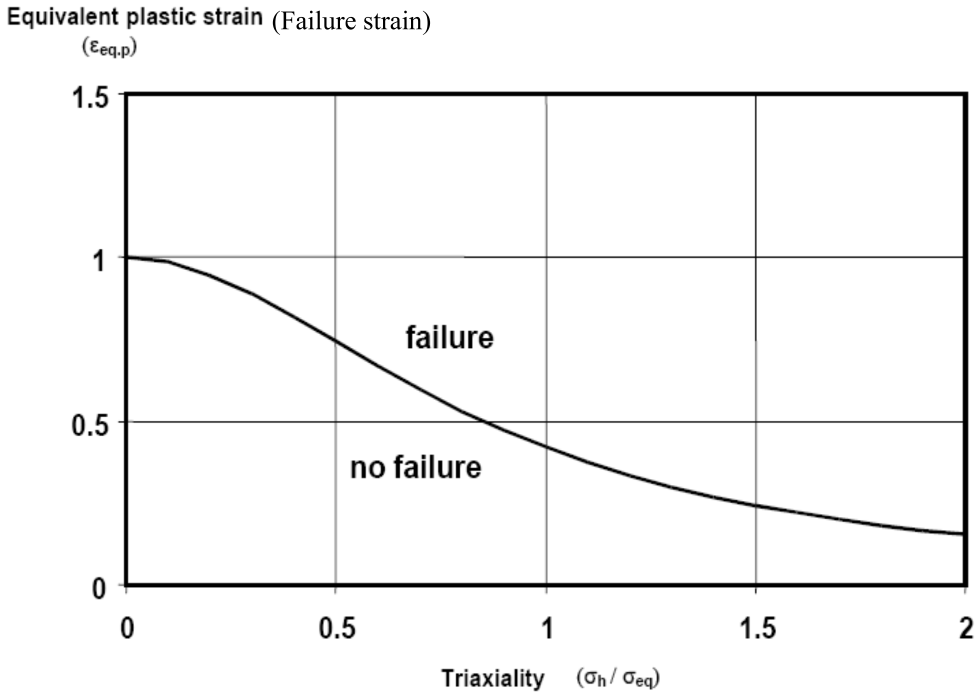

Figure 3.10: Master curve of Lemaitre failure criterion for ν=0.3

The Lemaitre criterion is checked for this type of connections to determine at which point the failure of this connection started. The node labels for which the Lemaitre criterion is investigated are shown in Figure 3.11. These nodes are selected because based on FEA results they give indication of failure based on accumulated plastic strain which occur in the nodes.

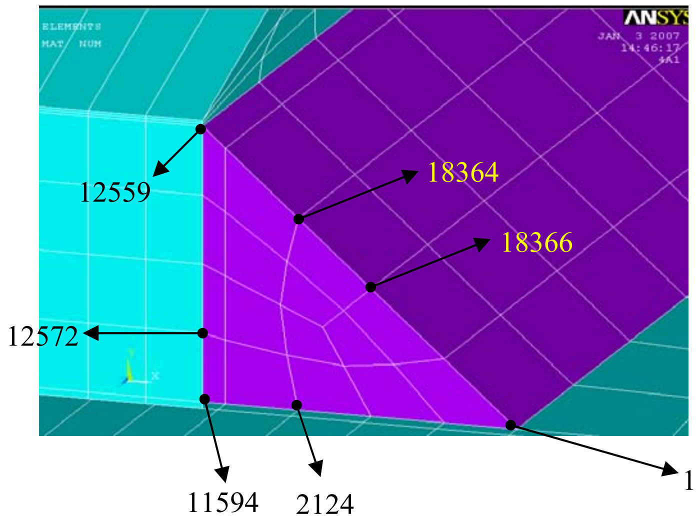

Figure 3.11: Nodes where Lemaitre criterion is checked

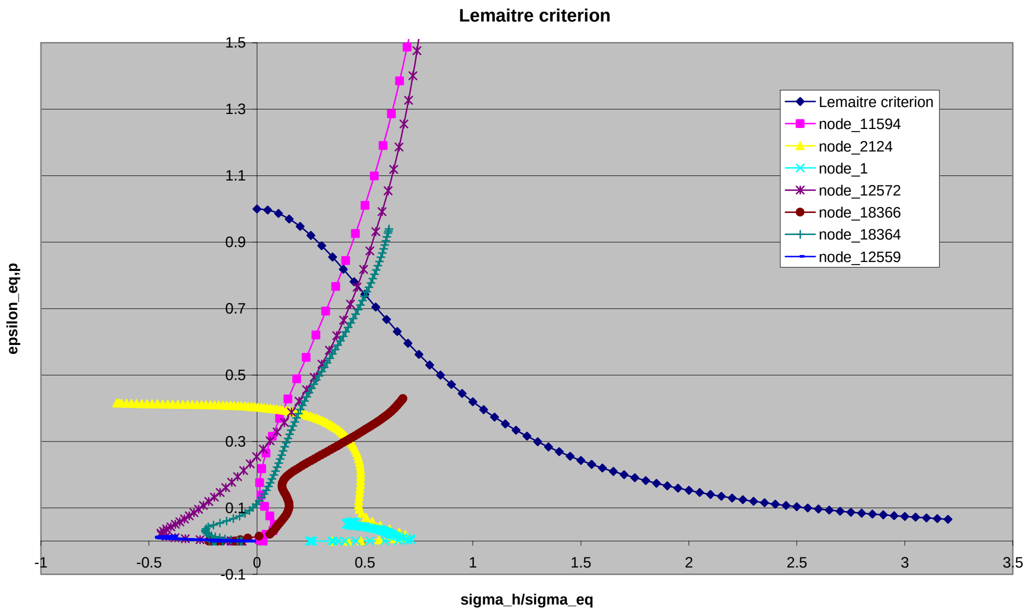

Figure 3.12: Lemaitre criterion

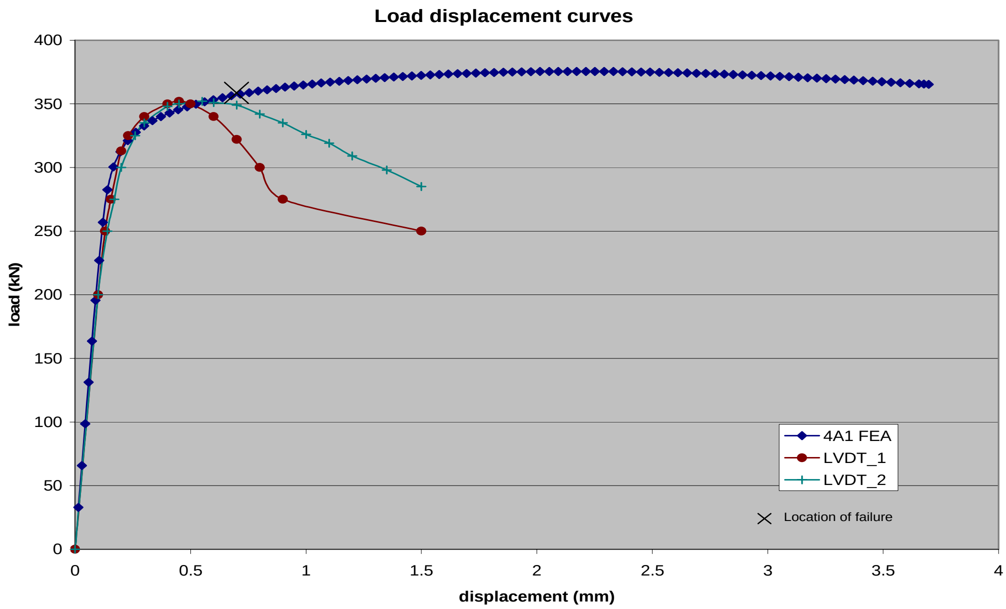

Figure 3.13: Location where failure started

According to Figure 3.12 the failure of the connections started from the weld root and expanded to the face of the weld (it is also validated as shown in Figure 3.14). This failure starts to occur at load step 25 out of 101 load steps. There are no failures at the weld toe. Furthermore, based on this criterion the place where failure starts to occur is plotted in the load displacement curve as shown in Figure 3.13. Apparently, this location is almost the same to that location where failure starts to occur in the connection of the experiment result. Finally, the corresponding failure load based on Lemaitre criterion for this connection is 356 kN.

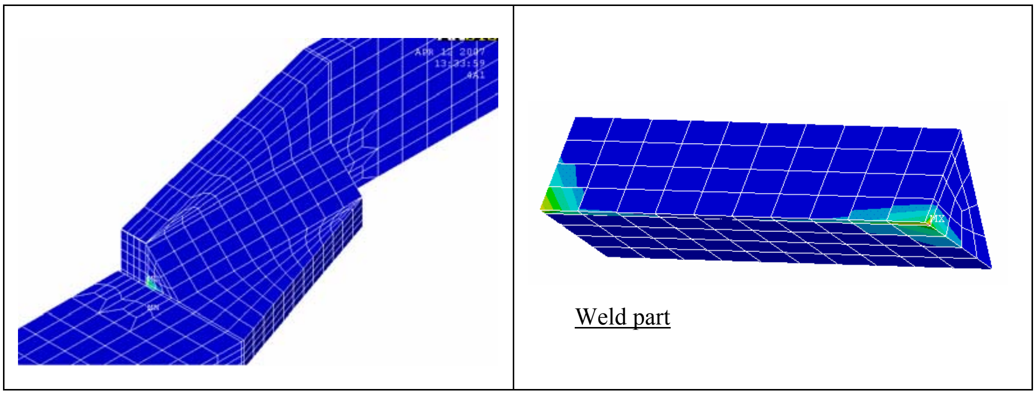

Figure 3.14: Contour plot of equivalent plastic strain at load step 25

2. Connection type 5A1

Once more convergence test is done firstly to determine the size of element which will be used later in the analysis for this type of connection. This test consists of test based on element size and test based on calculation time. The results of the analysis are shown in Table 3.2 and Figure 3.16.

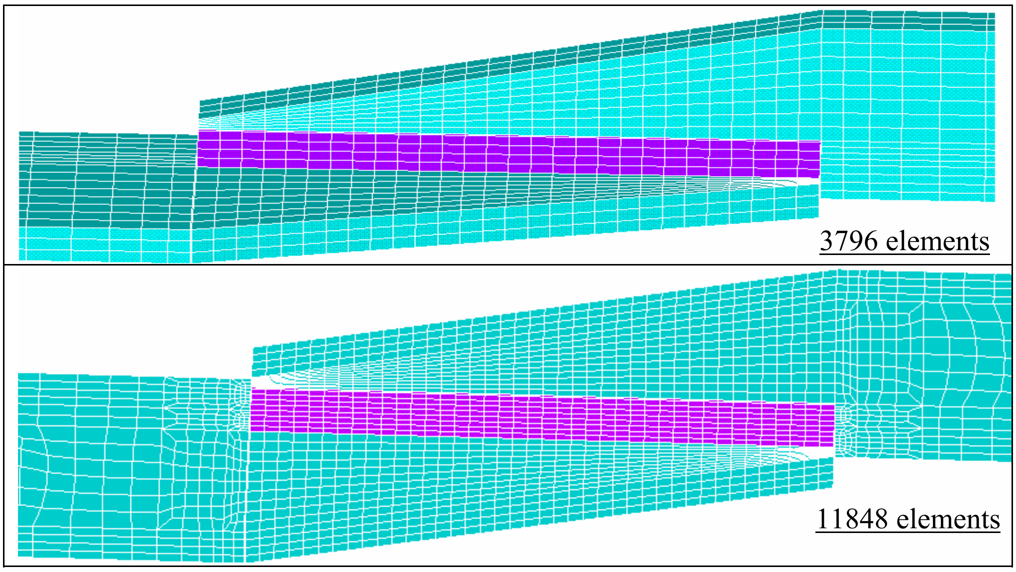

Figure 3.15: Type of mesh

Table 3.2 Convergence test results

No.	Number of element	Calculation time (Modern PC)
1.	8 nodes brick element (3796 elements)	24 minutes
2.	20 nodes brick element (3796 elements)	3 hours 34 minutes
3.	8 nodes brick element (11848 elements	3 hours

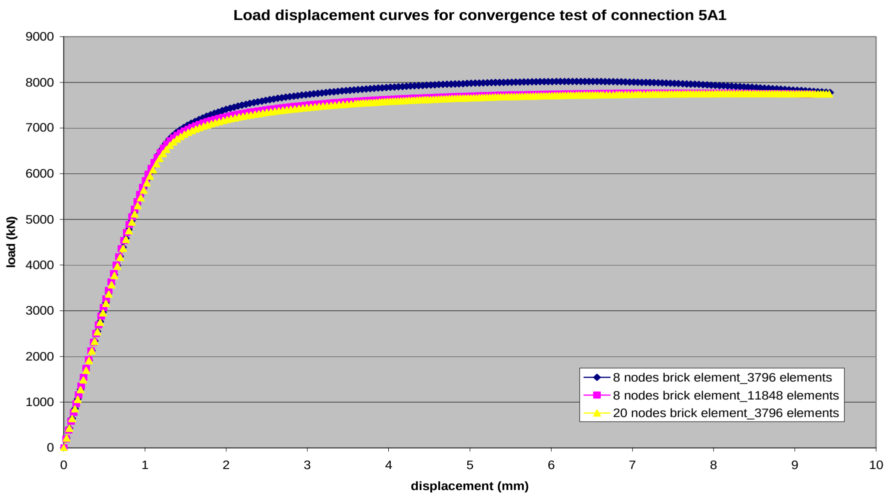

Figure 3.16: Convergence test results

From Figure 3.16 it can be seen that by using 20 nodes element, the convergence is faster to achieve compare to that of using 8 nodes element. In addition based on Table 3.2, for less number of elements 20 nodes element gives almost the same result in comparison to that of 8 nodes element with not so much difference in computation time.

To validate the FE analysis a comparison to the experimental results [6] is made. The result of the related connection from [6] (at LVDT positions which is shown in Figure 3.17) is replotted then it is compared to the FE analysis result. The result of this comparison is given in Figure 3.18.

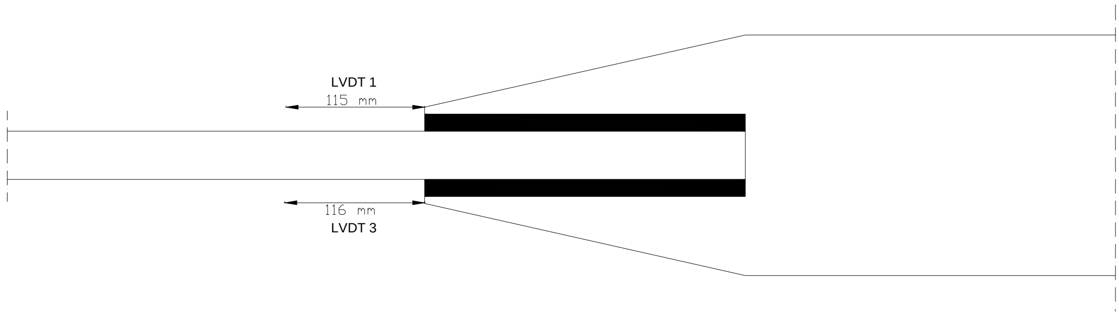

Figure 3.17: LVDT positions

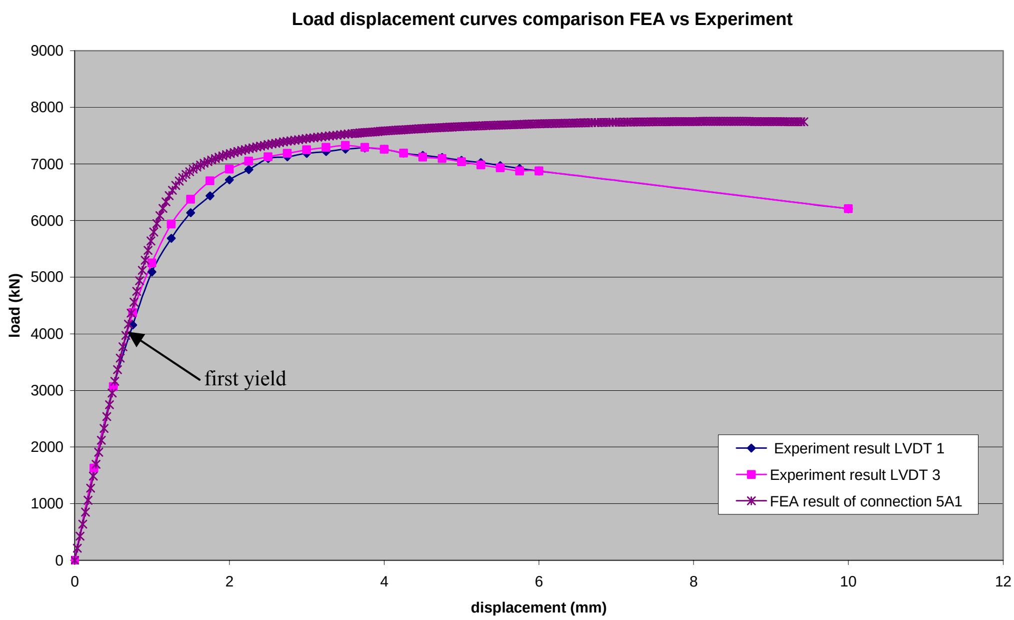

Figure 3.18: Comparison of FEA result and experiment result

The result presented in Figure 3.23 shows that the FEA only matches to that of experiment result in the elastic region. After this region the results show differences. First difference can be seen in the load capacity of the connection. Based on the experiment, the maximum load capacity which can be taken by the connection is 7300 kN. On contrary it is 7751 kN which can be taken by the connection based on FEA. Secondly, the FEA result shows that the connection has more ductility capacity compare to that of the experiment result has. The location where first yield occur in the connection is also shown in Figure 3.18. This yield load corresponds to approximately 50% of the failure load.

For determining the failure load of this connection, Lemaitre criterion is adopted. The node where Lemaitre criterion is investigated is shown in Figure 3.19.

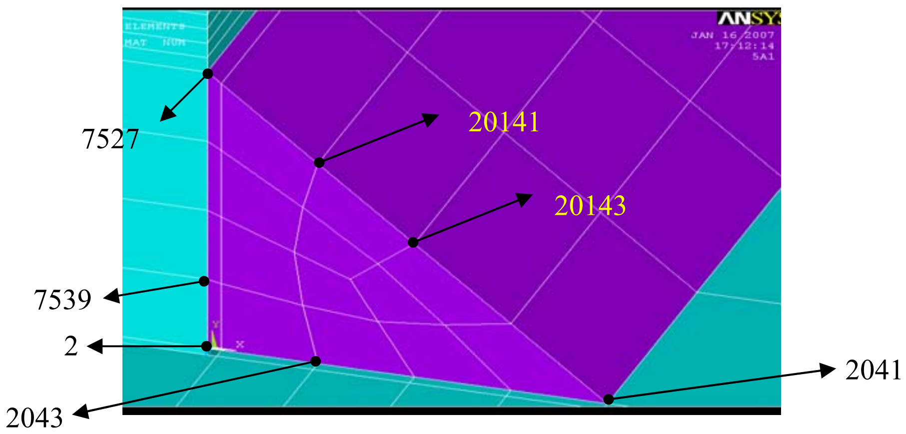

Figure 3.19: Nodes where Lemaitre criterion checked

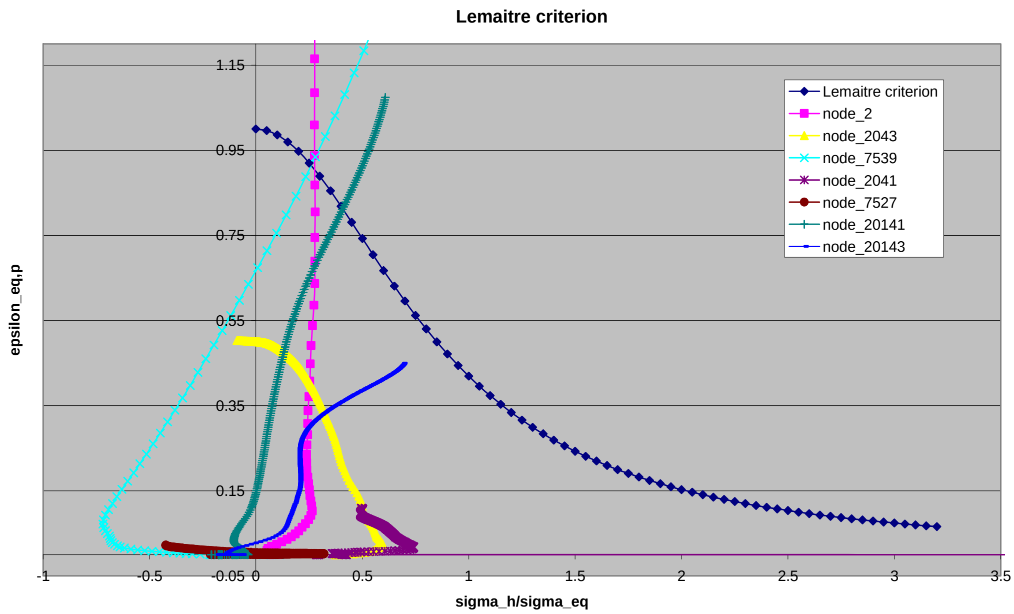

Figure 3.20: Lemaitre criteria

Figure 3.20 shows the state of failure of each node which is investigated. The nodes which pass the master curve of Lemaitre criterion is called starting to fail. The corresponding sub-step for each node at which the failure start is determined. Then the corresponding failure load can be determined correspond to this sub-step.

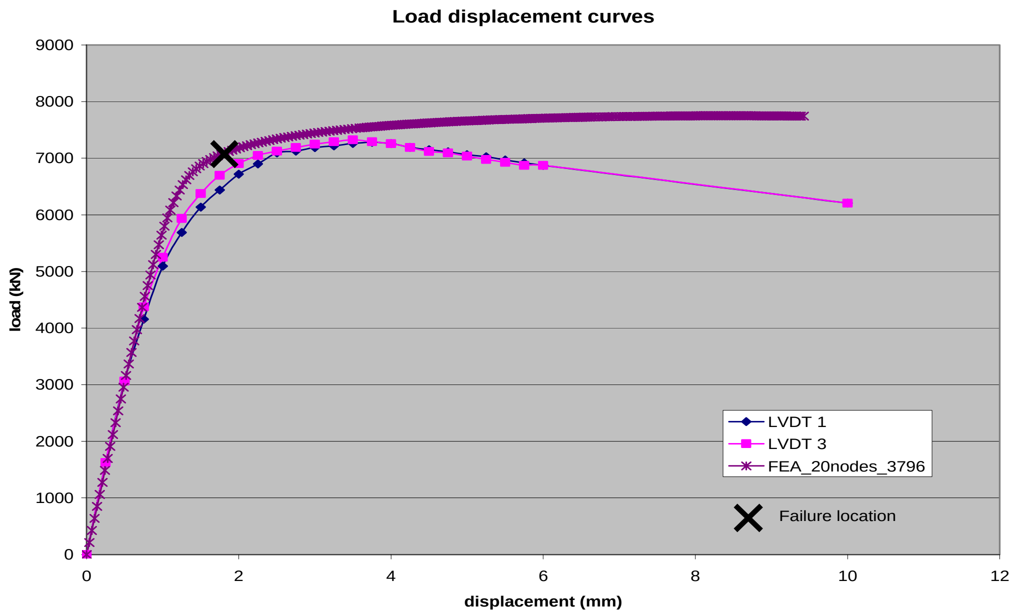

Figure 3.21: Location of failure load

According to Figure 3.20 the failure of the connections started from the weld root. There are no failures occur at the weld toe. This failure starts to occur at load step 45 out of 256 load steps. Furthermore, based on this criterion the place where failure starts to occur is plot in the load displacement curve as shown in Figure 3.21. Based on this figure the maximum load where the failure start is 7050 kN which is less than that of experiment results.

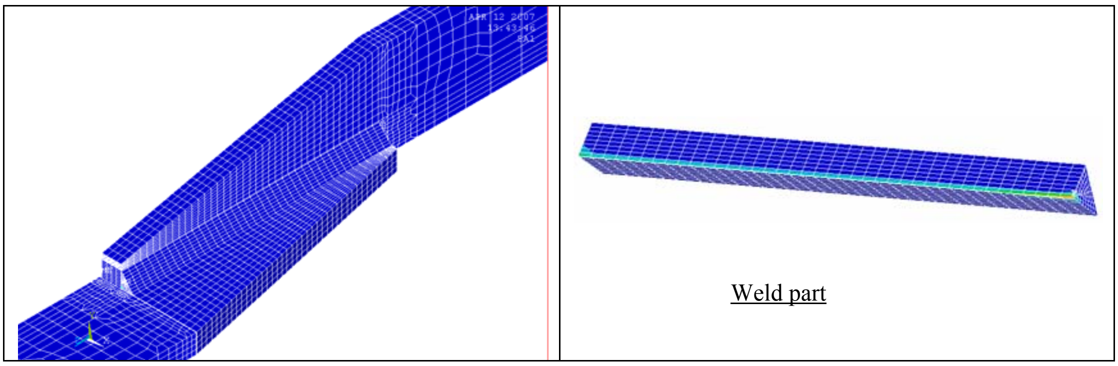

Figure 3.22: Contour plot of equivalent plastic strain at load step 45

In figure 3.22 the equivalent plastic strain contour plot is shown. It shows the state of plastic strain at load step 45 which is the step where failure start based on Lemaitre criterion. The plastic strain starts to grow from the weld root which implies that failure start in this connection at this place.

3.2.1.2 Connections type 2

Connection type 2 is a welded connection loaded by tension only. This load causes normal stress and shear stress in the weld. The geometry of this connection which is named connection 2A and connection 3A is shown in Figure 3.23. The differences of the two are in the plate thickness and in the weld throat size. Connection 2A consists of plate material with 10 mm thickness and 4.5 mm fillet weld and connection 2B has plate material thickness 40 mm with 10 mm fillet weld. Figure 3.23 also shows the part of the geometry which is modelled and in this case only one fourth of the connection which is modelled because of symmetry in geometry and loading.

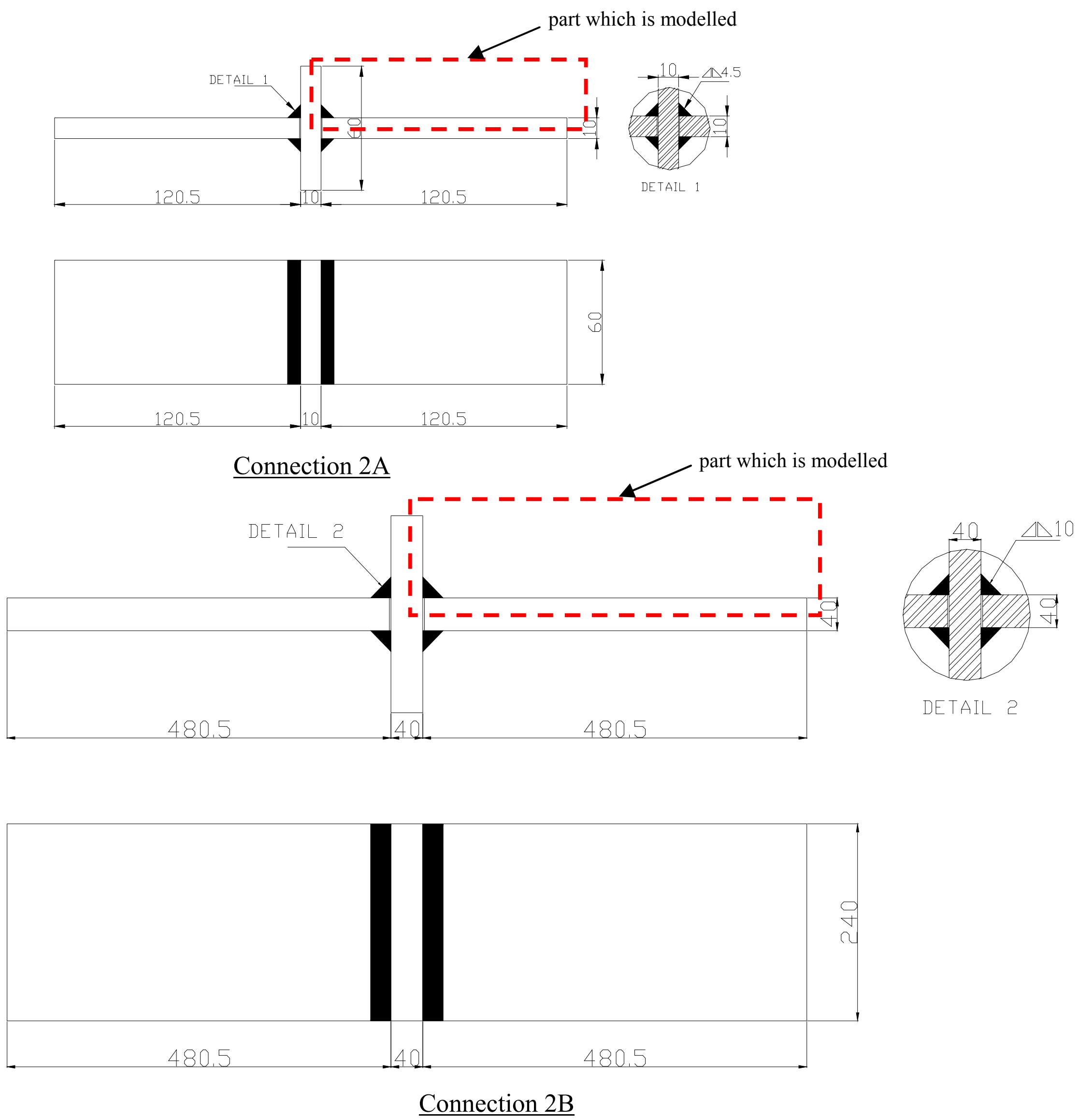

Figure 3.23: Geometry of connection type 2

For finite element modelling of connection 2A and 2B, the same material properties to that of connection type 4A and type 5A are applied respectively. Also the same procedure to the previous analysis is adopted. The boundary conditions for this connection are given in Figure 3.24. Displacement control is used for the loading which is increased gradually in order to get rid of convergence problem. This load is applied in the area where later on is transferred to the nodes before the analysis started.

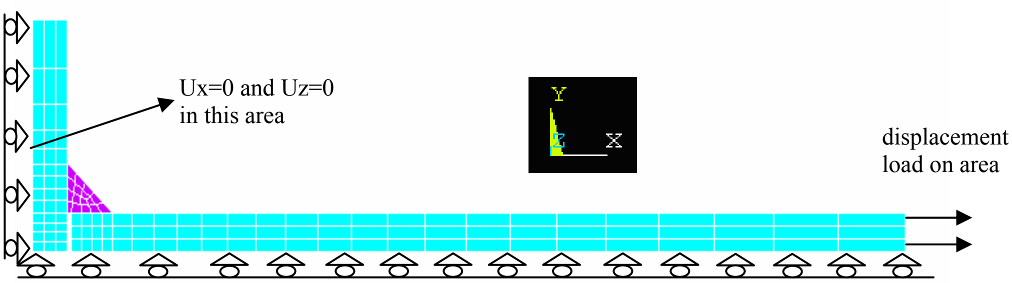

Figure 3.24: Boundary conditions

1. Connection 2A

Firstly, a convergence test is performed by varying the mesh which varied from coarse mesh to fine mesh and also test is done using 2 different types of element (8 nodes brick element and 20 nodes brick element). The mesh variations are shown in Figure 3.25 which also shows the number of elements in each mesh.

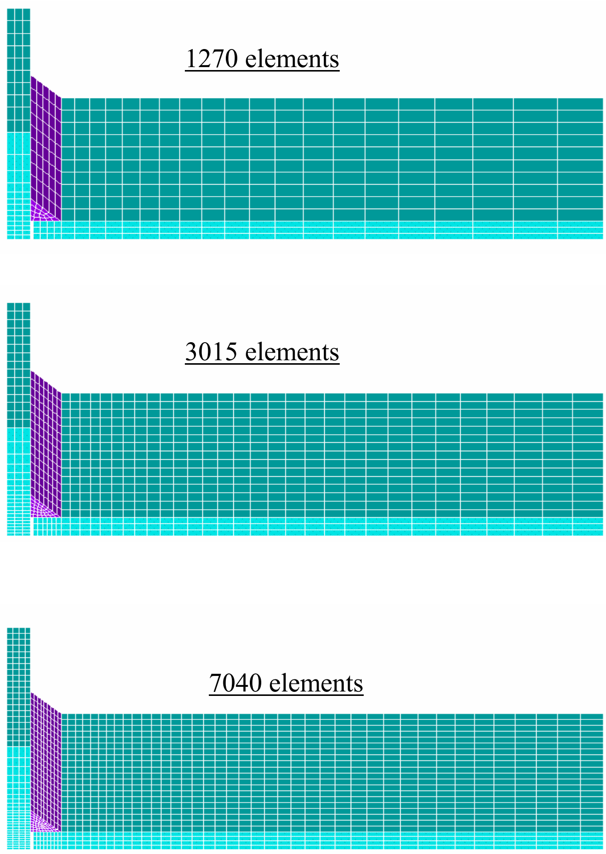

Figure 3.25: Types of mesh

The results of convergence test are given in Table 3.3 and Figure 3.26. Table 3.3 gives the computation time which is needed for each mesh. It is clear that the computational time increases as the number of nodes increased. Figure 3.26 shows the load displacement curve for each mesh. It can be seen that the higher order element gives smaller results in terms of failure load compare to smaller order element. In Figure 3.26 also can be seen that there is a locking problem during the analysis using 8 nodes brick element because the shape of the load displacement curves using this type of element differ remarkably to that of 20 nodes brick element has. Additionally, In order to see this problem more clearly, equivalent von Mises stresses for each mesh are plotted and it is shown in Figure 3.27. This contour plot is taken at sub-steps 21 for each mesh.

Table 3.3 Convergence test results connection type 2A

No.	Type of element	Calculation time
1.	8 nodes brick element (1270 elements)	1 minute 37 seconds
2.	20 nodes brick element (1270 elements)	9 minutes 35 seconds
3.	8 nodes brick element (3015 elements)	5 minutes 36 seconds
4.	20 nodes brick element (3015 elements)	35 minutes 56 seconds
5.	8 nodes brick element (7040 elements)	17 minutes 18 seconds
6.	20 nodes brick element (7040 elements)	2 hours 57 minutes and 40 seconds

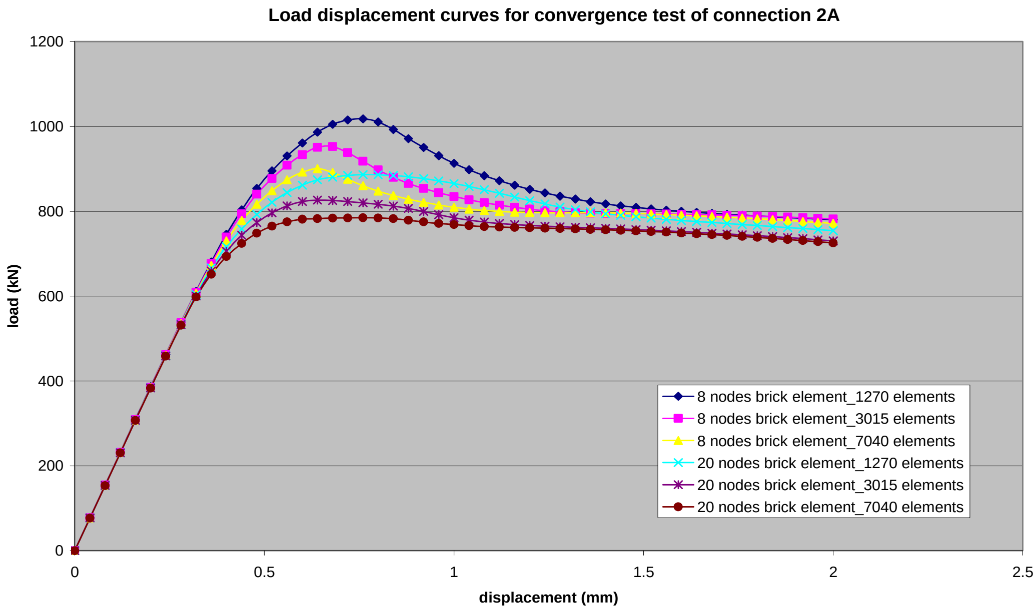

Figure 3.26: Convergence test results of connection 2A
(Selective reduced integration scheme is used for SOLID185 element)

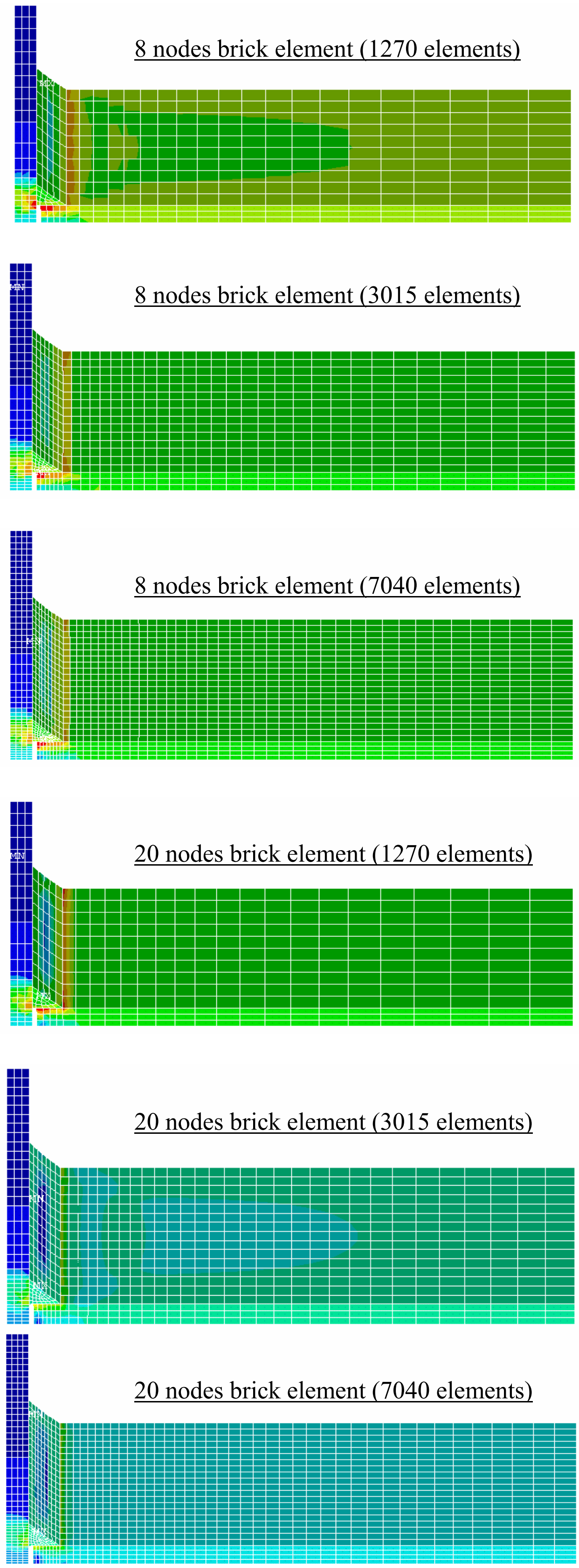

Figure 3.27: Equivalent Von Mises stress contour plot

Moreover, to investigate the problem which arises during convergence test particularly using 8 nodes brick element, sensitivity checked is performed by changing the type of integration point for this type of element. The type of integration point which is used is the enhanced strain formulation with 13 integration points replacing the selective reduced integration scheme which is used in previous analysis. The results of this analysis are given in Figure 3.28.

Several conclusions can be drawn based on Figure 3.28. Firstly, by using enhanced strain integration scheme result in almost the same shape of load displacement curve compare to that of 20 nodes brick element has. This is implies that locking problem which occur in the previous analysis is solved by using this integration point scheme. Secondly, it is visible in Figure 3.28 that the finer the mesh the less the plastic deformation which occurs in the connection. This is related to convergence problem which occur during the analysis where some of the elements experience turning inside out (overlapping between nodes at highly distorted condition).

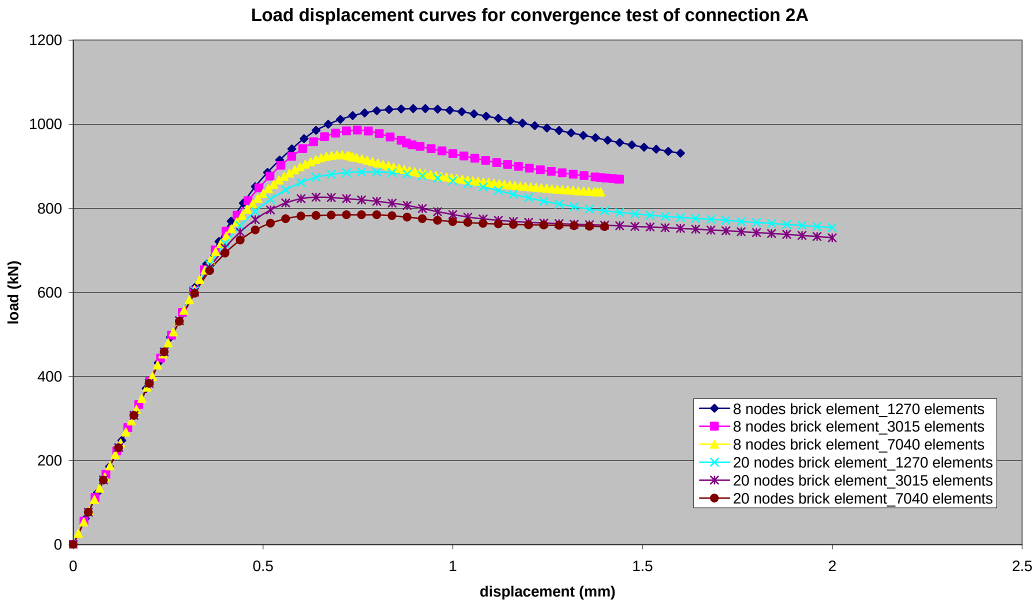

Figure 3.28: Convergence test results of connection 2A
(Enhanced strain integration scheme is used for SOLID185 element)

Finally, based on these results the 20 nodes brick element with 3015 number of elements is taken as the basis model for the next analysis of this type connection. The main reasons are because this model can converge quite fast to the solution, does not need longer calculation time and there is no locking problem encountered during the analysis.

The failure load should be calculated for the model which has been chosen based on convergence test. The Lemaitre criterion once again is adopted. Several numbers of nodes are checked in the weld location in order to know when failure starts to occur in the connection. These nodes are shown in Figure 3.29. These nodes are chosen because they give indication that failure start from their position and it can be seen clearly in the finite element model through the plot of the equivalent plastic strain of the nodal solution.

Figure 3.30 shows the plot of Lemaitre criterion for each node. The line which passed the master curve of the criterion is said starting to fail. For this case node 1731 which is located very close to the weld root is the part which fails first. This failure corresponding to sub-step 28 out of 50 sub-steps in the analysis.

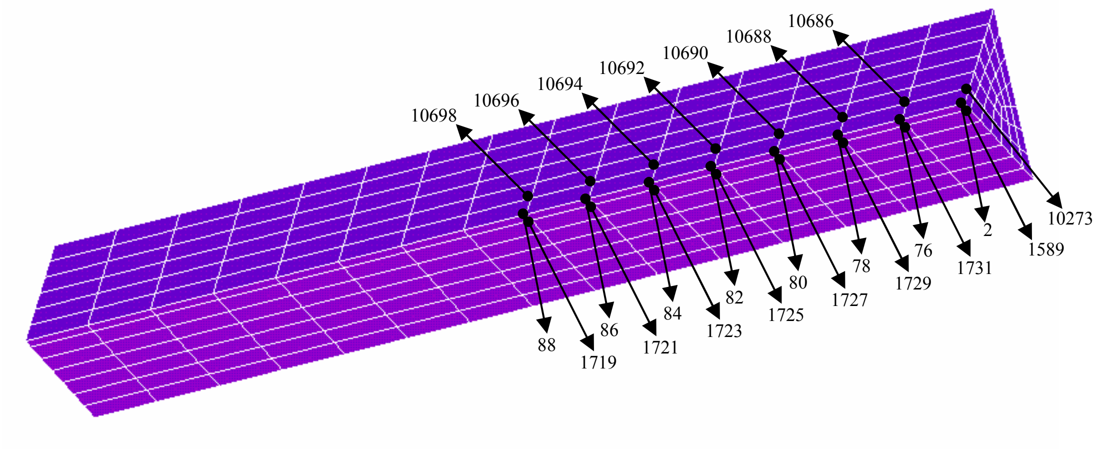

Figure 3.29: Nodes location where Lemaitre criterion is checked

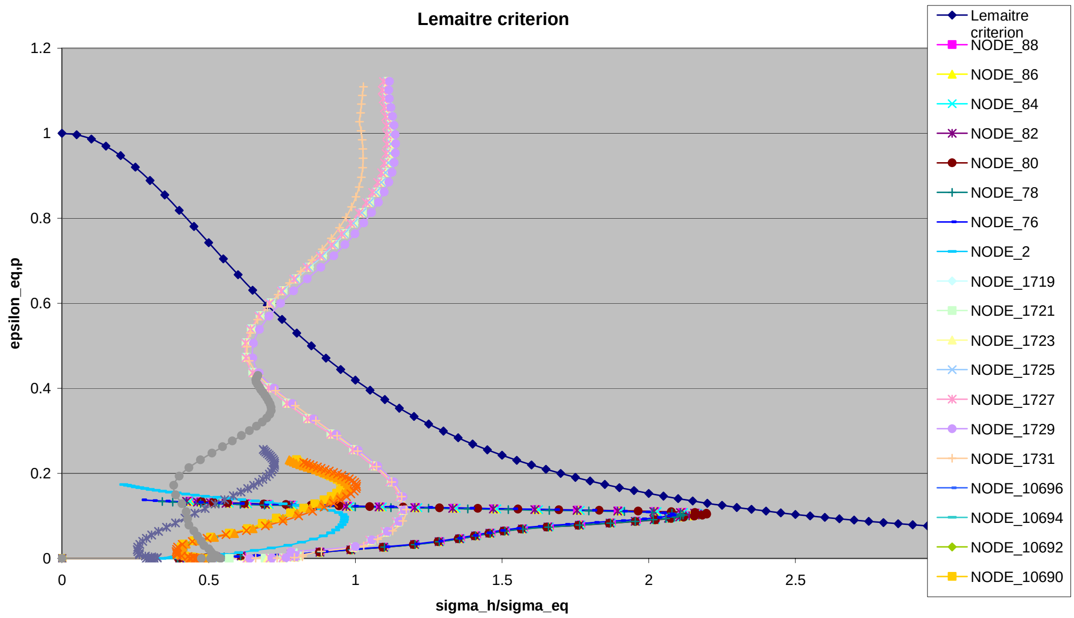

Figure 3.30: Lemaitre criteria

Furthermore, the load displacement curve which represents the response of this connection is plotted. The displacement is measured at distance 5t from the weld toe in order to have a global response where no influence of stress concentration. Subsequently the corresponding load step based on Lemaitre criteria is plotted in this curve in order to get the failure load of this connection. Figure 3.31 shows the result of this procedure and the failure load of this connection is 771 kN however this value cannot be used as the failure load because as can be seen the predicted failure load occur in the location after the maximum load in the load displacement curve. Consequently the maximum failure load 826 kN is used for this connection.

Figure.44 Lemaitre criteria

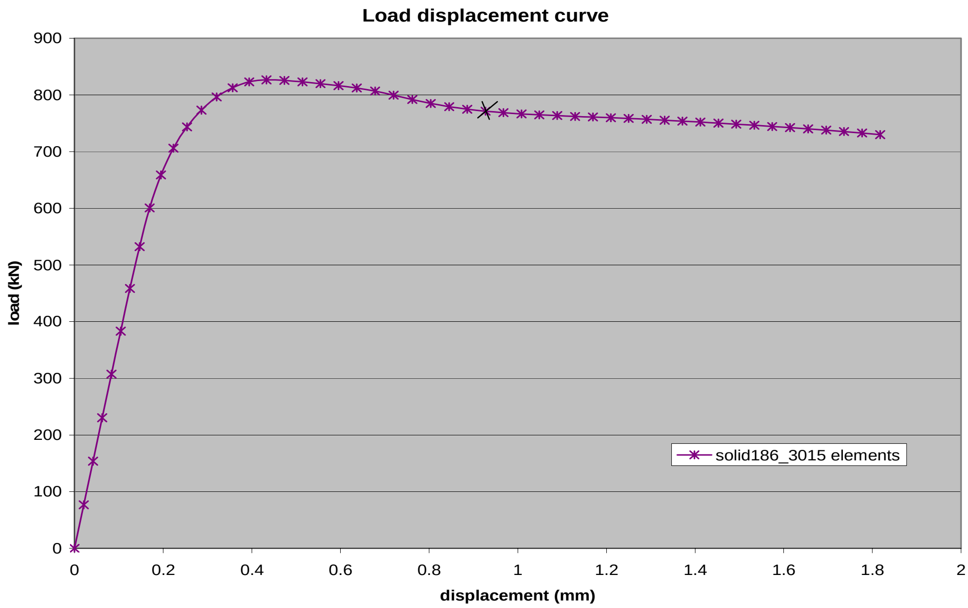

Figure 3.31: Position of failure load based on Lemaitre criterion

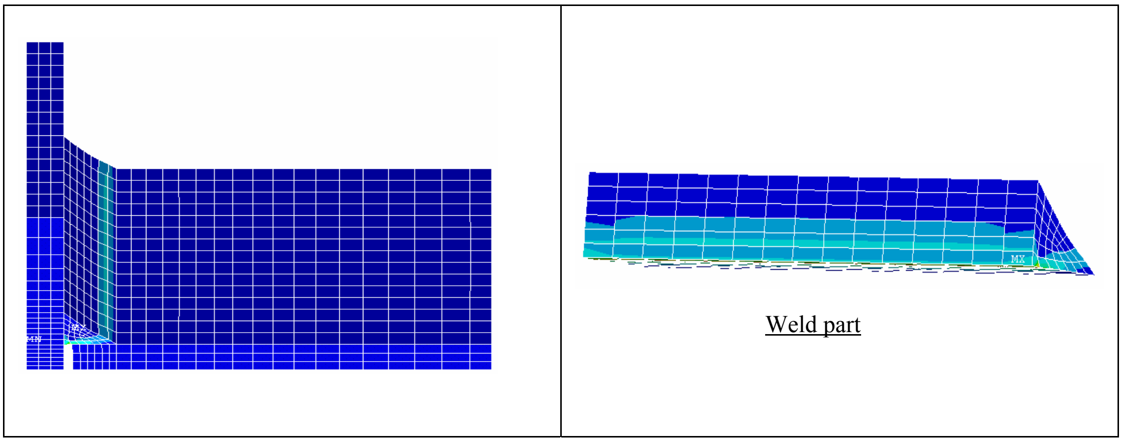

Figure 3.32: Contour plot of equivalent plastic strain at load step 28

Figure 3.32 shows the equivalent plastic strain of the connection at sub-step 28 out of 50. Based on this figure, the failure of the connection starts from the weld root which is indicated by the accumulation of the plastic strain in this location.

2. Connection 2B

The same procedure step to that of connection 2A is applied in modelling this connection. First the convergence test is done and Figure 3.33 shows the variation of the mesh.

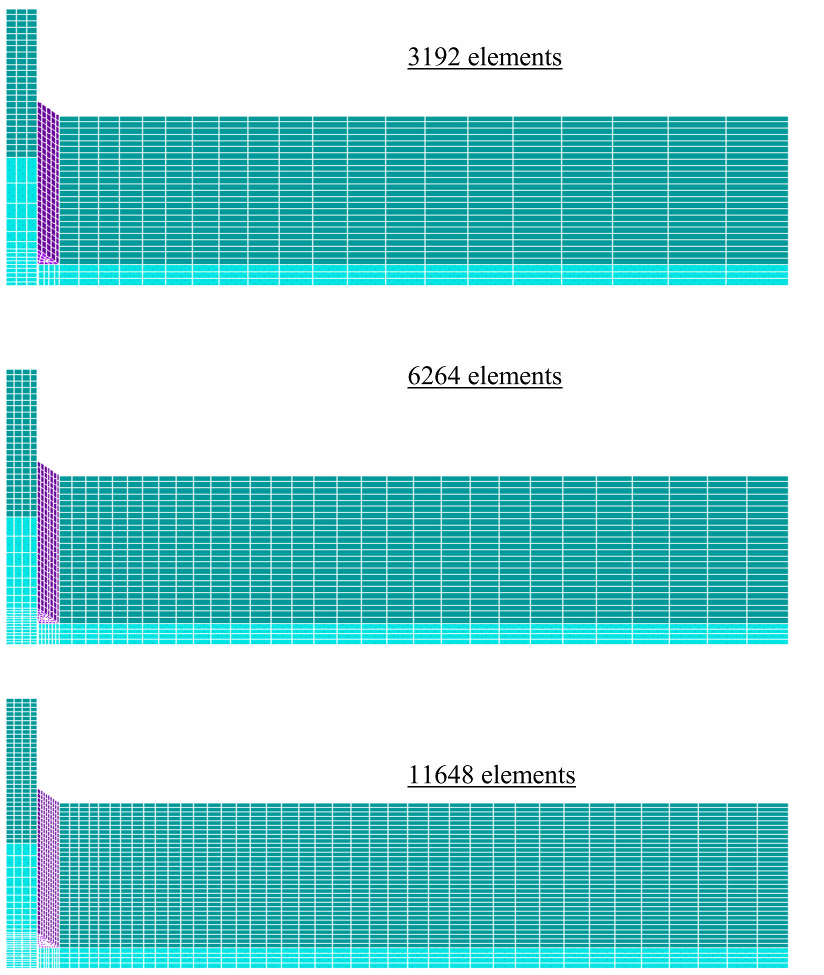

Figure 3.33: Types of mesh

The result of this test is given in Table 3.4 and Figure 3.34. Based on this result, the 20 nodes brick element with 6264 number of elements is used as the basis model for further analysis. In addition, the same phenomena occur in this convergence test for 8 nodes brick element that is locking as can be seen in Figure 3.34.

Table 3.4 Convergence test results connection type 2B

No.	Number of element	Calculation time (Modern PC)
1.	8 nodes brick element (3192 elements)	10 minutes 55 seconds
2.	20 nodes brick element (3192 elements)	52 minutes 59 seconds
3.	8 nodes brick element (6264 elements)	27 minutes 7 seconds
4.	20 nodes brick element (6264 elements)	3 hours 59 minutes and 12 seconds
5.	8 nodes brick element (11648 elements)	51 minutes 31 seconds

The response of the higher order elements show more ductility response compare to the smaller order element has.

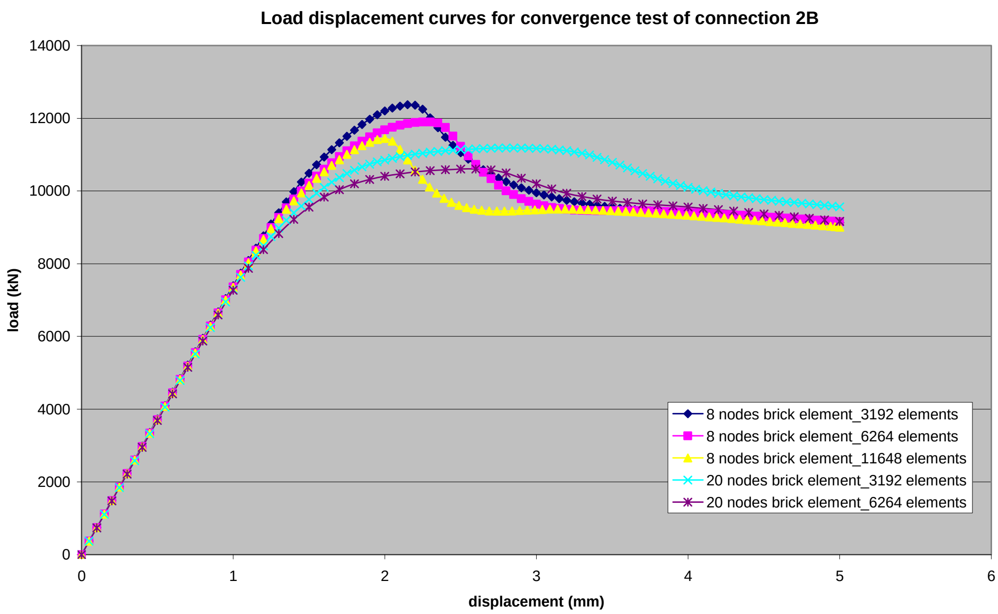

Figure 3.34: Convergence test results of connection 2B
(Selective reduced integration scheme is used for SOLID185 element)

Equivalent von Mises stress contour plot is shown in Figure 3.35 for each mesh. This plot is based on result at sub-step 44 for all mesh except for 20 nodes brick element with 6264 elements which is plot at sub-step 33.

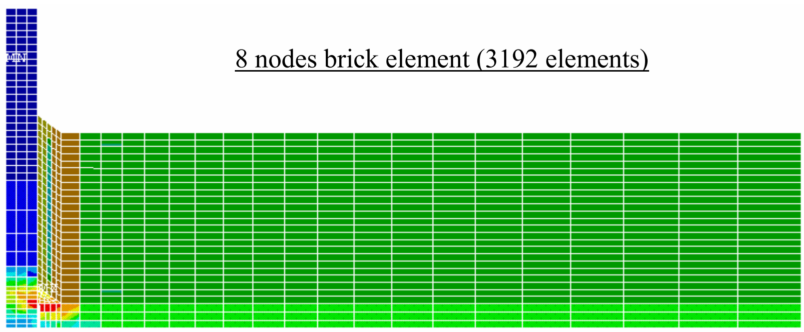

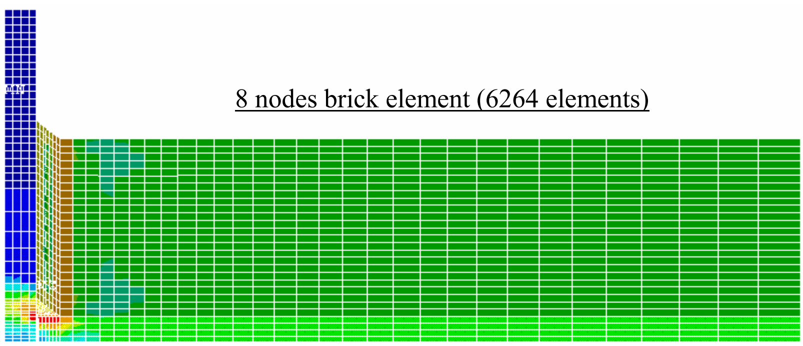

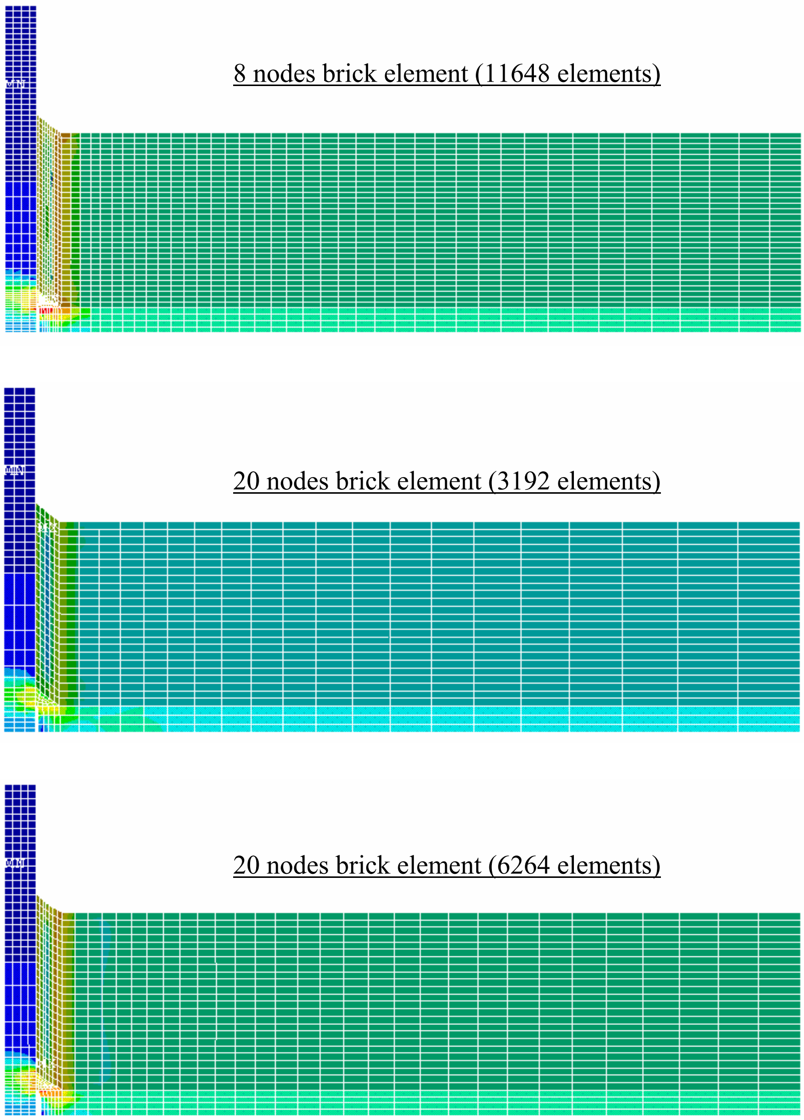

Figure 3.35: Equivalent Von Mises stress contour plot

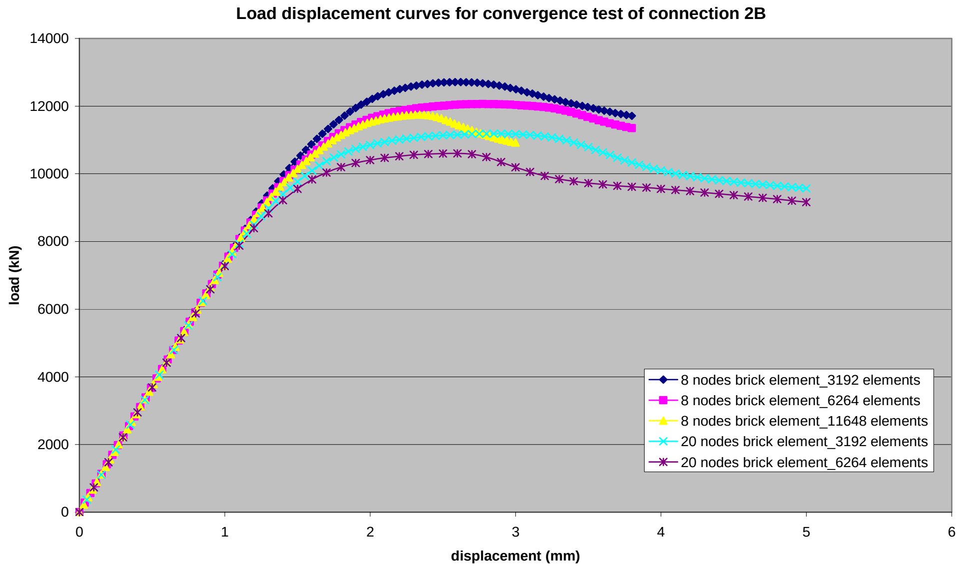

Figure 3.36: Convergence test results of connection 2B
(Enhanced strain integration scheme is used for SOLID185 element)

Due to locking problem which occur in the first convergence test another test for 8 nodes brick element using enhanced strain integration scheme is performed and the result is shown in Figure 3.36. The conclusion which can be drawn from this result is the same to that of previous analysis for connection 2A.

To determine the failure load of this connection, Lemaitre criterion is calculated for several nodes which are located in the region that show indication of failure. These nodes are shown in Figure 3.37. The corresponding Lemaitre criteria for each node are presented in Figure 3.38. Based on this figure, node 3834 is the the node location where failure starts to occur and corresponding to sub-step 20 out of 50 sub-steps.

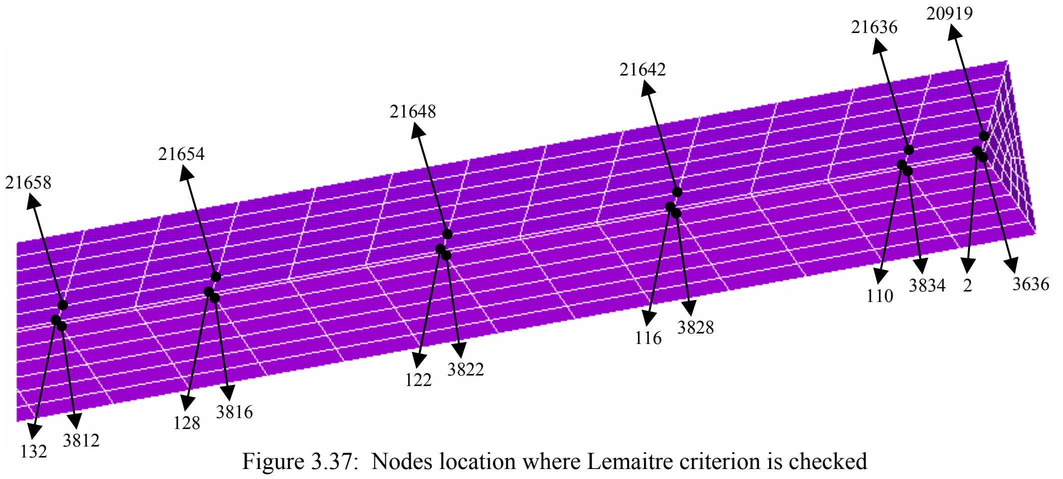

Figure 3.37: Nodes location where Lemaitre criterion is checked

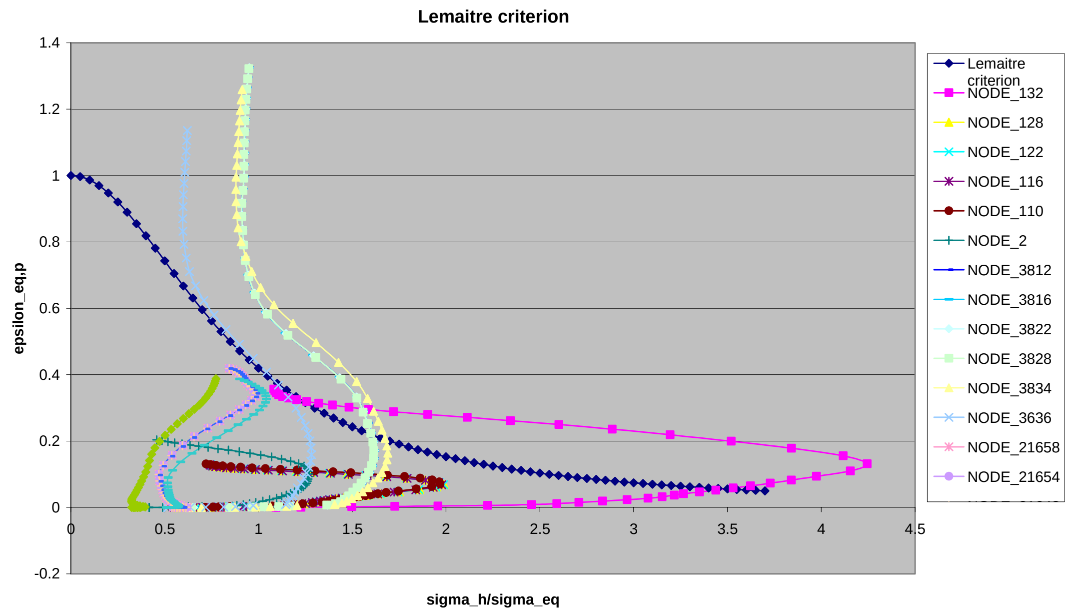

Figure 3.38: Lemaitre criteria

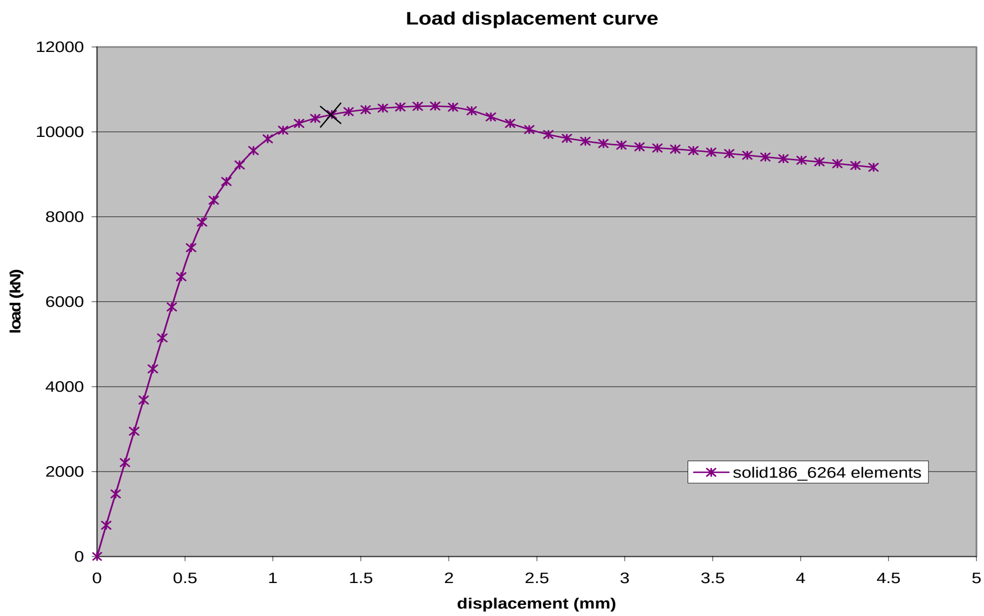

Figure 3.39: Location of failure load

Moreover, the load displacement curve which represents the response of this connection is plotted. The displacement is measured at distance 5t from the weld toe in order to have a global response where no influence of stress concentration. Subsequently the corresponding load step based on Lemaitre criteria is plotted in this curve in order to get the failure load of this connection. Figure 3.39 shows the result of this procedure and the failure load of this connection is 10406 kN.

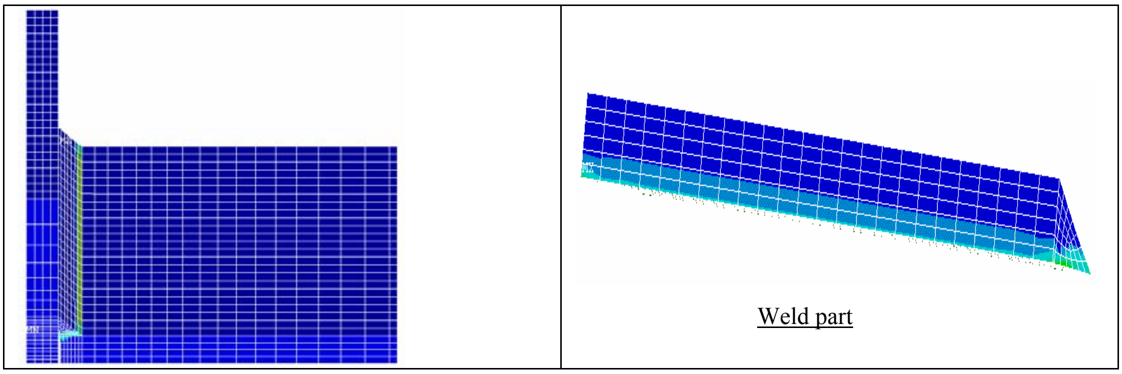

Figure 3.40: Contour plot of equivalent plastic strain at load step 20

Figure 3.40 shows also that the failure of this connection starts from the weld root which indicated by the accumulation of plastic strain in this area.

3.4.1.3 Connections type 3

Connection type is also a connection statically loaded by tension. Geometry of connection type 3 is presented in Figure 3.41. Due to this geometry, there will be three type of stresses occur in the weld that are perpendicular normal stress to the weld, perpendicular shear stress to the weld and parallel shear stress to the weld. In addition, this type of connection has 2 type of geometry with differences in the plate thickness and weld throat size.

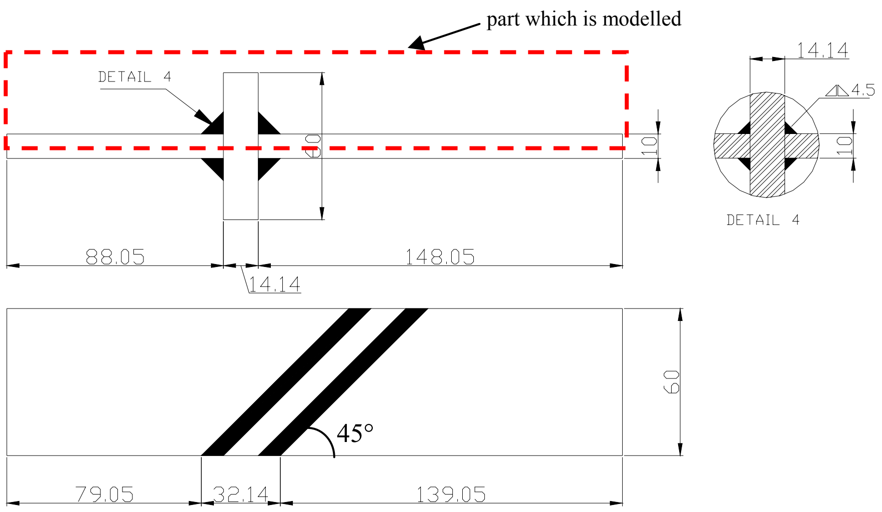

Connection 3A

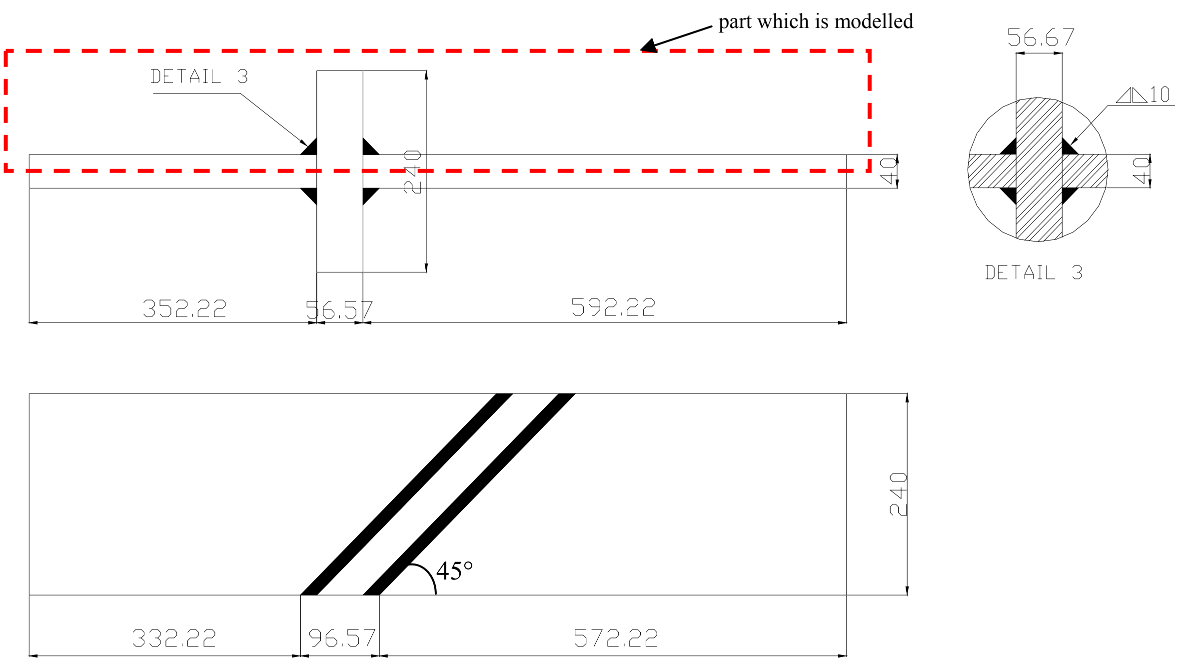

Connection 3B

Figure 3.41: Geometry of connection type 3

The same procedure from previous analysis is used in modelling this connection. A half of this connection will be modelled taking symmetry advantage of geometry and loading. The boundary conditions which are applied to this modelled is shown in Figure 3.42. One end of the connection is clamped and the other side is used to apply the load.

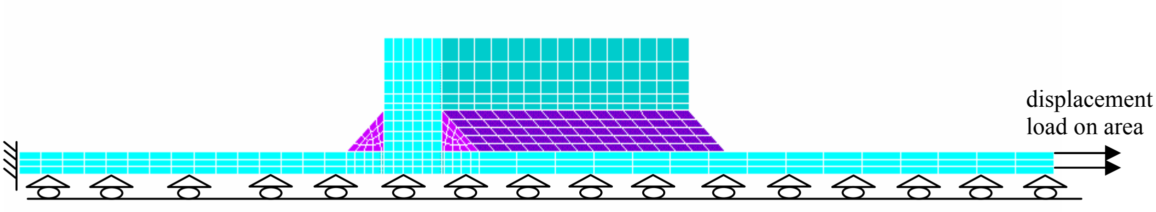

Figure 3.42: Boundary conditions

1. Connection 3A

The procedure in modelling this type of connections is exactly the same to the previous procedure for connection type 2. These are as follow:

1. Perform convergence test

2. Choose the basis model based on convergence test

All the results of this procedure are shown in Table 3.5 and Figure 3.44.

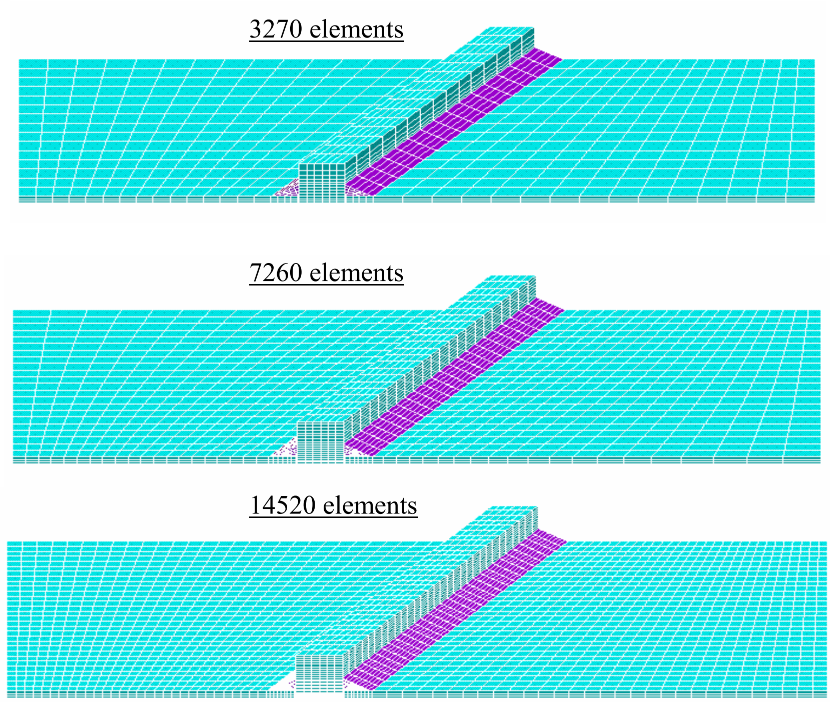

Figure 3.43: Types of mesh

Figure 3.43 shows the types of mesh which are used in convergence test. These meshes start from the coarser mesh to the finer mesh. The numbers of element for each mesh are also indicated in this figure.

Table 3.5 Convergence test results connection type 3A

No.	Number of element	Calculation time (Modern PC)
1.	8 nodes brick element (3270 elements)	3 minutes 25 seconds
2.	20 nodes brick element (3270 elements)	23 minutes 45 seconds
3.	8 nodes brick element (7260 elements)	10 minutes 13 seconds
4.	20 nodes brick element) (7260 elements)	3 hours 28 minutes 3 seconds
5.	8 nodes brick element (14520 elements)	34 minutes 35 seconds

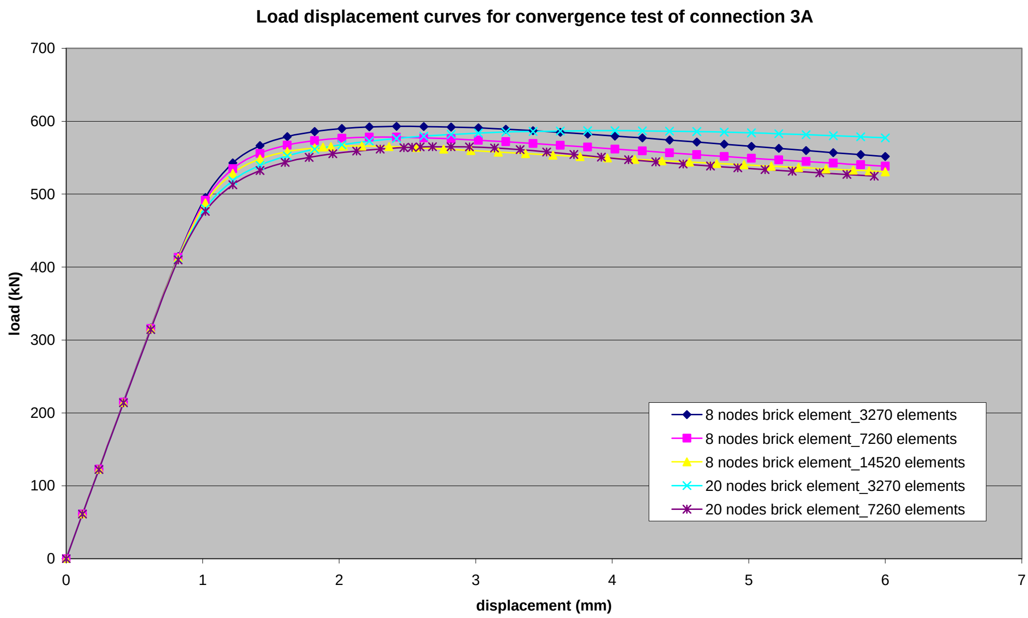

Figure 3.44: Convergence test results of connection 3A

Based on the results in Table 3.5 and Figure 3.44, the type of element which is used for further analysis is 20 nodes brick element with 7260 elements.

In order to determine the failure load for this type of connection, the Lemaitre criterion is adopted. The first step to do is to check this criterion in several nodes in the connection modelled which give indication that failure starts in that location. Figure 3.45 shows the nodes which are investigated. The result of this investigation is shown in Figure 3.46.

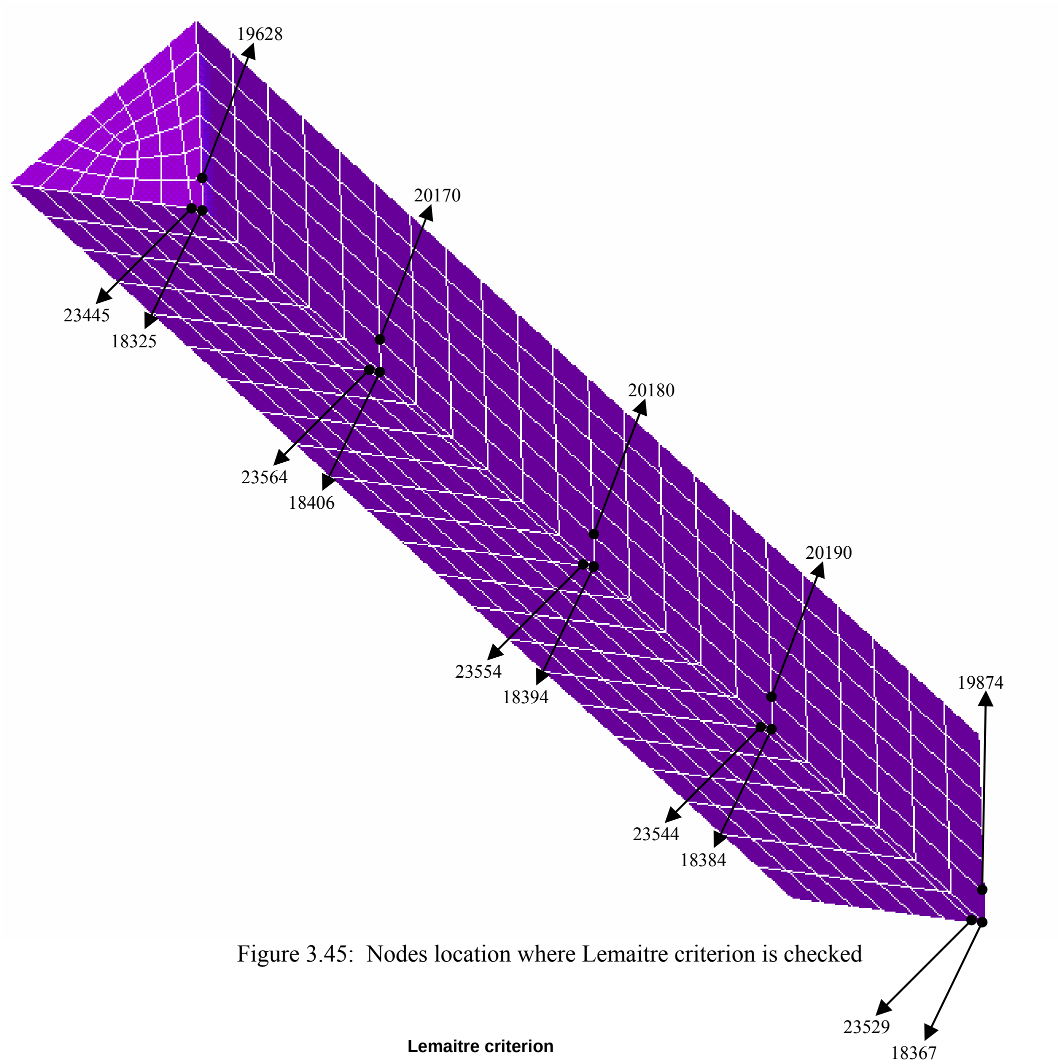

Figure 3.45: Nodes location where Lemaitre criterion is checked

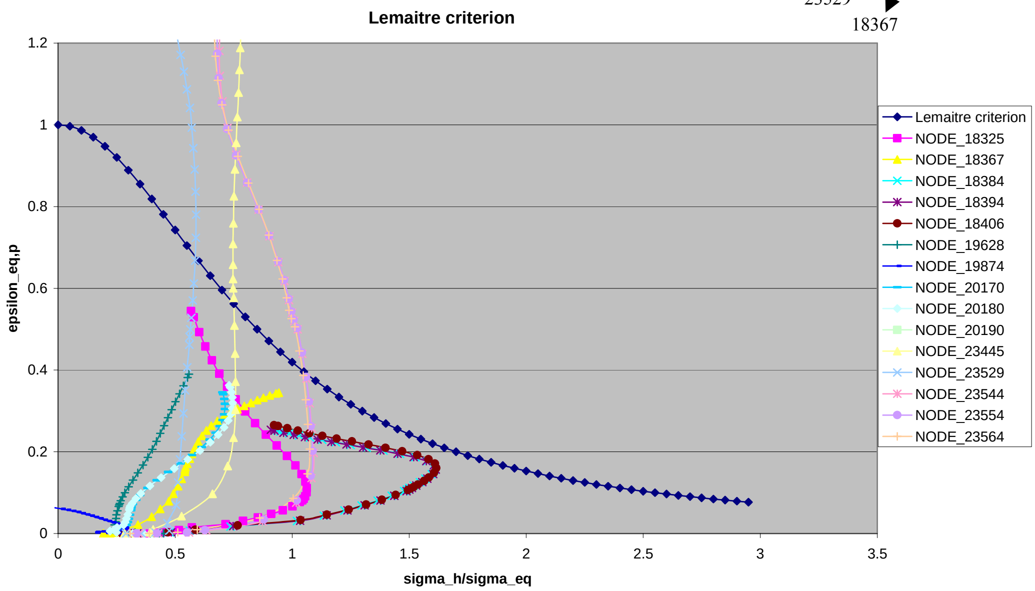

Figure 3.46: Lemaitre criteria

Based on Figure 3.46, the node which is corresponding to the first failure is node 23564 at sub-step 13 out of 34 sub-steps. The failure load at this sub-step is 560 kN which is shown in Figure 3.47.

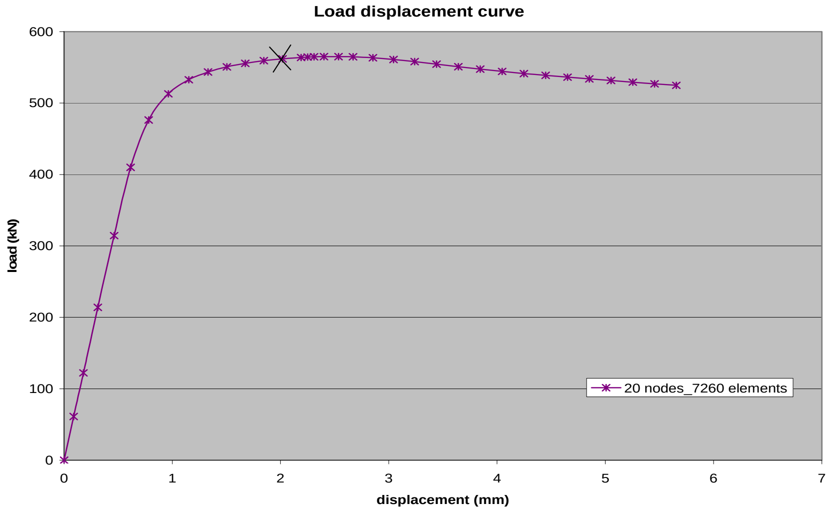

Figure 3.47: Location of failure load

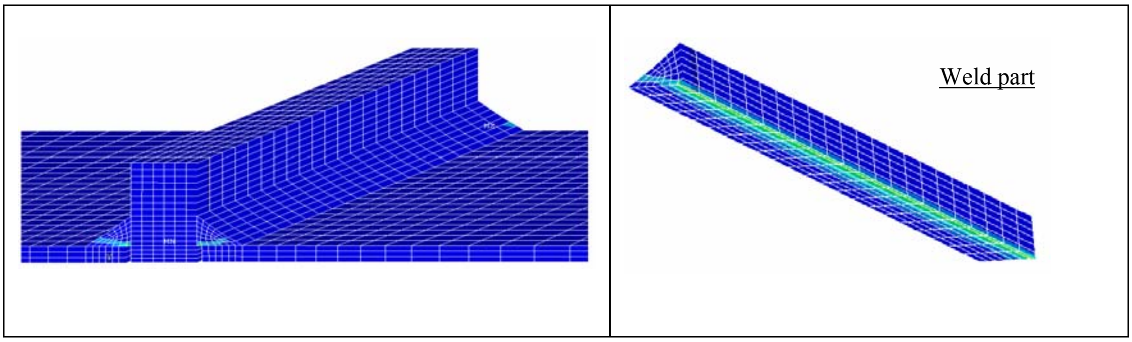

Figure 3.48: Contour plot of equivalent plastic strain at load step 13

Figure 3.48 shows the contour plot of equivalent plastic strain at load step 13. It can be seen that failure starts at the weld root which indicate by the accumulation of plastic strain in this area.

2. Connection 3B

The same procedure for modelling this connection is adopted as mentioned previously for other connections. The results of each procedure are given in figures and table below.

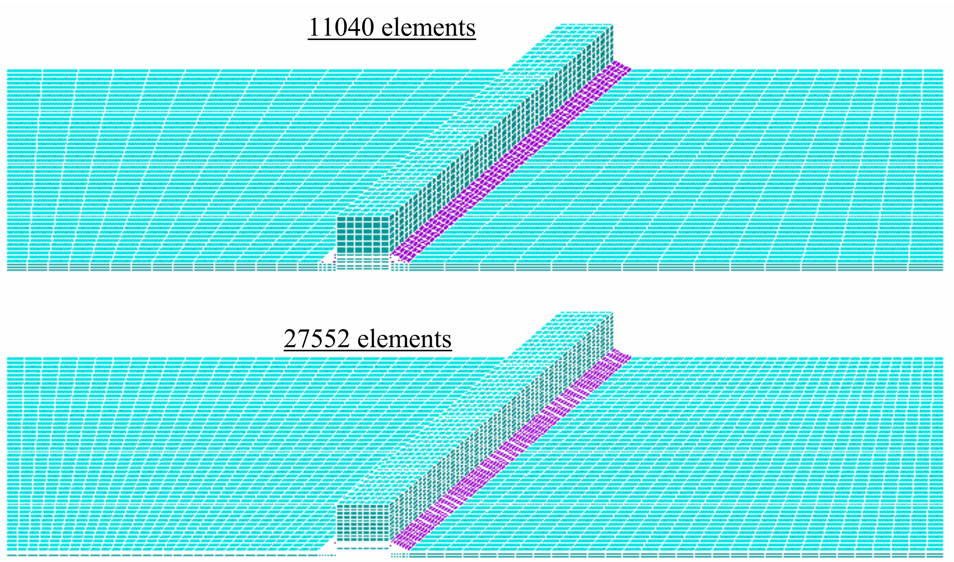

Figure 3.49: Types of mesh

Figure 3.49 shows types of mesh which are used in convergence test. The result of this test is given in Table 3.6 related to the computation time needed for each mesh. In addition, Figure 3.50 shows the result in term of load displacement curve for each mesh.

Table 3.6 Convergence test results connection type 3B

No.	Number of element	Calculation time
1.	8 nodes brick element (11040 elements)	39 minutes 18 seconds
2.	20 nodes brick element (11040 elements)	10 hours 31 minutes and 28 seconds
3.	8 nodes brick element (27552 elements)	1 hour 43 minutes 37 seconds

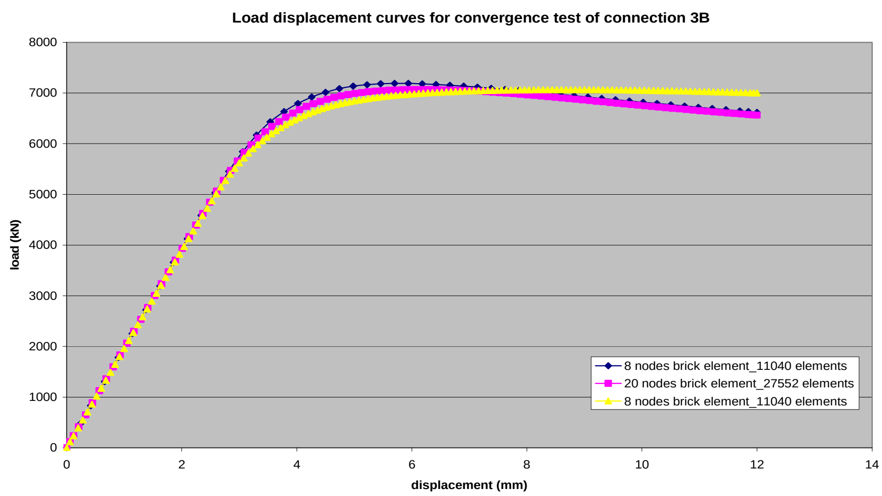

Figure 3.50: Convergence test results of connections 3B

Based on the convergence test in Table 3.6 and Figure 3.50, the type of element which is used for further analysis is 8 nodes brick element with 27552 elements. To continue, the Lemaitre criterion is used to determine the failure load of this connection. Figure 3.51 shows the nodes which are investigated using Lemaitre criterion in order to know when the connection start to fail.

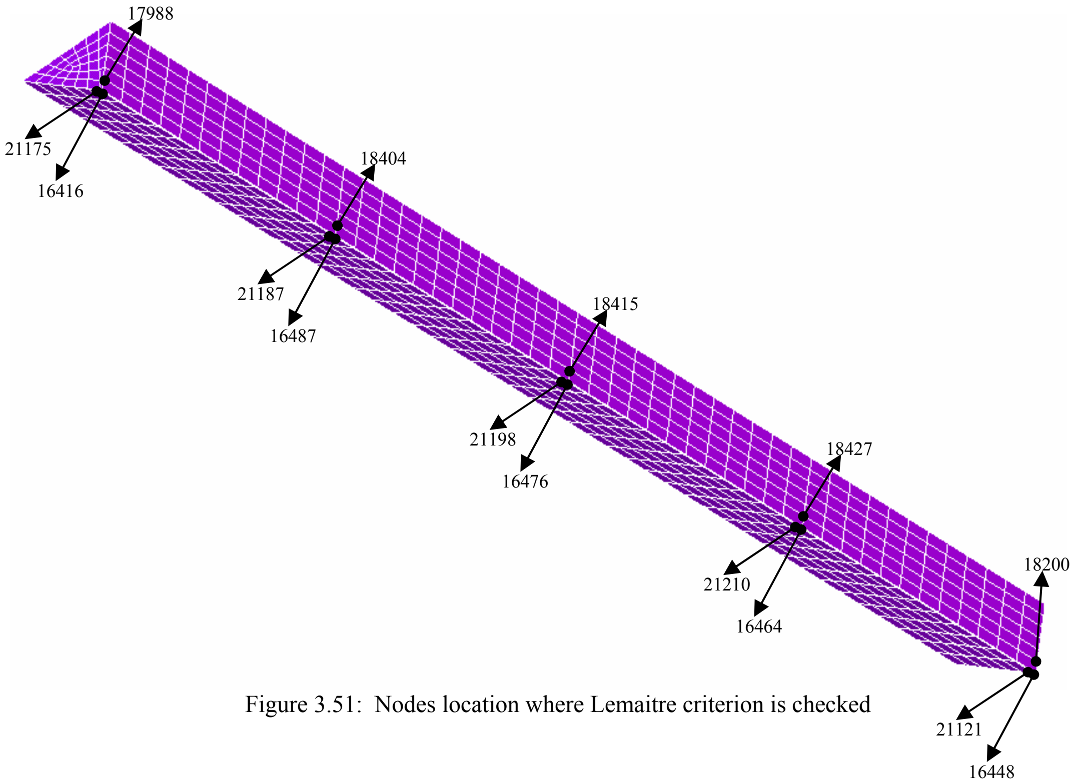

Figure 3.51: Nodes location where Lemaitre criterion is checked

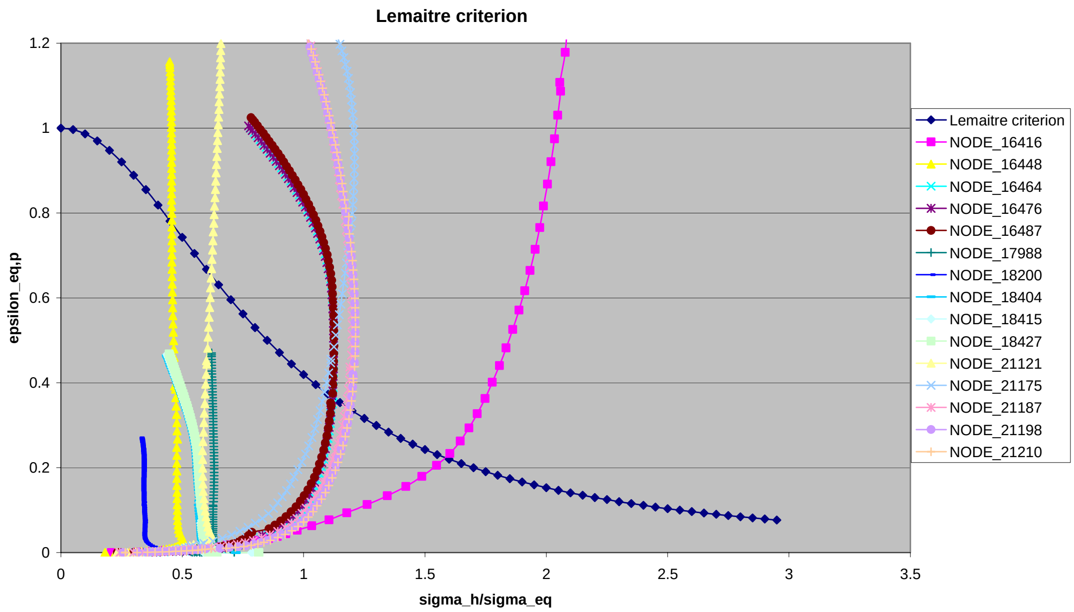

Figure 3.52: Lemaitre criteria

Figure 3.52 shows the result of the investigation using Lemaitre criterion. Node 21210 is the node that corresponding to the first failure of the connection based on this figure.

This failure occurs at sub-step 48. The failure load for this sub-step is 7055 kN and it is indicated in Figure 3.53 by a cross sign.

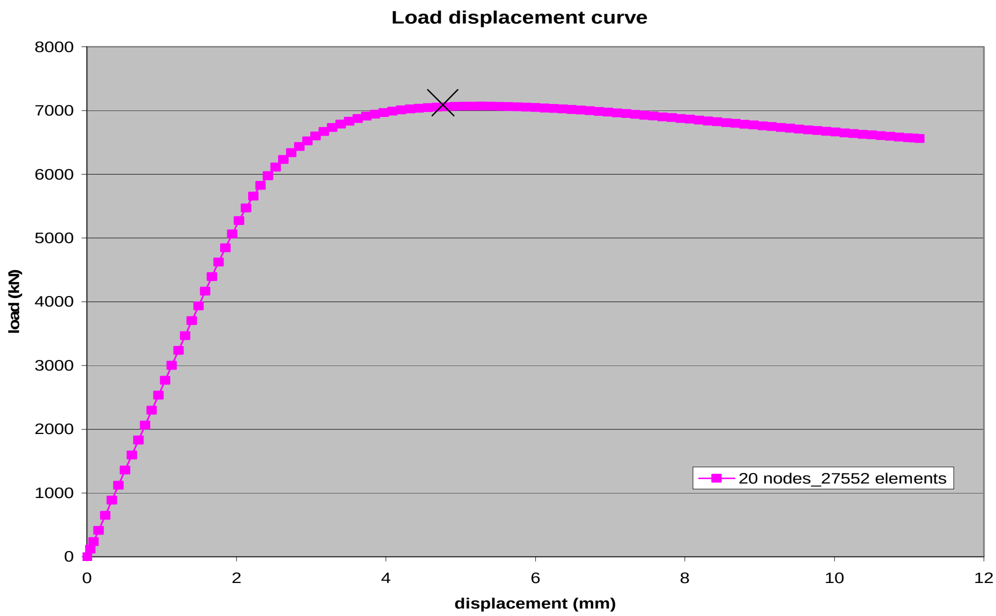

Figure 3.53: Location of failure load

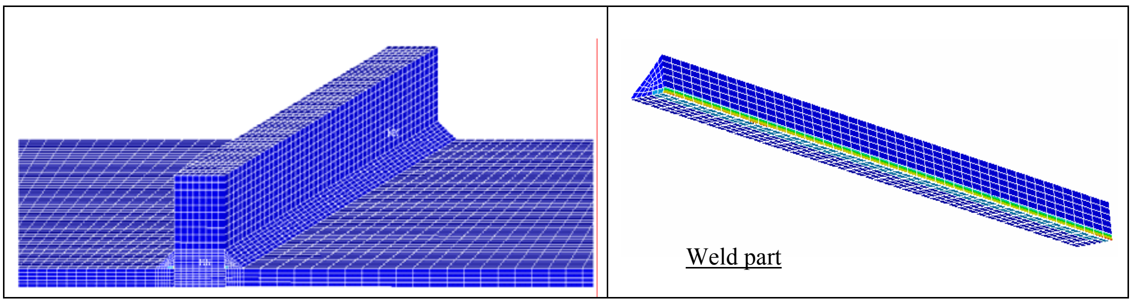

Figure 3.54: Location of failure load

Figure 3.54 shows that failure starts at the weld root of this connection which indicated by the accumulated plastic strain in this location.

Finally to conclude the FEM of connections using steel S1100, a list of failure load for each connection analysed is shown in Table 3.7. It is clear from this table that connection type 2 has larger failure load compare to connection type 3. The numbers of stress components which occur in the weld play a big role for this case.

Table 3.7 Failure loads

No.	Type of connection	Failure load numerical (kN)	Failure load experiment (kN)
1.	4A1	356	352
2.	5A1	7050	7300
3.	2A	826	
4.	2B	10406	
5.	3A	560	
6.	3B	7055	

3.4.2 FEM connections using steel S355

The same geometries of all types of connection which are modelled using steel S1100 are adopted with differences in weld throat thickness only. For each connection with 4.5 mm and 10 mm weld throat thickness, the new applied thickness is 2.5 mm and 5.5 mm respectively. These changes are aimed to make sure that the failure will be in the weld material instead of in the base material.

As the material input, the true stress strain relations of steel S355 which have already developed in the previous section are used. Modulus of elasticity and Poisson's ratio are taken 2.1E6 MPa and 0.3 respectively. There are no convergence tests for this particular case. The types of element which are used in the FE analysis are the same to the previous analysis for steel S1100 for each type of connection.

The results of the FE analysis for all types of connection are shown in Figure 3.55 and Figure 3.56.

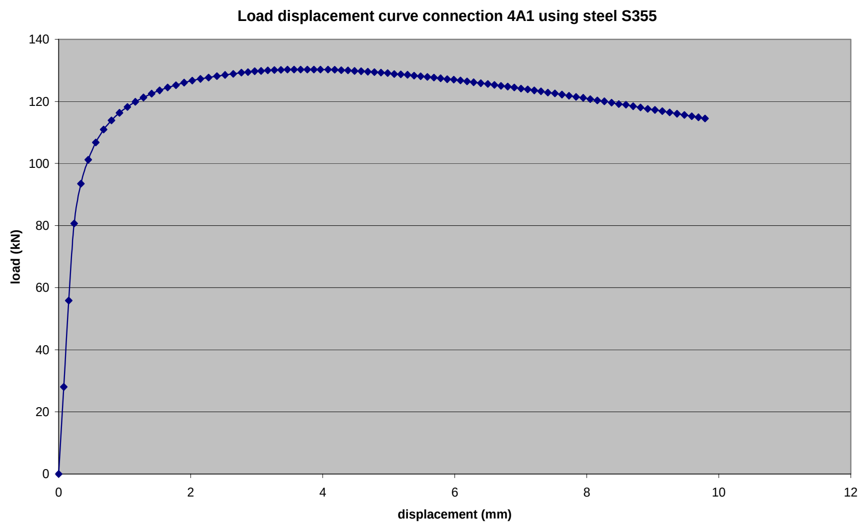

(a)

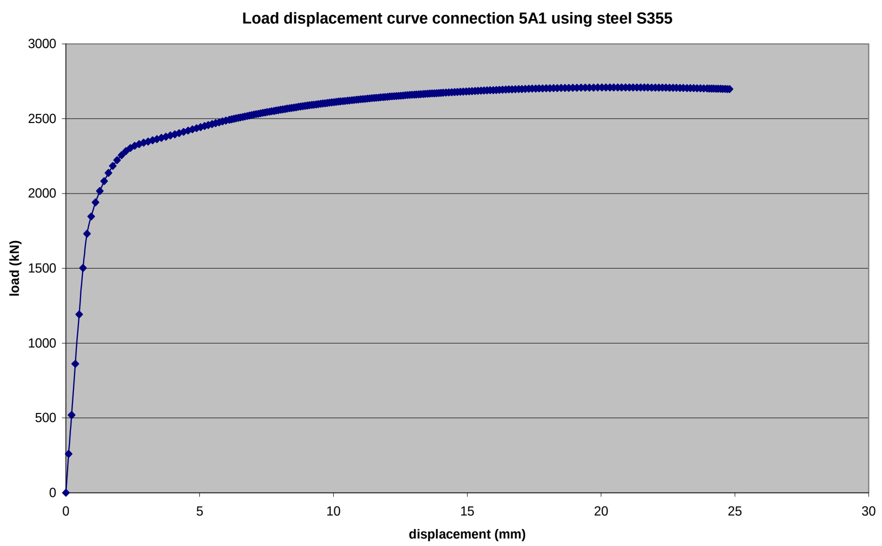

(b)

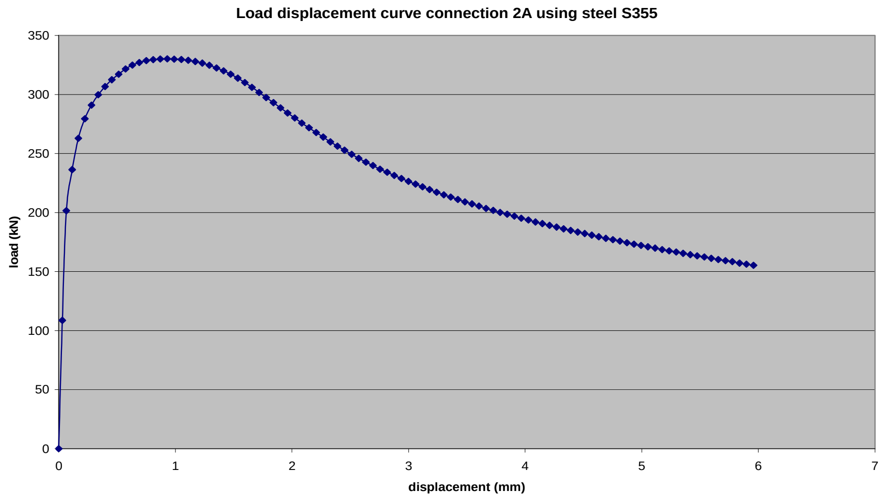
Load displacement curve connection 2A using steel S355
load (kN)
displacement (mm)
0
50
100
150
200
250
300
350
0
1
2
3
4
5
6
7

(c)

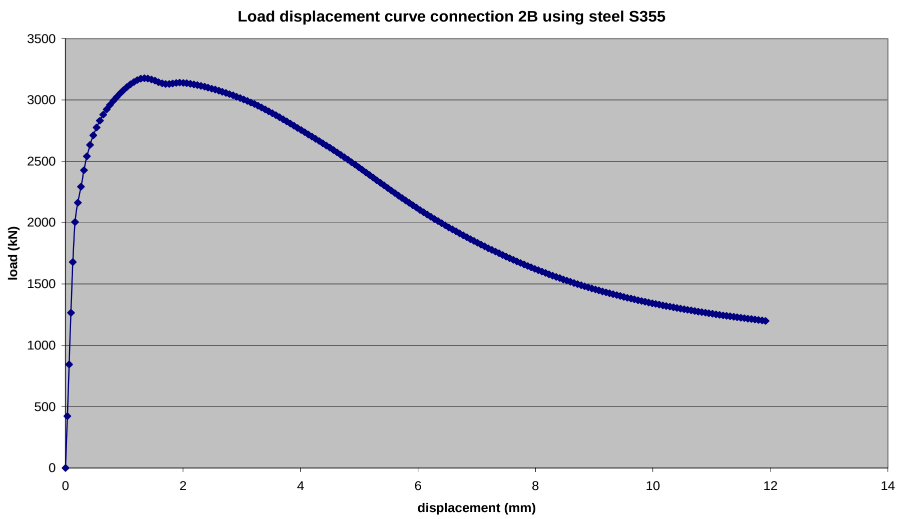
Load displacement curve connection 2B using steel S355
load (kN)
displacement (mm)
0
500
1000
1500
2000
2500
3000
3500
0
2
4
6
8
10
12
14

(d)

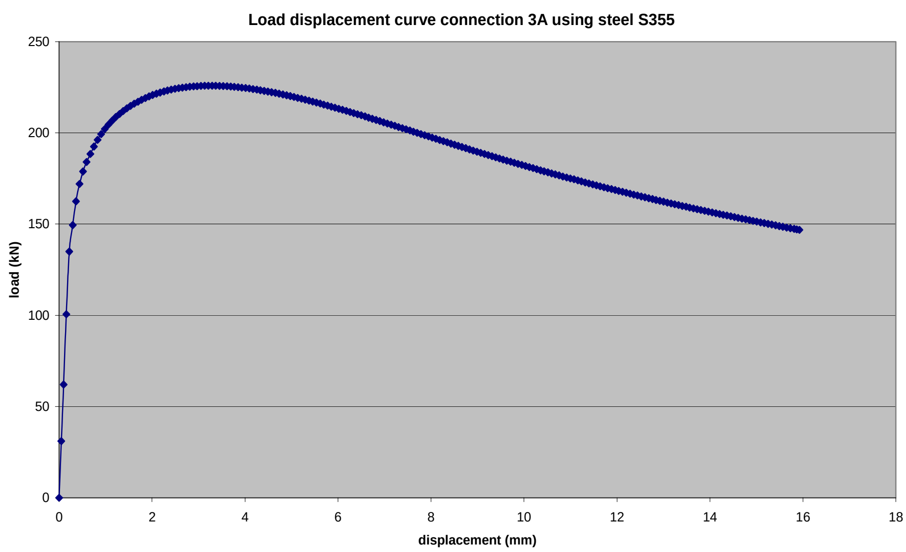
Load displacement curve connection 3A using steel S355
load (kN)
displacement (mm)
0
50
100
150
200
250
0
2
4
6
8
10
12
14
16
18

(e)

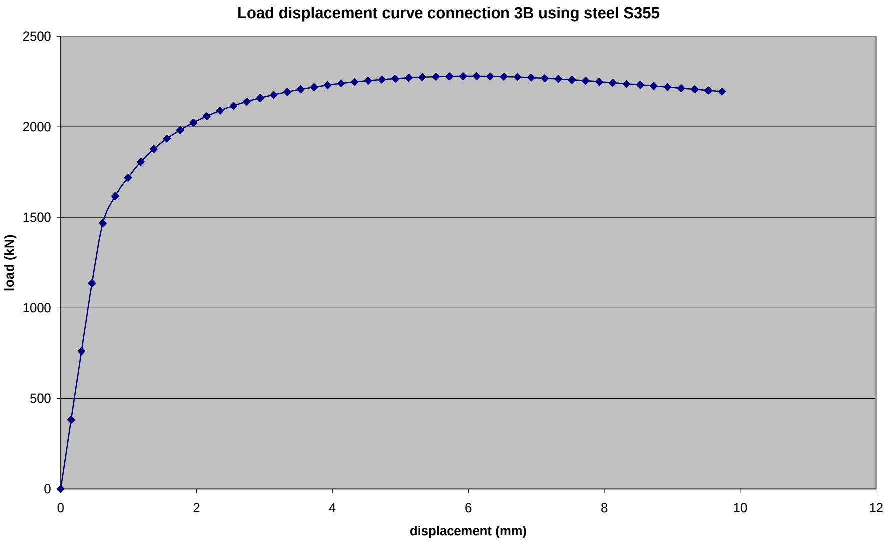

(f)

Figure 3.55: Load displacement curves
(a) connection 4A1, (b) connection 5A1, (c) connection 2A, (d) connection 2B,
(e) connection 3A, (f) connection 3B

Figure 3.55 shows a tendency that a connection with thicker plate gives more ductility which means has more deformation capacity compare to the thinner one.

Connection 4A1 using steel S355

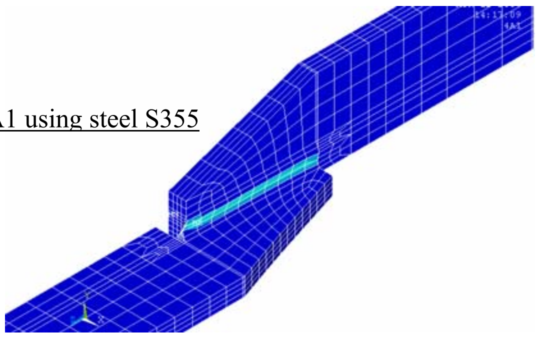

Connection 5A1 using steel S355

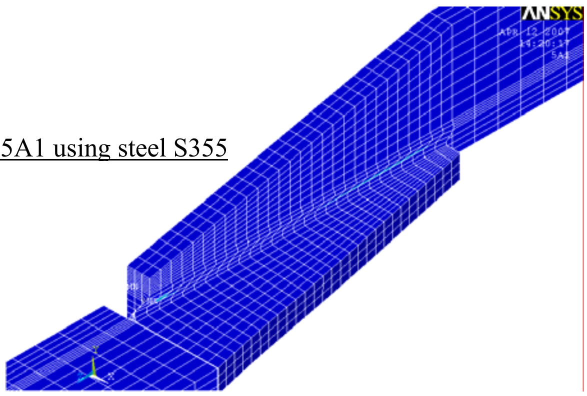

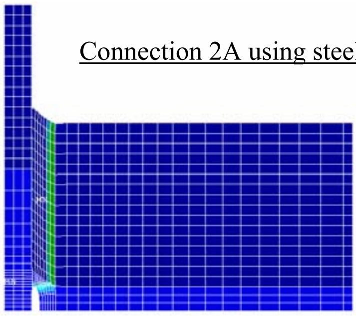

Connection 2A using steel S355

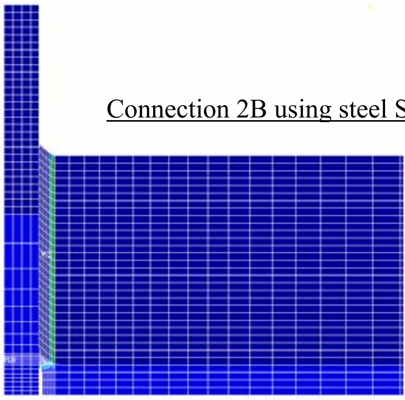

Connection 2B using steel S355

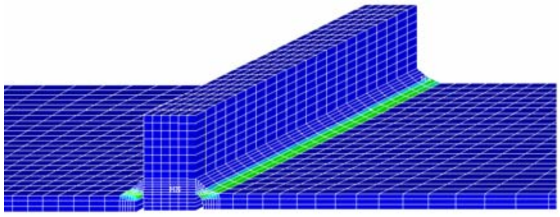

Connection 3A using steel S355

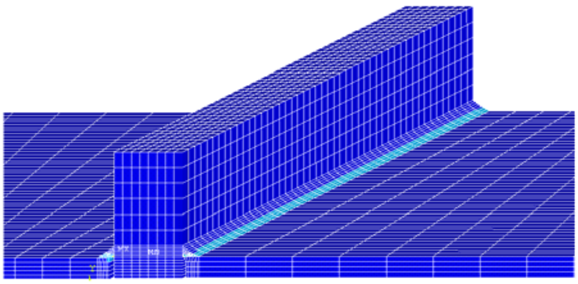

Connection 3B using steel S355

Figure 3.56: Equivalent plastic strain contour plot

In Figure 3.56, the equivalent plastic strain contour plot for each connection is shown. Based on this plot it is concluded that the failure starts from the weld root to the weld face.

To conclude, corresponding failure load for each connection is given in Table 3.8. These failure loads directly determined based on load displacement curve corresponds to each connection. The Lemaitre criterion cannot be used for this case because the failure load which results based on that criterion will located somewhere after the maximum load in the load displacement curve.

Table 3.8 Failure loads

No.	Type of connection	Failure load (kN)
1.	4A1	130
2.	5A1	2709
3.	2A	330
4.	2B	3141
5.	3A	226
6.	3B	2280

As can be seen in Table 3.8, connection type 3 has smaller failure load compare to connection type 2. For this case the numbers of stress components which occur in the connection play a role in reducing the failure load. Failure loads which are shown in Table 3.8 will be used later in calculation of β value.

Chapter 4 β values

4.1 Introduction

Based on the FEA results, the calculation of β value for steel S1100 and S355 is performed. This value will be compared to that of Huisman-Itrec standard. The used formula to calculate fillet weld connections will be given firstly with the appropriate criterion which is available in several codes [3, 8 and 10]. Secondly the corresponding formula to calculate β is given for each type of connection which is derived from the previous given formulas. Thirdly the ratio of corresponding yield load to failure load F/Fu is plotted with the β value from the previous calculation. This plot will be used in determining the β value after the yield load criterion is determined.

4.2 Formulas

The formulas which are shown below are used to derive the formula for determining the β value.

$$\boxed{\begin{array}{l}\sigma_c=\beta\sqrt{\sigma_\perp^2+3\left(\tau_{//}^2+\tau_\perp^2\right)}\le\dfrac{f_u}{\gamma_{MW}}\text{ and }\sigma_\perp\le\dfrac{f_u}{\gamma_{MW}}\\ \gamma_{MW}=1.25\end{array}}\qquad\text{(Eurocode3)}\qquad(4.1)$$

$$\boxed{\begin{array}{l}\sigma_c=\beta\sqrt{\sigma^2{}_\perp+3\left(\tau_{//}^2+\tau_{/\perp}^2\right)}\le\dfrac{f_y}{\gamma}\\ \text{with } f_y=\text{minimum yield stress}\\ \gamma=1.0\end{array}}\qquad\text{(NEN 2062)}\qquad(4.2)$$

$$\boxed{\begin{array}{l}\sigma_c=\beta\sqrt{\sigma_\perp^2+3\left(\tau_{//}^2+\tau_\perp^2\right)}\le\dfrac{f_{av}}{\gamma}\\ \text{with } f_{av}=0.41\left(f_y+f_u\right)\\ \gamma=1.0\end{array}}\qquad\text{(Lloyd Standard)}\qquad(4.3)$$

Equation (4.1), equation (4.2) and equation (4.3) are based on [3], [10] and [8] respectively. In those equations, minimum yield stress f_y and the ultimate tensile strength f_u values are based on the properties of base metal. Equation (4.2) is used in Huisman-Itrec standard to calculate fillet weld connections. The explanation regarding stress components which appears in those formulas is given in Appendix I.

The corresponding formulas to calculate the β value are given for each type of connection (after some elaborations) as follow.

1. Connection type 4A1 and 5A1
   This connection is mainly loaded by shear and there will be only one corresponding stress direction in the weld. The following formulas are used to determine the β values.

   In this case only $\tau_{//}$ occurs in the weld then equation (4.1), (4.2) and (4.3) are reduced to:

$$\boxed{\beta=\frac{f_u}{\gamma_{MW}\ \sigma_{weld}\ \sqrt{3}}}\qquad(4.4)$$

$$\boxed{\beta = \frac{f_y}{\sigma_{weld}\sqrt{3}}} \tag{4.5}$$

$$\boxed{\beta = \frac{f_{av}}{\sigma_{weld}\sqrt{3}}} \tag{4.6}$$

where: $\tau_{//} = \sigma_{weld} = \dfrac{F}{4\,a\,l}$

2. Connection type 2
   For this type of connection, there will be two corresponding equal stresses in the weld that are $\sigma_{\perp}$ and $\tau_{//}$ then equation (4.1), (4.2) and (4.3) will be:

$$\boxed{\beta = \frac{f_u}{\gamma_{MW}\,\sigma_{weld}\sqrt{2}}} \tag{4.7}$$

$$\boxed{\beta = \frac{f_y}{\sigma_{weld}\sqrt{2}}} \tag{4.8}$$

$$\boxed{\beta = \frac{f_{av}}{\sigma_{weld}\sqrt{2}}} \tag{4.9}$$

where: $\sigma_{weld} = \dfrac{F}{4\,a\,l}$

3. Connection type 3
   In this type of connection all stresses which are shown in equation (4.1), (4.2) and (4.3) occur in the weld and the corresponding formulas to calculate the β value are as follow.

$$\boxed{\beta = \frac{2\,f_u}{\gamma_{MW}\,\sigma_{weld}\sqrt{10}}} \tag{4.10}$$

$$\boxed{\beta = \frac{2\,f_y}{\sigma_{weld}\sqrt{10}}} \tag{4.11}$$

$$\boxed{\beta = \frac{2\,f_{av}}{\sigma_{weld}\sqrt{10}}} \tag{4.12}$$

$$where:\ \sigma_{\perp} = \tau_{\perp} = \frac{\sigma_{weld}}{2}$$

$$\tau_{//} = \frac{\sigma_{weld}}{\sqrt{2}}$$

$$\sigma_{weld} = \frac{F}{4\sqrt{2}\,a\,l_y}$$

4.3 β plots

Based on the formulas given above, the β values are calculated and the results for different type of connection are plotted against the ratio of F/Fu (safety margin) and it is shown in Figure 4.1 and Figure 4.2 for steel S1100 and steel S355 respectively. As a remark, the value of F is taken arbitrary and Fu is a defined value. Based on these figures, it is clear that the β value increases as F/Fu decreases which means that for a bigger β it will result in a conservative yield load F and it is not an advantage from economic point of view. For example, in Figure 4.1b for β=1.38 the corresponding value of F/Fu for connection type 2B equals to 0.52 and for β=1.5 the corresponding value of F/Fu equals to 0.48 which are more conservative.

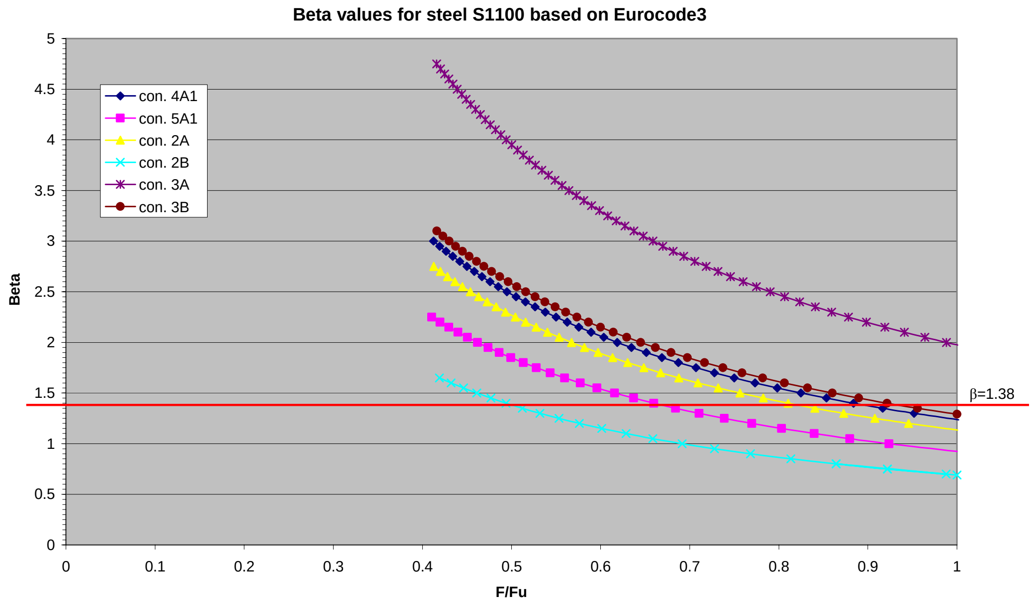

(a)

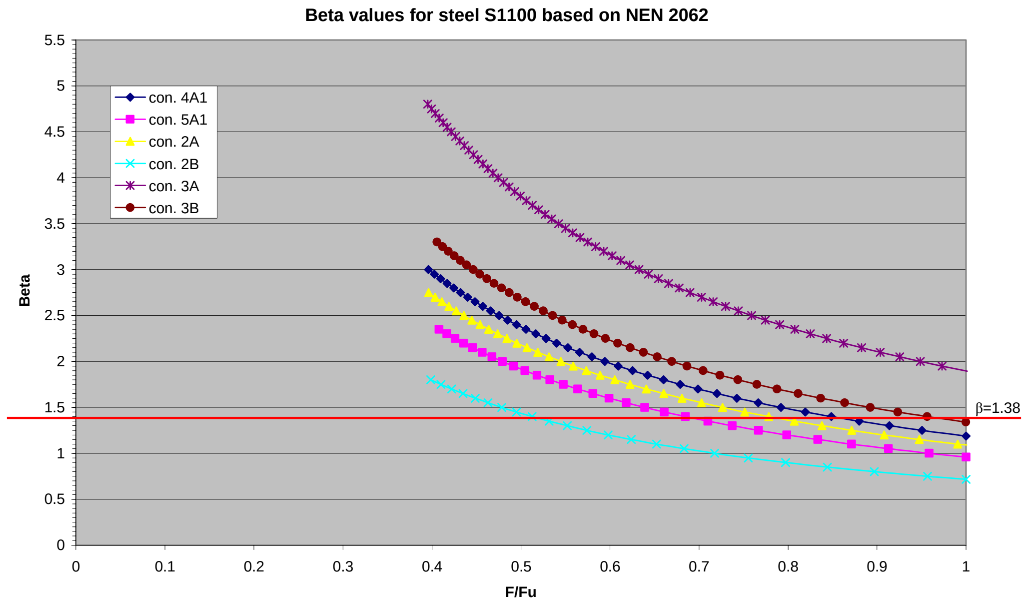

(b)

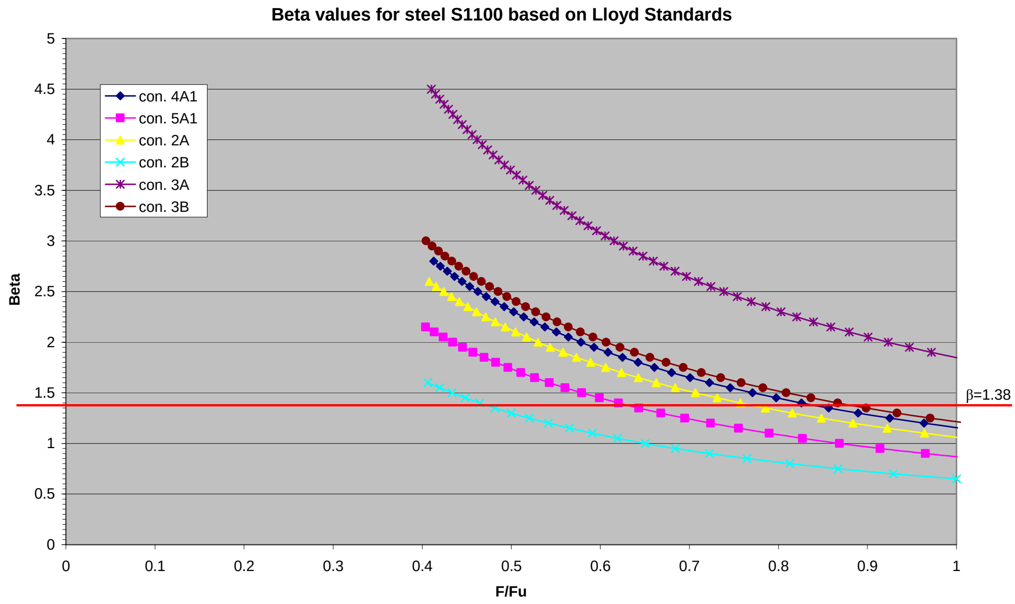

(c)

Figure 4.1: β values for steel S1100
(a) Eurocode3, (b) NEN 2062 and (c) Lloyd standards

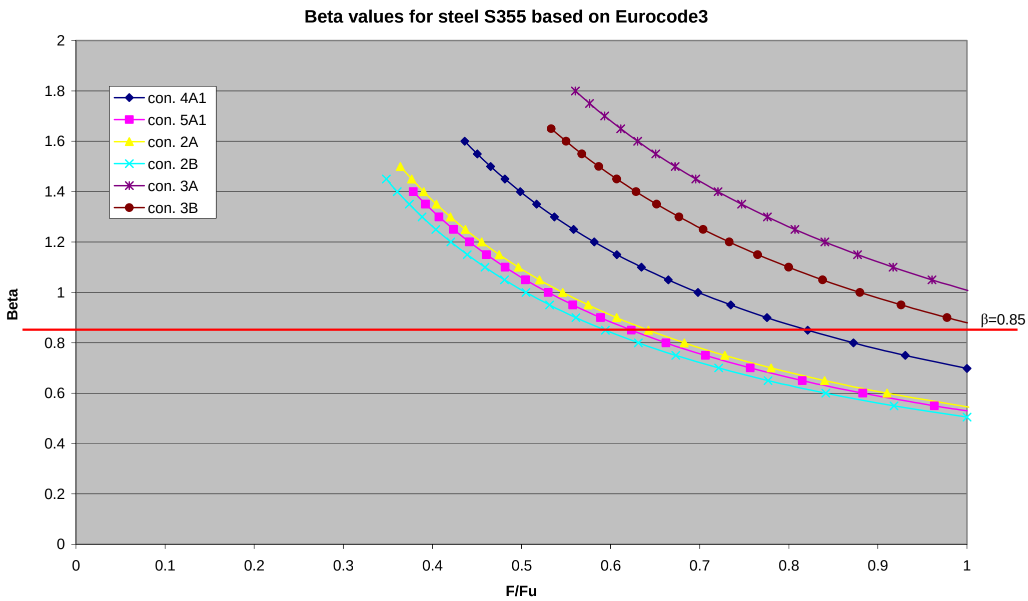

(a)

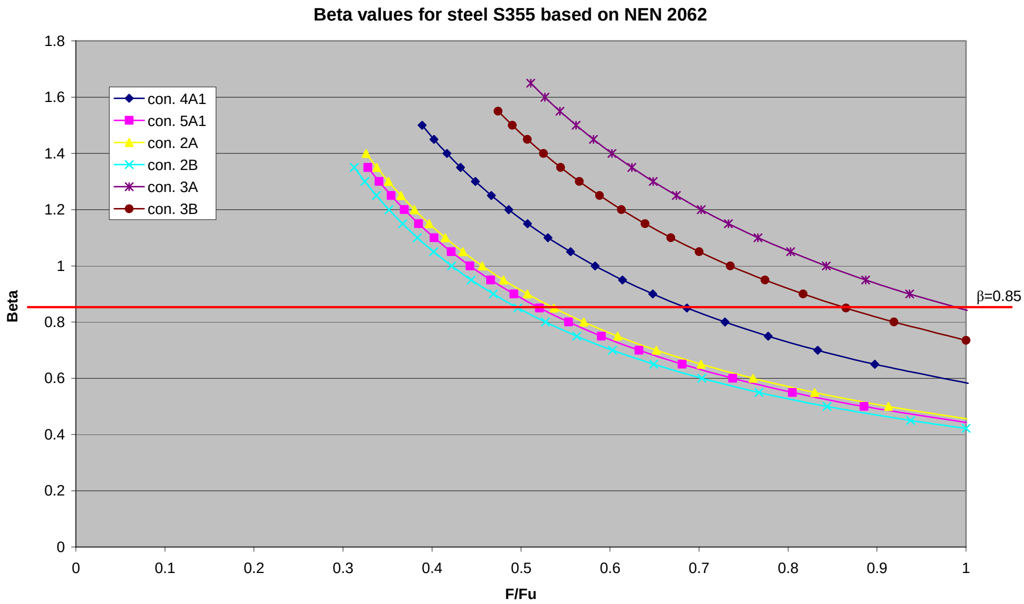

(b)

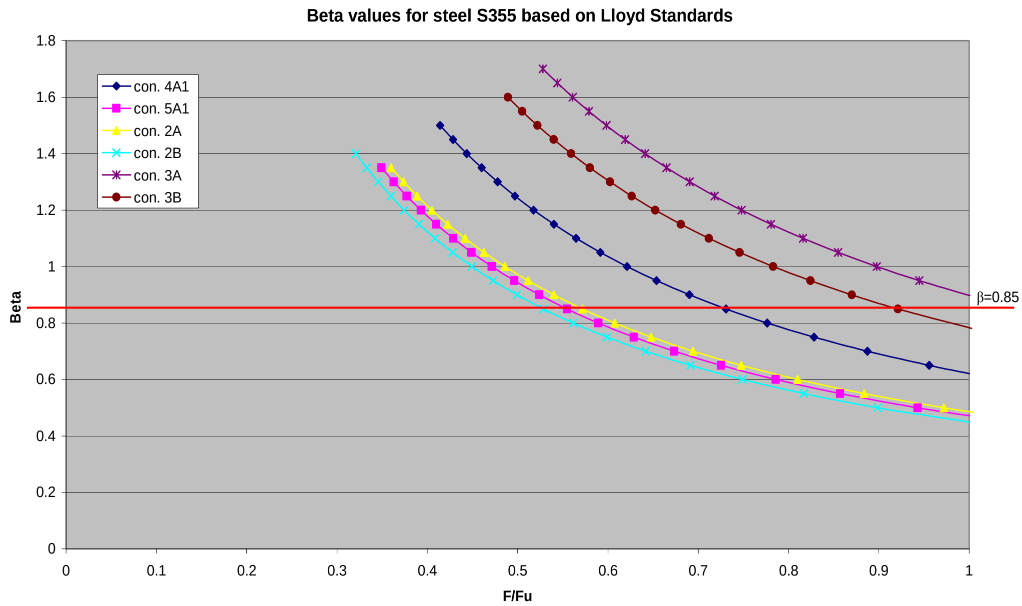

(c)

Figure 4.2: β values for steel S355
(a) Eurocode3, (b) NEN 2062 and (c) Lloyd standards

4.4 Yield Load Criterion

The yield load criterion which is used in this case is based on the comparison of the displacement plastic (Δ_{pl}) over the displacement elastic (Δ_{el}) in load displacement curve for each type of connection in order to know the influence of plastic strain in the connection which causes yield. This is done mainly because the fact that it is quite difficult to determine at which point the corresponding yield loads from FE results. In Figure 4.3 an example is given in the determination of Δ_{el} and Δ_{pl}. The procedures in order to get these values are as follow.

1. Draw a straight line which is based on the position of the first and second sub-step in the load displacement curve.
2. Draw a horizontal straight line corresponding to each sub-step and for this example sub-step 10 is the one which is investigated.
3. The first intersection of this line to the line which is made in procedure 1 gives Δ_{el}. Δ_{pl} is measured from the first intersection above to the intersection of the line in procedure 2 to the point of sub-step 10 in load displacement curve.

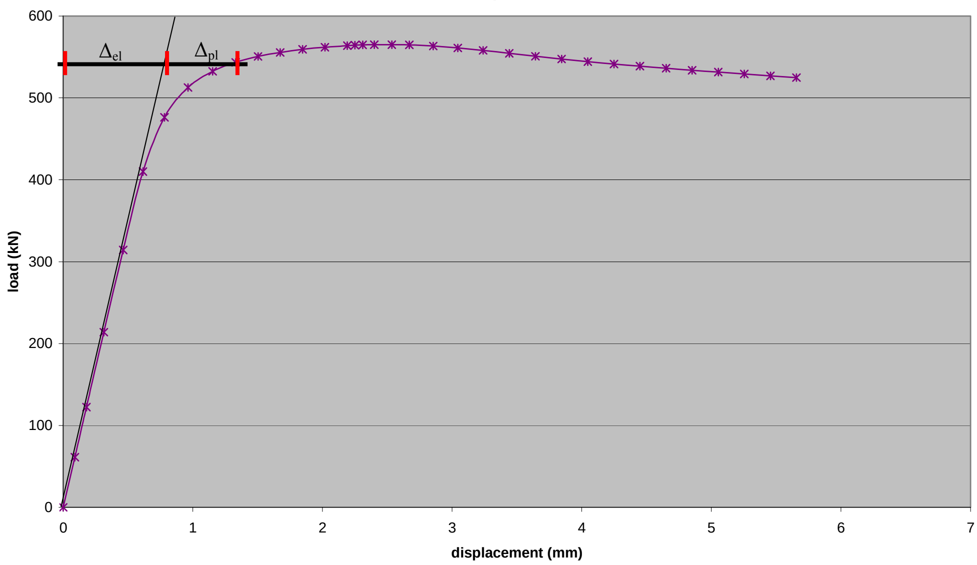

Figure 4.3: Yield load criterion

The criterion is shown in Figure 4.4 and it is plotted against the ratio of F/Fu.

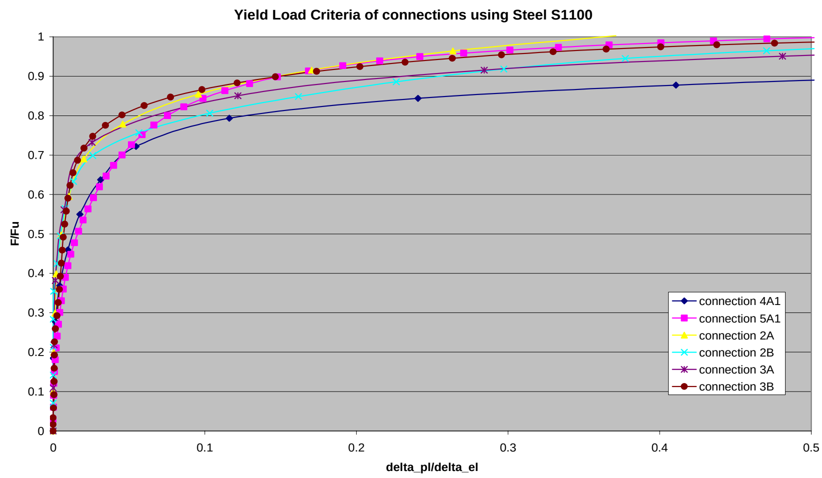

(a)

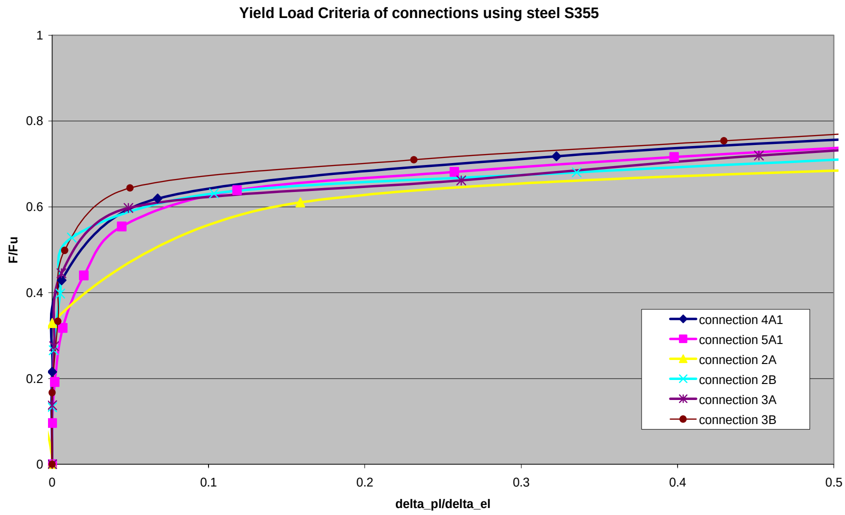

(b)

Figure 4.4: Yield load criteria based on $\Delta_{pl}/\,\Delta_{el}$
(a) steel S1100, (b) steel S355

4.5 Resulting β values

In Table 4.1 and Table 4.2 the β values of steel S1100 and steel S355 based on two yield load criteria are given. The criteria are Δ_{pl}/Δ_{el} equal to 5% and Δ_{pl}/Δ_{el} equal to 1%. These criteria are based on numerical results.

Table 4.1 β values for steel S1100

No.	Type of connection	Δ_{pl}/Δ_{el}	F/Fu	β		
				Eurocode3	NEN 2062	Lloyd standards
1	4A1	0.05	0.71	1.75	1.67	1.63
2	5A1		0.72	1.28	1.33	1.2
3	2A		0.79	1.48	1.38	1.34
4	2B		0.75	0.92	0.95	0.86
5	3A		0.78	2.54	2.44	2.37
6	3B		0.81	1.6	1.65	1.5
7	4A1	0.01	0.46	2.7	2.58	2.53
8	5A1		0.42	2.2	2.3	2.07
9	2A		0.59	1.92	1.85	1.8
10	2B		0.59	1.17	1.22	1.1
11	3A		0.6	3.3	3.2	3.07
12	3B		0.59	2.19	2.27	2.05

Table 4.2 β values for steel S355

No.	Type of connection	Δ_{pl}/Δ_{el}	F/Fu	β		
				Eurocode3	NEN 2062	Lloyd standards
1	4A1	0.05	0.76	0.92	0.77	0.82
2	5A1		0.74	0.72	0.6	0.64
3	2A		0.68	0.8	0.67	0.72
4	2B		0.71	0.71	0.59	0.63
5	3A		0.73	1.38	1.16	1.23
6	3B		0.77	1.14	0.95	1.02
7	4A1	0.01	0.64	1.09	0.91	0.97
8	5A1		0.62	0.86	0.71	0.76
9	2A		0.56	0.98	0.81	0.87
10	2B		0.63	0.8	0.67	0.72
11	3A		0.62	1.63	1.36	1.45
12	3B		0.67	1.31	1.1	1.17

An example of the procedures which are used to determine these β values are given in Appendix F.

As can be seen in Table 4.1 and Table 4.2, the resulting β values have a big scatter. This makes it is quite difficult to determine directly the appropriate β value which will be used in design formula for designing fillet weld connections especially for steel S1100.

The procedure in determining the β value is given as shown in Figure 4.5.

Calculate the ratio of Δ_{pl}/Δ_{el} based on load displacement curve of each type of connection for every sub-step. One example for determination of Δ_{el} and Δ_{pl} for one sub-step is shown in Figure 4.3

⇓

Calculate the F/Fu for each sub-steps based on load displacement curve of each connection.

⇓

Plot the corresponding Δ_{pl}/Δ_{el} and F/Fu for each sub-steps of each connection. This plot is given in Figure 4.4

⇓

Take a value of Δ_{pl}/Δ_{el} (0.01 or 0.05) as a yield load criterion and measure the corresponding F/Fu value from Figure 4.4. This is done for each type of connections.

⇓

Plot the F/Fu value to Figure 4.1 or Figure 4.2 based on type of steel grade used in the connection and determine the corresponding β value for each type of connections.

Figure 4.5: Flowchart to determine β value

For this particular case, it is assumed that the resulting β value based on [10] is the appropriate one for designing fillet weld connections. Consequently the β value for both materials can be determined by taking the average of those values and the results are shown in Table 4.3.

Table 4.3 β values

No.	Δ_{pl}/Δ_{el}	β	
		Steel S355	Steel S1100
1.	0.01	0.93	2.24
2.	0.05	0.79	1.57

Based on Table 4.3 it can be seen that for steel S355 with Δ_{pl}/Δ_{el} = 5% results in smaller β value compared to that stated in the code [10] whereas for Δ_{pl}/Δ_{el} = 1% results in higher β value compare to that mentioned in the code [10]. It is also the case for steel S1100 where smaller Δ_{pl}/Δ_{el} ratio gives bigger β value. These values are bigger than that is used in Huisman-Itrec standard.

Based on the resulting β values in Table 4.3, the margin of safety to failure can be determined for each type of connection using graph in Figure 4.1. One example which shows the plot which explains the meaning of safety margin from yield to failure is shown in Figure 4.6. As comparison, the safety margin that used in Huisman-Itrec will be used. Table 4.4 and Table 4.5 show the resulting safety margin to failure and the comparison value.

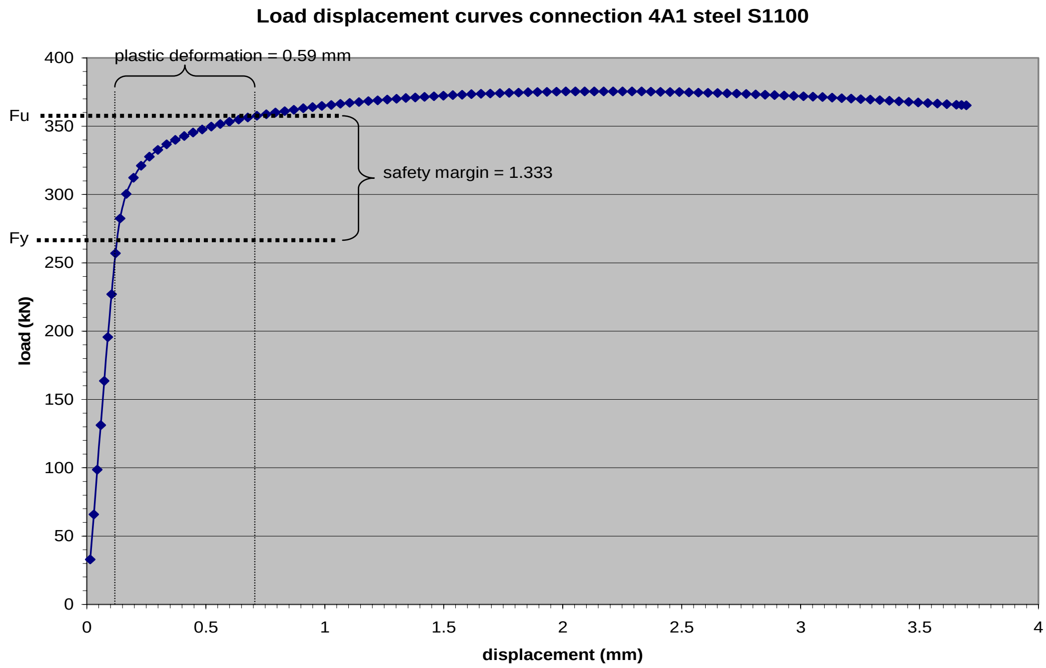

Figure 4.6: Safety margin plot

Table 4.4 Safety margin to failure for steel S355

No.	Type of connection	Steel S355				
		β = 0.79		β = 0.93		
		Fyield	safety margin to failure	Fyield	safety margin to failure	Minimum safety margin from yield to failure
1	4A1	0.740 Fu	1.351	0.627 Fu	1.595	1.5
2	5A1	0.560 Fu	1.786	0.475 Fu	2.105	1.5
3	2A	0.580 Fu	1.724	0.490 Fu	2.041	1.5
4	2B	0.530 Fu	1.887	0.453 Fu	2.208	1.5
5	3A	> Fu	< 1.000	0.970 Fu	1.031	1.5
6	3B	0.930 Fu	1.075	0.790 Fu	1.266	1.5

Table 4.5 Safety margin to failure for steel S1100

No.	Type of connection	steel S1100				
		β = 1.57		β = 2.24		
		Fyield	safety margin to failure	Fyield	safety margin to failure	Minimum safety margin from yield to failure
1	4A1	0.750 Fu	1.333	0.528 Fu	1.894	1.5
2	5A1	0.604 Fu	1.656	0.428 Fu	2.336	1.5
3	2A	0.687 Fu	1.456	0.484 Fu	2.066	1.5
4	2B	0.450 Fu	2.222	0.320 Fu	3.125	1.5
5	3A	> Fu	< 1.000	0.845 Fu	1.183	1.5
6	3B	0.840 Fu	1.190	0.600 Fu	1.667	1.5

In Huisman-Itrec standard, the safety margin to failure is expected 2.25 which can be explained as follows.

$F_{allow} = \frac{F_y}{1.5}$ and $F_y = \frac{F_{UTS}}{1.5}$ consequently $F_{allow} = \frac{F_{UTS}}{2.25}$

As can be seen in Table 4.4 and Table 4.5, the bigger the β values are the bigger the safety margin to failure which implies that it is safe. Consequently, β = 0.93 and β = 2.24 is chosen for steel S355 and steel S1100 respectively which can be used in design formula of fillet weld connection as state in [10]. Additionally, to validate the chosen β value for steel S1100, Monte Carlo Simulation is performed and the complete calculation is given in Appendix G. Based on this calculation, it is concluded that the chosen β = 2.24 is a safe value because it gives lower probability failure compared to that is suggested in code of practice.

4.6 Improvement formula proposal

In this section, improvement formulas are proposed in designing fillet weld connections using steel S355 and fillet weld connections using steel S1100. These formulas are derived based on the failure load results of FEA. Firstly, based on these failure loads each stress components which occur in the weld are calculated for each connection. The results are shown in Table 4.6 and Table 4.7 for fillet weld connections using steel S355 and fillet weld connections using steel S1100 respectively.

Table 4.6 Weld stresses component values of connection using steel S355

Type of connection	F_u (kN)	a (mm)	l (mm)	$\sigma_\perp$ (N/mm^2)	$\tau_\perp$ (N/mm^2)	$\tau_{//}$ (N/mm^2)
4A1	130	2.5	37	0.00	0.00	351.35
5A1	2709	5.5	266	0.00	0.00	462.92
2A	330	2.5	60	388.91	388.91	0.00
2B	3141	5.5	240	420.65	420.65	0.00
3A	226	2.5	60	133.17	133.17	188.33
3B	2280	5.5	240	152.67	152.67	215.91

Table 4.7 Weld stresses component values of connection using steel S1100

Type of connection	F_u (kN)	a (mm)	l (mm)	$\sigma_\perp$ (N/mm^2)	$\tau_\perp$ (N/mm^2)	$\tau_{//}$ (N/mm^2)
4A1	356	4.5	37	0	0	534.53
5A1	7050	10	266	0	0	662.59
2A	771	4.5	60	504.80	504.80	0
2B	10406	10	240	766.47	766.47	0
3A	560	4.5	60	183.32	183.32	259.26
3B	7055	10	240	259.82	259.82	367.45

Secondly, linear regression analyses are performed for the stress combinations which occur in the weld. It is noted that because $\sigma_\perp$ and $\tau_\perp$ have the same value (couple) for all type of connections as can be seen in Table 4.6 and Table 4.7, it is assumed that they had the same effect in the weld. Consequently, only combination of $\tau_{//}$ and $\sigma_\perp$ or $\tau_{//}$ and $\tau_\perp$ which will be used in regression analyses. The results of these analyses (linear curves) are shown in Figure 4.7 and Figure 4.8 for fillet weld connections using steel S355 and fillet weld connections using steel S1100 respectively.

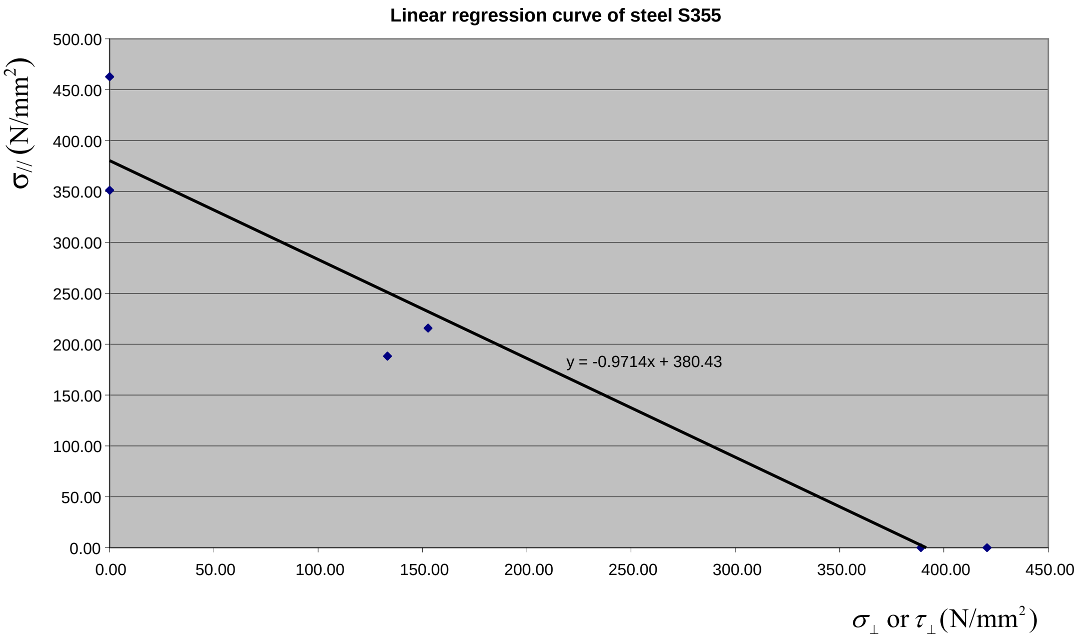

Figure 4.7: Linear regression curve of steel S355

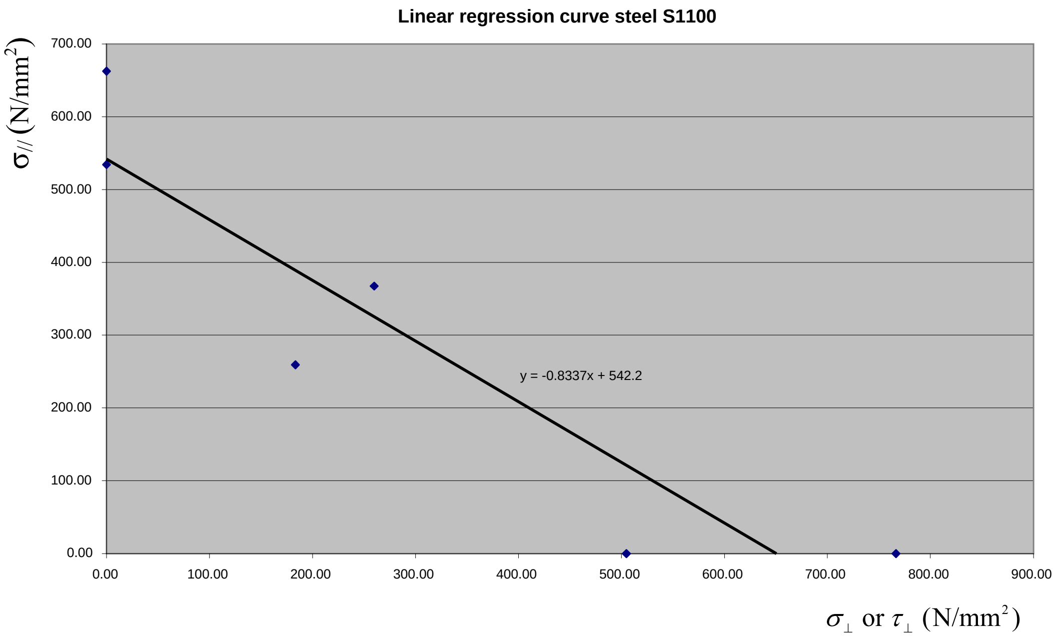

Figure 4.8: Linear regression curve steel S1100

Finally, the improvement formulas are elaborated based on the equations of the curves resulting from the regression analyses.

The equations for fillet weld connections using steel S355 and fillet weld connections using steel S1100 based on regression analyses are given as follow:

$$y = -0.9714x + 380.43 \quad \text{(Fillet weld connections using S355)} \tag{4.13}$$

$$y = -0.8337x + 542.2 \quad \text{(Fillet weld connections using S100)} \tag{4.14}$$

which after some elaborations and written in terms of inequalities equation (4.13) and (4.14) results in:

$2.62.10^{-3}\tau_{//} + 2.55.10^{-3}\sigma_{\perp} \leq 1.0$ (Fillet weld connections using S355) (4.15)

$1.84.10^{-3}\tau_{//} + 1.54.10^{-3}\sigma_{\perp} \leq 1.0$ (Fillet weld connections using S1100) (4.16)

Equation (4.15) and (4.16) implies that all stress combinations position below or position at the curves is safe.

For steel S355 with minimum tensile stress σ_y = 355 N/mm^2 and for steel S1100 with minimum tensile stress σ_y = 1100 N/mm^2 equation (4.15) and (4.16) can be modified by multiplying it by the correspond σ_y which results:

$0.93\tau_{//} + 0.905\sigma_{\perp} \leq \sigma_y$ (Fillet weld connections using S355) (4.17)

$2.029\tau_{//} + 1.692\sigma_{\perp} \leq \sigma_y$ (Fillet weld connections using S1100) (4.18)

where: $\sigma_{\perp} = \tau_{\perp}$

Equation (4.17) and equation (4.18) are the proposed improvement formula in designing fillet weld connections using steel S355 and fillet weld connection using steel S1100 respectively with one restriction that $\sigma_{\perp}$ and $\tau_{\perp}$ should always have the same value (couple) whenever they appear in the connections.

Finally equation (4.17) and (4.18) are compared to equation based on [10]. These comparisons are made by calculating the corresponding yield load F for each type of connection which has been analysed in this project. β = 0.93 and β = 2.24 for steel S355 and steel S1100 are used respectively in equation based on [10]. The result of this comparison is shown in Table 4.8 and Table 4.9.

Table 4.8 Yield load comparison for steel S355

No.	Type of connection	F_y	
		NEN 2062	Equations (4.17)
1.	A1	2.48 σ_y . a . l	4.30 σ_y . a . l
2.	2	3.04 σ_y . a . l	6.25 σ_y . a . l
3.	3	3.85 σ_y . a . l	5.10 σ_y . a . l

Table 4.9 Yield load comparison for steel S1100

No.	Type of connection	F_y	
		NEN 2062	Equations (4.18)
1.	A1	1.03 σ_y . a . l	1.97 σ_y . a . l
2.	2	1.26 σ_y . a . l	3.34 σ_y . a . l
3.	3	1.60 σ_y . a . l	2.48 σ_y . a . l

Based on the comparison results shown in Table 4.8 and Table 4.9, it can be seen that equation (4.17) and (4.18) results in less conservative yield load compared to that of NEN 2062.

A comparison is also made between the proposed formula given previously and the β formula (NEN 2062) for steel S355 and steel S1100 by plotting the curve of the formulas. The results are shown in Figure 4.9.

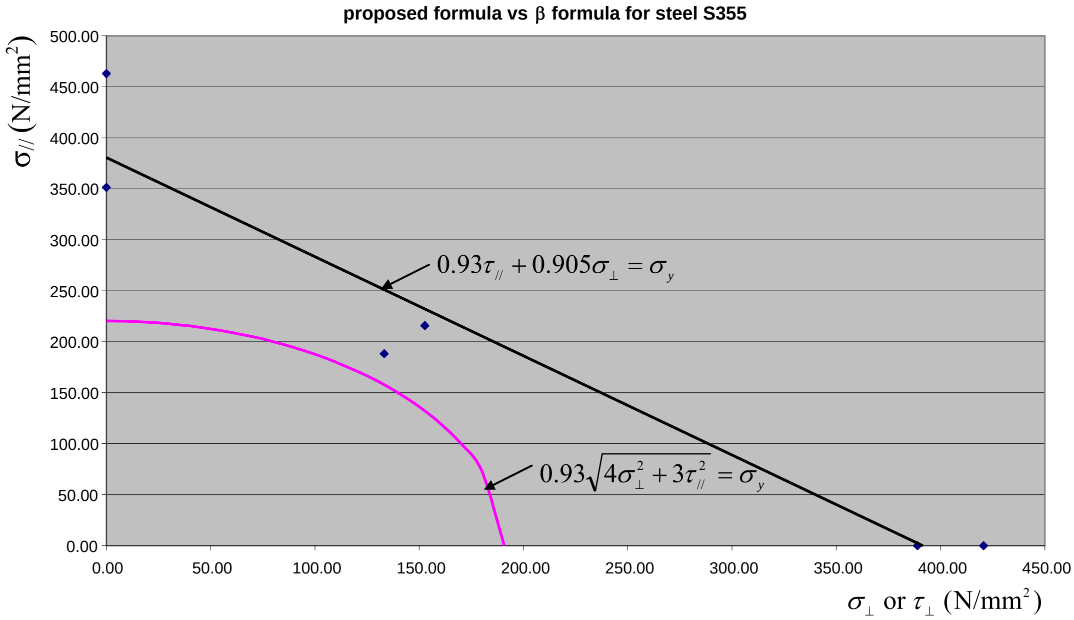

(a)

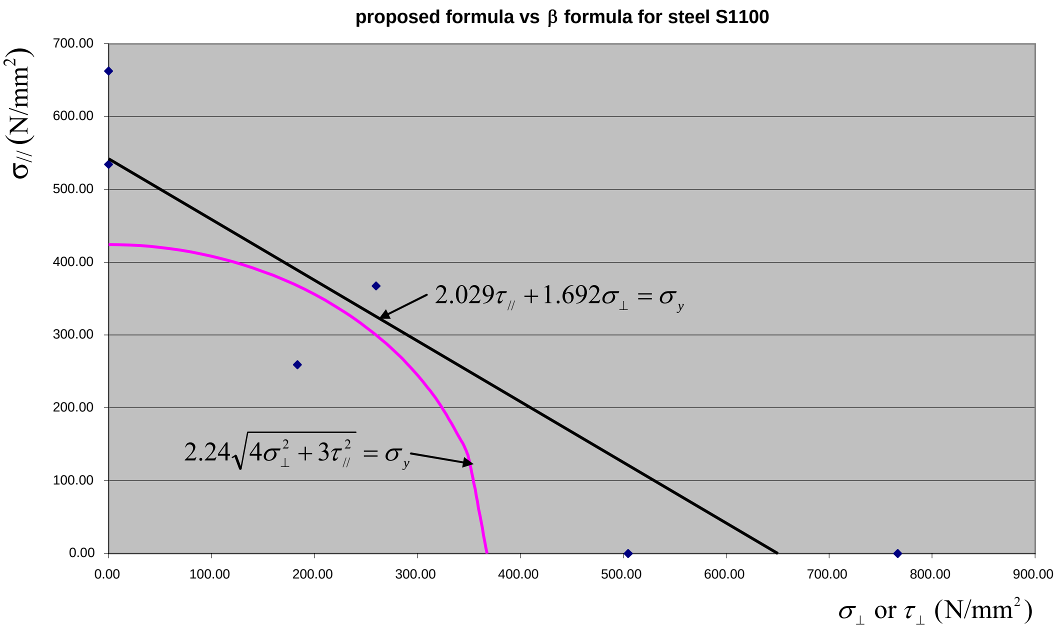

(b)

Figure 4.9: Proposed formula vs β formula (NEN 2062)
(a) steel S355, (b) steel S1100

In Figure 4.9, β=0.93 and β=2.24 is used in β formulation. In addition, $\sigma_{\perp}$ and $\tau_{\perp}$ are coupled. Based on Figure 4.9, it can be concluded the β formulation (NEN 2062) give more conservative yield load compare to that of the proposed formula.

Chapter 5 Conclusions and Recommendations

5.1 Conclusions

Several conclusions can be made regarding the results of this research project as follows.

A. Finite Element Modelling

1. Some mesh sensitivities are shown in the results of FEA especially in yielding area (e.g. Figure 2.9). The finer the mesh in the yielding area is the more sensitive the results.

2. Using higher order brick element in the FEM prevents the mesh locking problem during the analysis.

3. Non linear FEM in combination with Lemaitre criterion can predict the failure load in high strength steel fillet weld connections accurately.

B. β values

1. A big scatter appears in the calculated β values using formulas given in several codes [3, 8 and 10] for steel S1100 and S355. It is clear that for different types of weld detail (different combination of $\sigma_\perp$, $\tau_\perp$ and $\tau_{//}$) produce different β values and in turn gives different margin to failure which implies that those formulas in those codes can be improved.

2. In this project, β = 2.24 for steel S1100 is found and after validation using Monte Carlo simulation it is concluded as a safe value if to be used in designing fillet weld connections using design equations based on [10]. However, few joints are included in the determination of this value, which means that it can be reduced if more experiments or analysis are available.

3. The proposed formula for designing fillet weld connection of steel S1100 will predict the failure load more accurate compare to β formulation [10]; however, in the derivation of the formula the influence of the uncoupled $\sigma_\perp$ and $\tau_\perp$ is not included and also it seems that there is dependency to the weld size (the bigger the welds the more strength in the connections).

4. Overmatching and undermatching conditions in a fillet weld connections do not directly determine the failure location in the connections because the thickness of the weld is also important.

5. In a welded connections, plastic deformation has already occurred at the first stage of the loading which implies that a design formulation based on yield cannot be formulated.

5.2 Recommendations

Several recommendations related to this project can be summarized as follow.

1. More experiments regarding fillet weld connections for steel S1100 need to be done in order to reduce the uncertainty in the determination of β value for this type of steel grade. In addition, FE modelling of fillet weld connections for steel S1100 only can be validated with a very good accuracy if there are enough experimental results for comparison are available.

2. In the FE modelling, the imperfections and flaws which occur during fabrication of the connections should be taken into account in the material properties which is used as the input and also in the model that is built. This can make sure that the results of the FEA accurate enough if comparison is done with the experiment results.

3. Other type of fillet weld connections geometry which result in uncoupled $\sigma_\perp$ and $\tau_\perp$ should be analysed and also other loading case should be included in order to have a complete formulation of designing fillet weld connection of steel S1100. A detail of fillet weld connections where $\sigma_\perp$ and $\tau_\perp$ are uncoupled is shown in Figure 5.1

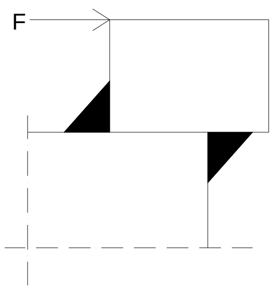

Figure 5.1: A detail of fillet weld connections where $\sigma_\perp$ and $\tau_\perp$ are uncoupled

References

[1] ANSYS Release 8.0 Documentation.

[2] A.C.W.M. Vrouwenvelder, J. Witteveen, "Plastic Analysis of Structures, The plastic behaviour and the calculation of beams and frames subjected to bending", Lecture book Delft University of Technology, March 2003.

[3] Eurocode 3 part 1.8, General rules-Design of joints, Dec. 2003.

[4] Integrity of High Strength Steel Structures-Validation FEM analyses, TNO Report 2005-BCS-R0446, February 2006.

[5] Integrity of High Strength Steel Structures-Pilot FEM analyses, TNO Report 2005-BC-R0054, December 2004.

[6] Kolstein M.H., Integrity of High Strength Steel Structures-Experimental results, TU-Delft, March 2006.

[7] Kolstein M.H, Dijkstra O.D., INTEGRITY OF HIGH STRENGTH STEEL STRUCTURES Analysis of the experiment, March 2006, TU-Delft.

[8] Lloyd's Register of Shipping, Code for Lifting Appliances in a Marine Environment, January 2003.

[9] Lubahn J.D, Felgar R.P., Plasticity and Creep of Metals, John Wiley & Sons, Inc, New York, 1961.

[10] NEN 2062, Arc Welding- Calculation of welded joints in unalloyed and low-alloy steel with up to and including Fe 510 (Fe 52) which are predominantly statically loaded, 1977.

[11] Stofregen M., Applicability of Design Rules for The Extra High Tensile Steel S1100Q, MSc thesis, 2004, TU-Delft, The Netherlands.

[12] Welding consumbales, DRAHTZUG STEIN wire and welding.

Appendices

Appendix A

The figures below are taken from a report by Kolstein [6].

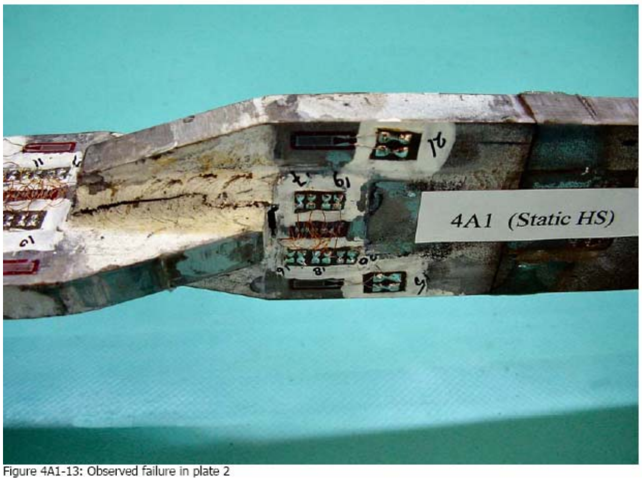

Figure A.1: Failure of connection 4A1

Figure A.2: Failure of connection 5A1

Appendix B

Material Nonlinearities

Strain Definition

For nonlinear material the definition of plastic strain is given as follow.

$$\varepsilon_{pl} = \varepsilon_{tot} - \varepsilon_{el} \tag{B.1}$$

where: ε_{pl} = plastic strain vector
ε_{tot} = total strain vector
ε_{el} = elastic strain vector

Rate Independent Plasticity

Rate-independent plasticity is characterized by the irreversible straining that occurs in a material once a certain level of stress is reached. The plastic strains are assumed to develop instantaneously, that is, independent of time. There are three components which included in this plasticity that are yield criterion, flow rule and hardening rule. Each component will be explained in the following section.

- Yield Criterion

The yield criterion determines the stress level at which yielding is initiated. For multi-component stresses, this is represented as a function of the individual components, f({σ}), which can be interpreted as an equivalent stress σ_e:

$$f = \{(\sigma)\} \tag{B.2}$$

(σ) = *stress vector*

When the equivalent stress is equal to a material yield parameter σ_y,

$$f\{(\sigma)\} = \sigma_y \tag{B.3}$$

the material will develop plastic strains. If σ_e is less than σ_y, the material is elastic and the stresses will develop according to the elastic stress-strain relations. Noting that the equivalent stress can never exceed the material yield since in this case plastic strains would develop instantaneously, thereby reducing the stress to the material yield. Equation (B.3) can be plotted in stress space as shown in Figure B.1 for some of the plasticity options. The surfaces in Figure 3.1 are known as the yield surfaces and any stress state inside the surface is elastic, that is, they do not cause plastic strains.

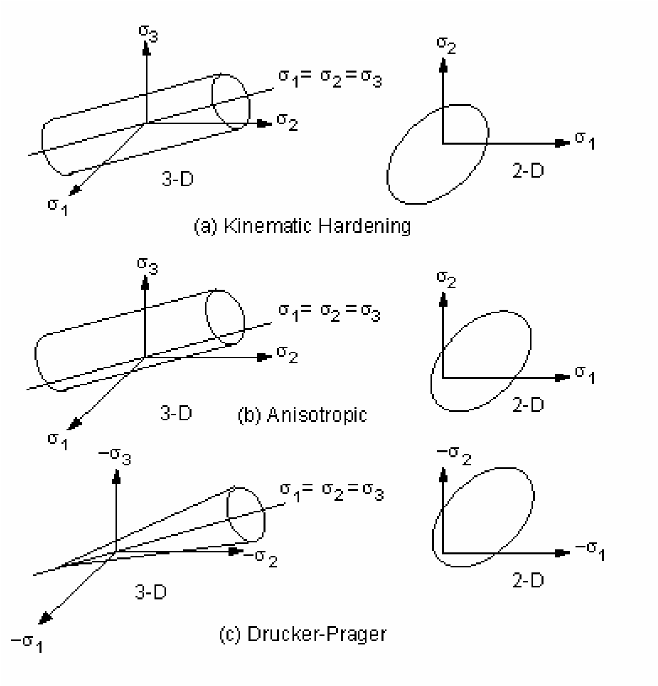

Figure B.1: Various yield surfaces

- Flow Rule

The flow rule describes the direction of the plastic deformation and gives relation between the loading function and the stress strain relation. Flow rule is defines as follows.

$$d\varepsilon_{ij}^{p} = d\lambda \frac{\partial g}{\partial \sigma_{ij}} \tag{B.4}$$

Where $d\lambda \geq 0$

The gradient of the plastic potential surface $\frac{\partial g}{\partial \sigma_{ij}}$ defines the direction of the plastic strain increment vector $d\varepsilon_{ij}^{p}$ and $d\lambda$ determines the length.

- Hardening Rule

Hardening rule is a phenomenon where yield stress increases with further plastic straining. There are several types of hardening rules which had been proposed in order to define the modification of the yield surface during plastic deformation. For example, isotropic hardening, kinematic hardening and mixed hardening which is the combination of both hardening. In the following section only the first two will be explained.

1. Isotropic hardening

This hardening rule assumed that the initial yield surface expands uniformly without distortion and translation as plastic flow occurs. The size of the yield surface is governed by the plastic strain history. Figure B.2 shows the representation of this hardening rule.

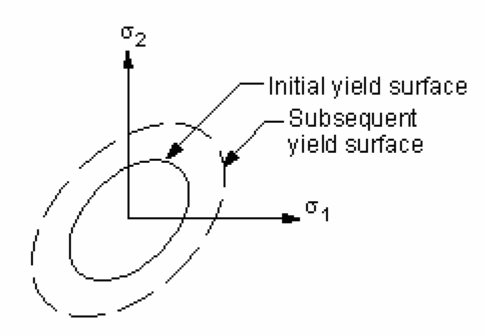

Figure B.2: Isotropic Hardening

2. Kinematic hardening

The kinematic hardening assumes that the yield surface translate in the stress space during plastic deformation as a rigid body which means the size, shape and orientation of the surface is the same as before plastic deformation occurs and it is shown in Figure B.3. This hardening rule take into account the Bauschinger effect which is not considered in isotropic hardening rule.

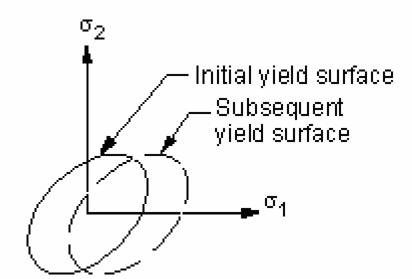

Figure B.3: Kinematic Hardening

Appendix C

This explanation is based on [1].

A. Numerical integration of SOLID 185 (8 nodes brick element)

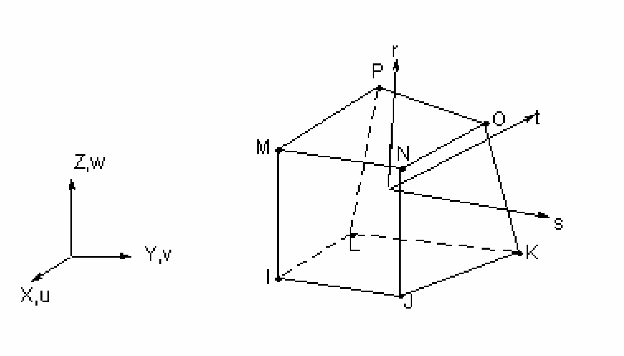

Figure C.1: SOLID 185 element

This element uses 2 x 2 x 2 integration point if KEYOPT(2) = 0, 2, or 3 and use 1 integration point if KEYOPT(2) = 1.

The explanation regarding every KEYOPT ( ) are as follow.

- If KEYOPT(2) = 0, this element uses method (selective reduced integration technique for volumetric terms).
- If KEYOPT(2) = 1, the uniform reduced integration technique is used.

- If KEYOPT(2) = 2 or 3, the enhanced strain formulations are used. It introduces 13 internal degrees of freedom to prevent shear and volumetric locking for KEYOPT(2) = 2, and 9 degreess of freedom to prevent shear locking only for KEYOPT(2) = 3. If mixed u-P formulation is employed with the enhanced strain formulations, only 9 degrees of freedom for overcoming shear locking are activated.

B. Numerical integration of SOLID 186 (20 nodes brick element)

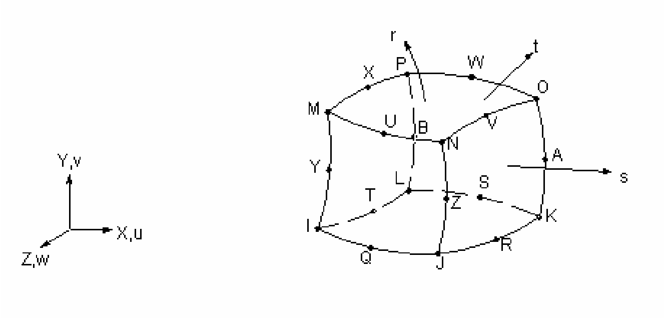

Figure C.2: SOLID 186 element

This element uses 14 integration point if KEYOPT (2) = 1 and uses 2 x 2 x 2 integration point if KEYOPT (2) = 0

Appendix D

This explanation is based on [1].

Free or Mapped Mesh

Before meshing the model, and even before building the model, it is important to think about whether a free mesh or a mapped mesh is appropriate for the analysis. A *free* mesh has no restrictions in terms of element shapes, and has no specified pattern applied to it.

Compared to a free mesh, a *mapped* mesh is restricted in terms of the element shape it contains and the pattern of the mesh. A mapped area mesh contains either only quadrilateral or only triangular elements, while a mapped volume mesh contains only hexahedron elements. In addition, a mapped mesh typically has a regular pattern, with obvious rows of elements. If you want this type of mesh, you must build the geometry as a series of fairly regular volumes and/or areas that can accept a mapped mesh. The figure below shows an example of free and mapped mesh.

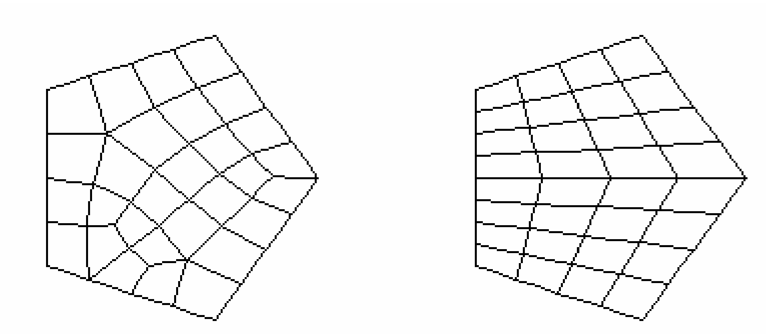

(a) (b)

Figure D.1: (a) Free mesh; (b) Mapped mesh

Appendix E

This explanation is based on [1].

Interpretation of Equivalent Strains

The equivalent strains for the elastic, plastic, creep and thermal strains are computed in postprocessing using the von Mises equation:

$$\varepsilon_{eq} = \frac{1}{\sqrt{2}(1+\nu')}\left[(\varepsilon_x - \varepsilon_y)^2 + (\varepsilon_y - \varepsilon_z)^2 + (\varepsilon_z - \varepsilon_x)^2 + \frac{3}{2}(\gamma_{xy}^2 + \gamma_{yz}^2 + \gamma_{xz}^2)\right]^{\frac{1}{2}}$$

where:

ε_x, ε_y, etc. = appropriate component strain values

ν' = effective Poisson's ratio

Physical Interpretation of Equivalent Strain

The von Mises equation is a measure of the “shear” strain in the material and does not account for the hydrostatic straining component. For example, strain values of $\varepsilon_x = \varepsilon_y = \varepsilon_z = 0.001$ yield an equivalent strain εeq = 0.0.

Plastic Strain

For plasticity, the accumulated effective plastic strain is defined by:

$$\varepsilon_{eqa}^{pl} = \sum \Delta\varepsilon_{eq}^{pl}$$

where:

ε_{eqa}^{pl} = accumulated effective plastic strain

$$\Delta_{eq}^{pl} = \frac{\sqrt{2}}{3}\left[\left(\Delta\varepsilon_x^{pl} - \Delta\varepsilon_y^{pl}\right)^2 + \left(\Delta\varepsilon_y^{pl} - \Delta\varepsilon_z^{pl}\right)^2 + \left(\Delta\varepsilon_z^{pl} - \Delta\varepsilon_x^{pl}\right)^2 + \frac{3}{2}\left(\Delta\gamma_{xy}^{pl^2} + \Delta\gamma_{yz}^{pl^2} + \Delta\gamma_{xz}^{pl^2}\right)\right]^{\frac{1}{2}}$$

Appendix F

Steps of the procedure in determining β value of fillet weld connection are as follow.

1. Based on the yield load criteria, the corresponding F/Fu value can be determined based on Figure 5.3 for each type of steel and type of connections. For example, the β value of connection 4A1 using Lloyd standard will be determined for yield load criteria 5%. First draw a vertical straight line at position Δ_{pl}/Δ_{el} = 5% then from the intersection of this line with the line representing connection 4A1 draw another horizontal straight line which gives the value of F/Fu. For this particular case the F/Fu is 0.71. The complete example of the first procedure is given in the Figure F.1.

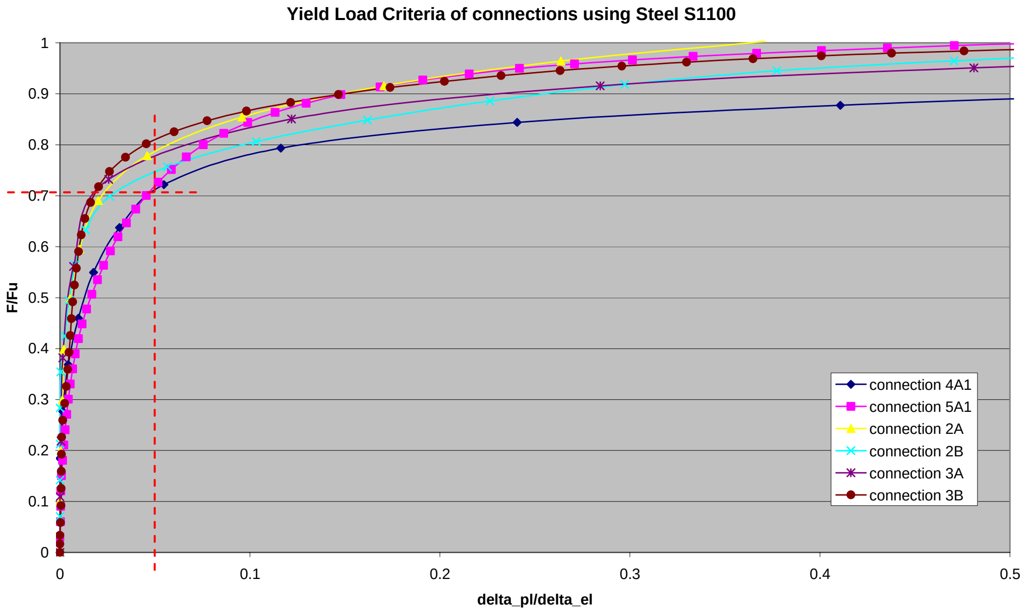

Figure F.1: Determination of F/Fu value

2. Using this F/Fu value the β value can be determined using Figure 5.3. Continue from the given example for Lloyd standard the corresponding β value for F/Fu equal to 0.71 is 0.94. Again the complete representation is given in the Figure F.2.

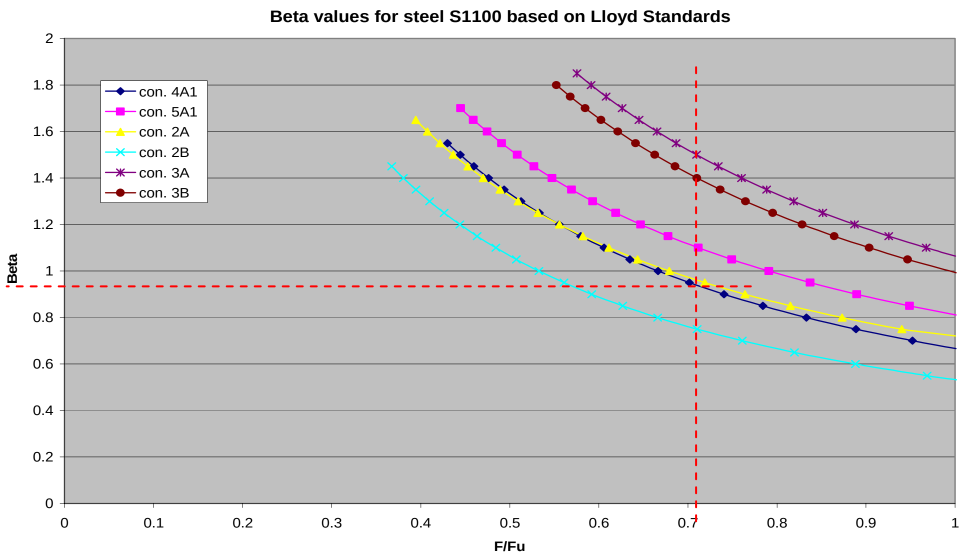

Figure F.2: Determination of β value

Appendix G

Monte Carlo simulation.

Monte Carlo simulation of 100000 virtual fillet weld connections is made to calculate the probability failure of the connection. For this simulation, connection type 3 using steel S1100 is used as the basis model. Normal distributions are taken for the material strength, the loading and the model factor. The 5% characteristic value is used for the yield strength of the material with variation coefficient 0.08 and the safety factor is taken 1.5 according to Huisman-Itrec standard. These values are used for the determination of mean and standard deviation of the yield strength. For the determination of mean and standard deviation of the loading, a load factor 1.5 is used for live load based on Huisman-Itrec standard. 5% characteristic value of the loading is calculated based on [10] for fillet weld connection with variation coefficient 0.08 corresponds to hoisting loading. This coefficient corresponds to the fact that during lifting operations of a crane, the operator of the crane should make sure that the crane is not overloaded.

For the model factor which is in this case the β value, a value 1.57 is used to see whether this value is a safe value. For the statistics β value, the mean and standard deviation is based on 5% yield load criteria which is given in Table G.1 which is the result from FEA. The mean is taken as the average of β value of 2 connections that are connection 3A and connection 3B. For standard deviation, β value of 6 type of connections are taken into account. The corresponding mean and standard deviation of β is given in Table G.1.

Table G.1 Mean and Standard deviation value of β

No.	Statistic properties	NEN 2062
1.	Mean	2.045
2.	Standard deviation	0.5

The probability result of the Monte Carlo simulation will be compared to a failure probability which is based on codes of practice. For this case, a probability failure of 0.00130 (β=3.0) will be used as a comparison value. This value is bigger comparing to that usually used 0.00016 (β=3.6). The reasons like professionals involvement in design and assembly process of the structure, structure economic live that less than 50 years and the awareness of the workers to the danger while working in a rig are all that make a bigger probability failure is possible to use.

Monte Carlo simulation program to calculate the probability failure of fillet weld connection (connection type 3B) is given below.

```
> restart:
> with(stats):
>
> # reliability of a weld connection
> # Maple 9.5
> w:=240:              # steel plate width       [mm]
> t:=20:               # steel plate thickness   [mm]
> a:=10:               # weld thickness          [mm]
> alpha:=evalf(Pi/4): # angle of the connection [-]
> fy:=1100:            # yield stress            [N/mm2] 5% characteristic value
> beta:=2.24:          # model factor
> loadfactor:=2.25:    # load factor
> n:=100000:           # number of simulations
>
> # material statistics
> eq1:=meanfy=fy+1.645*stanDevfy:
> eq2:=stanDevfy=meanfy*0.08:
> assign(solve({eq1,eq2},{meanfy,stanDevfy})):
>
> # FEA
> nrAnalysis:=6:
> meanBeta:=2.045:
> stanDevBeta:=0.5:
>
```

```
> # design calculation
> # tau1:=F/2*cos(alpha) / (a*w/sin(alpha)):
> # tau2:=F/2*sin(alpha)/sqrt(2) / (a*w/sin(alpha)):
> # sigma:=tau2:
> # eq1:=fy=beta*sqrt( sigma^2 +3*(tau1^2 +tau2^2)):
> # solve(eq1,F):
> F:=2*fy*a*w/(beta*sin(alpha)*sqrt(2*sin(alpha)^2+3*cos(alpha)^2)):
> Strength:=evalf(F/loadfactor);
>
> # load statistics
> eq1:=meanLoad=Strength-1.645*stanDevLoad:
> eq2:=stanDevLoad=meanLoad*0.08:
> assign(solve({eq1,eq2},{meanLoad,stanDevLoad}));
>
> # Monte Carlo simulation
> nF:=0:
> for i from 1 to n do
  # realisation of yield stress
  fyR:=meanfy+stats[random,normald](1)*stanDevfy:

  # realisation of the FEA
  t1:=0: t2:=0:
  for j from 1 to nrAnalysis do
    B:=meanBeta+stats[random,normald](1)*stanDevBeta:
    t1:=t1+B:
    t2:=t2+B*B:
  end do:
  meanB:=t1/nrAnalysis:
  stanDevB:=sqrt( (t2-nrAnalysis*meanB^2) / (nrAnalysis-1) ):
  betaR:=meanB+stats[random,normald](1)*stanDevB:

  # realisation connection strength
  R:=2*fyR*a*w/(betaR*sin(alpha)*sqrt(2*sin(alpha)^2+3*cos(alpha)^2));

  # realisation of load
  S:=meanLoad+stats[random,normald](1)*stanDevLoad:

  if (R<S) then nF:=nF+1: end if:
end do:
> P:=evalf(nF/n); # < 0.00130
```

$$P := 0.0009500000000$$

The dimension of the material connected such as width of the plate, thickness of the plate and thickness of the weld do not influence the result of the probability failure. The probability failure results of Monte Carlo simulation are given in Table G.2.

Table G.2 Probability failure results

No.	Probability failure	NEN 2062
1.	Limit	0.00130
2.	Monte Carlo Simulation	0.00095

It can be seen in Table G.2 that the probability factor based on Monte Carlo Simulation is smaller than the limit probability factor for all standards. It implies that the model factor $\beta = 2.24$ is a safe value.

Appendix H

Safety index (β)

Veiligheid

Tabel voor de normale verdeling

u/-β	kans	u/-β	kans	u/-β	kans	u/-β	kans
0,00	$5,00 \times 10^{-1}$	2,55	$5,45 \times 10^{-3}$	5,05	$2,30 \times 10^{-7}$	7,55	$2,22 \times 10^{-14}$
0,05	$4,80 \times 10^{-1}$	2,60	$4,70 \times 10^{-3}$	5,10	$1,70 \times 10^{-7}$	7,60	$1,51 \times 10^{-14}$
0,10	$4,60 \times 10^{-1}$	2,65	$4,10 \times 10^{-3}$	5,15	$1,35 \times 10^{-7}$	7,65	$1,02 \times 10^{-14}$
0,15	$4,40 \times 10^{-1}$	2,70	$3,50 \times 10^{-3}$	5,20	$1,00 \times 10^{-7}$	7,70	$6,93 \times 10^{-15}$
0,20	$4,20 \times 10^{-1}$	2,75	$3,05 \times 10^{-3}$	5,25	$7,90 \times 10^{-8}$	7,75	$4,68 \times 10^{-15}$
0,25	$4,00 \times 10^{-1}$	2,80	$2,60 \times 10^{-3}$	5,30	$5,80 \times 10^{-8}$	7,80	$3,15 \times 10^{-15}$
0,30	$3,80 \times 10^{-1}$	2,85	$2,25 \times 10^{-3}$	5,35	$4,55 \times 10^{-8}$	7,85	$2,12 \times 10^{-15}$
0,35	$3,60 \times 10^{-1}$	2,90	$1,90 \times 10^{-3}$	5,40	$3,30 \times 10^{-8}$	7,90	$1,42 \times 10^{-15}$
0,40	$3,40 \times 10^{-1}$	2,95	$1,60 \times 10^{-3}$	5,45	$2,60 \times 10^{-8}$	7,95	$9,49 \times 10^{-16}$
0,45	$3,25 \times 10^{-1}$	3,00	$1,30 \times 10^{-3}$	5,50	$1,90 \times 10^{-8}$	8,00	$6,33 \times 10^{-16}$
0,50	$3,10 \times 10^{-1}$	3,05	$1,14 \times 10^{-3}$	5,55	$1,50 \times 10^{-8}$	8,05	$4,21 \times 10^{-16}$
0,55	$2,90 \times 10^{-1}$	3,10	$9,70 \times 10^{-4}$	5,60	$1,10 \times 10^{-8}$	8,10	$2,80 \times 10^{-16}$
0,60	$2,70 \times 10^{-1}$	3,15	$8,20 \times 10^{-4}$	5,65	$8,50 \times 10^{-9}$	8,15	$1,85 \times 10^{-16}$
0,65	$2,55 \times 10^{-1}$	3,20	$6,70 \times 10^{-4}$	5,70	$6,00 \times 10^{-9}$	8,20	$1,22 \times 10^{-16}$
0,70	$2,40 \times 10^{-1}$	3,25	$5,75 \times 10^{-4}$	5,75	$4,65 \times 10^{-9}$	8,25	$8,05 \times 10^{-17}$
0,75	$2,25 \times 10^{-1}$	3,30	$4,80 \times 10^{-4}$	5,80	$3,30 \times 10^{-9}$	8,30	$5,29 \times 10^{-17}$
0,80	$2,10 \times 10^{-1}$	3,35	$4,05 \times 10^{-4}$	5,85	$2,55 \times 10^{-9}$	8,35	$3,47 \times 10^{-17}$
0,85	$1,95 \times 10^{-1}$	3,40	$3,30 \times 10^{-4}$	5,90	$1,80 \times 10^{-9}$	8,40	$2,27 \times 10^{-17}$
0,90	$1,80 \times 10^{-1}$	3,45	$2,80 \times 10^{-4}$	5,95	$1,38 \times 10^{-9}$	8,45	$1,48 \times 10^{-17}$
0,95	$1,70 \times 10^{-1}$	3,50	$2,30 \times 10^{-4}$	6,00	$1,02 \times 10^{-9}$	8,50	$9,63 \times 10^{-18}$
1,00	$1,60 \times 10^{-1}$	3,55	$1,95 \times 10^{-4}$	6,05	$7,45 \times 10^{-10}$	8,55	$6,25 \times 10^{-18}$
1,05	$1,50 \times 10^{-1}$	3,60	$1,60 \times 10^{-4}$	6,10	$5,45 \times 10^{-10}$	8,60	$4,05 \times 10^{-18}$
1,10	$1,40 \times 10^{-1}$	3,65	$1,35 \times 10^{-4}$	6,15	$3,98 \times 10^{-10}$	8,65	$2,62 \times 10^{-18}$
1,15	$1,30 \times 10^{-1}$	3,70	$1,10 \times 10^{-4}$	6,20	$2,90 \times 10^{-10}$	8,70	$1,69 \times 10^{-18}$
1,20	$1,20 \times 10^{-1}$	3,75	$9,10 \times 10^{-5}$	6,25	$2,11 \times 10^{-10}$	8,75	$1,08 \times 10^{-18}$
1,25	$1,10 \times 10^{-1}$	3,80	$7,20 \times 10^{-5}$	6,30	$1,53 \times 10^{-10}$	8,80	$6,95 \times 10^{-19}$
1,30	$1,00 \times 10^{-1}$	3,85	$6,00 \times 10^{-5}$	6,35	$1,11 \times 10^{-10}$	8,85	$4,44 \times 10^{-19}$
1,35	$9,05 \times 10^{-2}$	3,90	$4,80 \times 10^{-5}$	6,40	$7,97 \times 10^{-11}$	8,90	$2,83 \times 10^{-19}$
1,40	$8,10 \times 10^{-2}$	3,95	$4,00 \times 10^{-5}$	6,45	$5,74 \times 10^{-11}$	8,95	$1,80 \times 10^{-19}$
1,45	$7,40 \times 10^{-2}$	4,00	$3,20 \times 10^{-5}$	6,50	$4,12 \times 10^{-11}$	9,00	$1,15 \times 10^{-19}$
1,50	$6,70 \times 10^{-2}$	4,05	$2,65 \times 10^{-5}$	6,55	$2,95 \times 10^{-11}$	9,05	$7,25 \times 10^{-20}$
1,55	$6,10 \times 10^{-2}$	4,10	$2,10 \times 10^{-5}$	6,60	$2,11 \times 10^{-11}$	9,10	$4,58 \times 10^{-20}$
1,60	$5,50 \times 10^{-2}$	4,15	$1,70 \times 10^{-5}$	6,65	$1,50 \times 10^{-11}$	9,15	$2,89 \times 10^{-20}$
1,65	$4,95 \times 10^{-2}$	4,20	$1,30 \times 10^{-5}$	6,70	$1,07 \times 10^{-11}$	9,20	$1,82 \times 10^{-20}$
1,70	$4,50 \times 10^{-2}$	4,25	$1,05 \times 10^{-5}$	6,75	$7,57 \times 10^{-12}$	9,25	$1,14 \times 10^{-20}$
1,75	$4,05 \times 10^{-2}$	4,30	$7,93 \times 10^{-6}$	6,80	$5,35 \times 10^{-12}$	9,30	$7,12 \times 10^{-21}$
1,80	$3,60 \times 10^{-2}$	4,35	$6,38 \times 10^{-6}$	6,85	$3,78 \times 10^{-12}$	9,35	$4,44 \times 10^{-21}$
1,85	$3,25 \times 10^{-2}$	4,40	$4,83 \times 10^{-6}$	6,90	$2,66 \times 10^{-12}$	9,40	$2,77 \times 10^{-21}$
1,90	$2,90 \times 10^{-2}$	4,45	$4,11 \times 10^{-6}$	6,95	$1,87 \times 10^{-12}$	9,45	$1,72 \times 10^{-21}$
1,95	$2,60 \times 10^{-2}$	4,50	$3,40 \times 10^{-6}$	7,00	$1,31 \times 10^{-12}$	9,50	$1,06 \times 10^{-21}$
2,00	$2,30 \times 10^{-2}$	4,55	$2,74 \times 10^{-6}$	7,05	$9,14 \times 10^{-13}$	9,55	$6,57 \times 10^{-22}$
2,05	$2,05 \times 10^{-2}$	4,60	$2,09 \times 10^{-6}$	7,10	$6,37 \times 10^{-13}$	9,60	$4,05 \times 10^{-22}$
2,10	$1,80 \times 10^{-2}$	4,65	$1,70 \times 10^{-6}$	7,15	$4,43 \times 10^{-13}$	9,65	$2,49 \times 10^{-22}$
2,15	$1,60 \times 10^{-2}$	4,70	$1,31 \times 10^{-6}$	7,20	$3,08 \times 10^{-13}$	9,70	$1,53 \times 10^{-22}$
2,20	$1,40 \times 10^{-2}$	4,75	$1,04 \times 10^{-6}$	7,25	$2,13 \times 10^{-13}$	9,75	$9,34 \times 10^{-23}$
2,25	$1,25 \times 10^{-2}$	4,80	$7,75 \times 10^{-7}$	7,30	$1,47 \times 10^{-13}$	9,80	$5,70 \times 10^{-23}$
2,30	$1,10 \times 10^{-2}$	4,85	$6,26 \times 10^{-7}$	7,35	$1,01 \times 10^{-13}$	9,85	$3,47 \times 10^{-23}$
2,35	$9,60 \times 10^{-3}$	4,90	$4,77 \times 10^{-7}$	7,40	$6,95 \times 10^{-14}$	9,90	$2,11 \times 10^{-23}$
2,40	$8,20 \times 10^{-3}$	4,95	$3,83 \times 10^{-7}$	7,45	$4,76 \times 10^{-14}$	9,95	$1,28 \times 10^{-23}$
2,45	$7,20 \times 10^{-3}$	5,00	$2,90 \times 10^{-7}$	7,50	$3,25 \times 10^{-14}$	10,00	$7,72 \times 10^{-24}$
2,50	$6,20 \times 10^{-3}$						

Appendix I

Stress components in fillet weld connection.

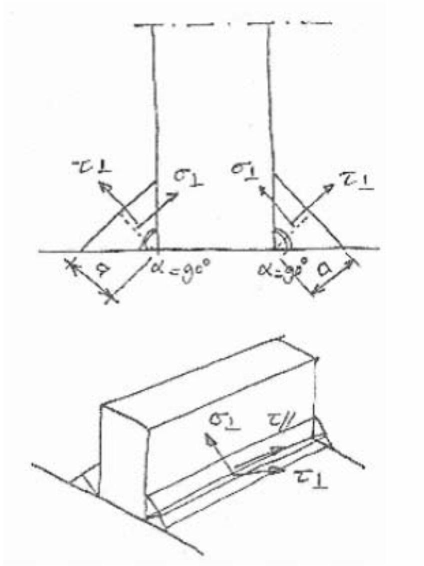

Figure I.1: Stress components in fillet weld connection
(based on Huisman-Itrec manual calculation, pg 5-20)

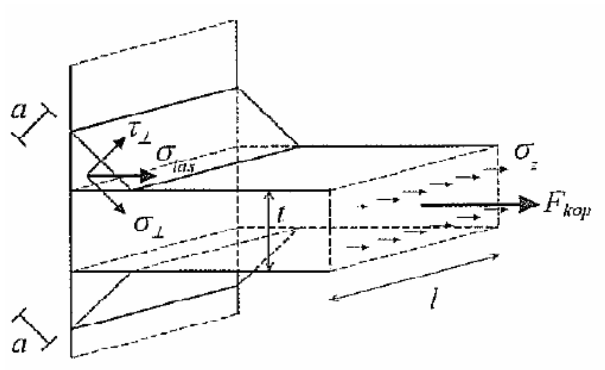

(a)

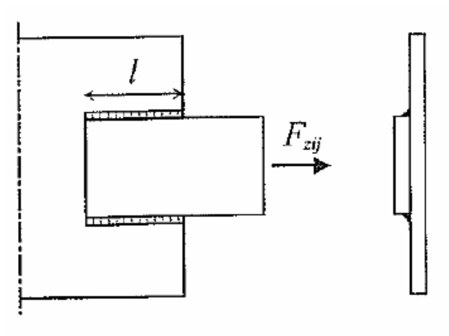

(b)

Figure I.2: Stress components in fillet weld connection
(a) two stress components occur in the connection, (b) one stress component occur in the connection
(based on metaalmagazine 2 2007, pg 36)